

PARAMETRIC DESIGN METHODOLOGY FOR MANUFACTURING OF METALLIC AND COMPOSITE  
STRUCTURES

by

Saptarshi Datta

Bachelor of Engineering, Ryerson University (2015)

A thesis

presented to Ryerson University

in partial fulfillment of the

requirements for the degree of

Master of Applied Science

in the program of

Aerospace Engineering

Toronto, Ontario, Canada, 2018

© Saptarshi Datta, 2018

## AUTHOR'S DECLARATION FOR ELECTRONIC SUBMISSION OF A THESIS

I hereby declare that I am the sole author of this thesis. This is a true copy of the thesis, including any required final revisions, as accepted by my examiners.

I authorize Ryerson University to lend this thesis to other institutions or individuals for the purpose of scholarly research.

I further authorize Ryerson University to reproduce this thesis by photocopying or by other means, in total or in part, at the request of other institutions or individuals for the purpose of scholarly research.

I understand that my thesis may be made electronically available to the public.

# **PARAMETRIC DESIGN METHODOLOGY FOR MANUFACTURING OF METALLIC AND COMPOSITE STRUCTURES**

Saptarshi Datta

Master of Applied Science, Aerospace Engineering, Ryerson University, Toronto (2018)

## **ABSTRACT**

A parametric, concurrent design methodology for manufacturing of metallic and composite structures is established. Often, during a new product development, designs prepared using the “Sequential” or “Waterfall” approach are rejected or require significant rework during manufacturing, as designers are not always versed with manufacturing principles. Similarly, manufacturers are not always versed in design principles resulting in designs that do not cater to the functional requirements. The goal of this study is to establish a methodology right from the scope to the detailed design for developing manufacturable structures using the “Concurrent Engineering” approach.

Existing literature on “Design Optimization for Manufacturing” predominantly focus on single variable optimization problems geared towards conceptual designs. The designs developed through such optimization cater towards functional performance within a “Fixed Design Space” while not accounting for manufacturing or operational challenges. The methodology developed in this study enables “Design for Manufacturing” for “Detailed Designs” through selection of a conceptual design and subsequently optimizing the selected conceptual design for a set of functional parameters. An “Integrated Product Development” approach is used, whereby, the functional requirements are linked to both design and manufacturing variables and optimization is conducted in an “Augmented Design Space” which is not available when only considering design or manufacturing variables.

Three case studies involving both “Conceptual” and “Detailed” designs have been used to illustrate the methodology presented. Case I documents the design of a Flight Control System Bracket. Case II illustrates

the use of “2D” composite structures to fabricate a roll frame. Case III involves the development of a “3D” composite door for a light unpressurized aircraft. For each of the three case studies a separate development approach has been employed. Case I uses an analytical approach, Case II uses FEM while CASE III employs a hybrid approach comprising of both FEM and analytical techniques.

## ACKNOWLEDGEMENTS

The completion of this thesis would not have been possible without the sustained academic, educational and psychological support of my supervisors:

- Dr. Fengfeng (Jeff) Xi, Professor, Ryerson University
- Dr. Seyed M. Hashemi, Professor, Ryerson University

I would also like to thank my colleagues at the Department of Aerospace Engineering for their continued backing throughout my university career.

My colleagues at SPP Canada Aircraft Inc., Diamond Aircraft Industries Canada Inc. and Bombardier Aerospace provided me with many valuable insights without which the thesis would not have the spirit that it has today.

Finally, I would like to thank my family for supporting me unrelentingly throughout this period.

## ABBREVIATIONS

AoA	Angle of Attack
CE	Concurrent Engineering
DFM	Design for Manufacturing
DFMA	Design for Manufacturing and Assembly
DFX	Design for X
EIS	Entry Into Service
F.S.	Factor of Safety
FAR	Federal Aviation Regulations
HOQ	House of Quality
HOQ	House of Quality
IPDT	Integrated Product Development Team
MTOW	Maximum Take-Off Weight
NASA	National Aeronautics and Space Administration
NCR	Non-Conformance Report
NLG	Nose Landing Gear
OML	Outer Mold Line
PuCC	Pugh Controlled Convergence
QFD	Quality Function Deployment
RFP	Request for Proposal
RFQ	Request for Quotation
SBCE	Set Based Concurrent Engineering
TPS	Total Production System
TRD	Technical Requirement Documents
OML	Outer Mold Line
IML	Inner Mold Line

# TABLE OF CONTENTS

AUTHOR'S DECLARATION FOR ELECTRONIC SUBMISSION OF A THESIS.....	ii
Abstract.....	iii
Acknowledgements.....	v
Abbreviations .....	vi
Table of Contents .....	vii
List of Tables .....	ix
List of Figures .....	x
1 Introduction .....	1
1.1 Preamble.....	1
1.2 Background .....	3
1.3 Problem Definition and Scope .....	7
1.4 Report Structure .....	7
2 Literature Review .....	9
2.1 Conceptual Product Development Methods .....	9
2.1.1 Set Based Concurrent Engineering Model .....	9
2.1.2 Pugh Controlled Convergence .....	15
2.1.3 Quality Function Deployment .....	17
2.2 Detailed Product Optimization Methods.....	21
2.2.1 Classical Methods.....	21
2.2.2 Vector Evaluated Genetic Algorithm (VEGA) .....	22
2.2.3 Nondominated Sorting Genetic Algorithm (NSGA).....	23
3 Methodology.....	26
3.1 Part I: Parameter Space Generation .....	27
3.2 Part II: Parameter Space Integration .....	29
3.3 Limitations of the Method .....	34
4 Case Studies .....	36
4.1 Case Study 1: Metallic Flight Control System Bracket .....	36
4.1.1 Design Objective .....	36
4.1.2 Parameter Space Generation - Conceptual Design Selection .....	37
4.1.3 Parameter Space Integration for Design Parameters .....	39
4.1.4 Parameter Space Integration for Manufacturing Parameters .....	47

4.2	Case Study 2: Roll Frame for a light unpressurized aircraft .....	61
4.2.1	Design Objective .....	61
4.2.2	Parameter Space Generation - Conceptual Design Selection .....	64
4.2.3	Parameter Space Integration for Design Parameters .....	66
4.2.4	Parameter Space Integration for Manufacturing Parameters .....	74
4.3	Case Study 3: Composite Door for a FAR 23 Aircraft .....	88
4.3.1	Design Objective .....	88
4.3.2	Parameter Space Generation - Conceptual Design Selection .....	88
4.3.3	Parameter Space Integration for Design Parameters .....	91
4.3.4	Parameter Space Integration for Manufacturing Parameters .....	98
5	Conclusion and Future Work .....	104
	Appendices.....	106
	Appendix-I: Rod End Bearings.....	106
	Appendix-II: Analysis of Clevis Joints .....	107
	Bearing Analysis .....	109
	Lug Analysis.....	111
	Pin Analysis .....	118
	Appendix-III: Finite Element Model Details .....	123
	Roll Frame .....	123
	NLG bay Door .....	126
	References .....	128



## LIST OF TABLES

Table 1: Design Matrix for Communicating Alternatives .....	12
Table 2: Conceptual Design Selection Matrix .....	28
Table 3: Comparative Summary of Material Properties [25] .....	42
Table 4: Sheet Metal Bracket - Relationship Matrix - Design .....	46
Table 5: Sheet Metal Bracket - Relationship Matrix - Manufacturing .....	59
Table 6: Value of Weight Savings in Dollars [30] .....	68
Table 7: Comparative Summary of Fiber Properties [30] .....	69
Table 8: Comparative Summary of Thermosetting Resins [30] .....	69
Table 9: Roll Frame - Relationship Matrix - Design .....	73
Table 10: Comparison of various composite material forms [30] .....	77
Table 11: Comparison of composite fiber weaves [30] .....	78
Table 12: Comparison of common mold materials [30] .....	82
Table 13: Roll Frame - Relationship Matrix - Manufacturing .....	82
Table 14: Comparison of common core types [30] .....	92
Table 15: Door - Relationship Matrix - Design .....	95
Table 16: Door - Relationship Matrix - Manufacturing [30] .....	101

## LIST OF FIGURES

Figure 1: Traditional Product Development Model .....	4
Figure 2: Waterfall Model [3].....	5
Figure 3: Concurrent Engineering [5].....	6
Figure 4: Principles of Set Based Concurrent Engineering [7] .....	11
Figure 5: Set Based Concurrent Engineering Model [6].....	15
Figure 6: PuCC Matrix [10] [11].....	17
Figure 7: Four Phases of QFD [13].....	18
Figure 8: House of Quality Model [12].....	20
Figure 9: HOQ Example [14].....	20
Figure 10: Initial Model before optimization [22].....	24
Figure 11: Final Model after optimization [22] .....	24
Figure 12: An optimized bracket [23] .....	25
Figure 13: Relationship Matrix – Scoring Methodology .....	30
Figure 14: Standard Product Development Approach.....	35
Figure 15: Proposed Product Development Approach.....	35
Figure 16: Partial schematic of the Flight Control System.....	39
Figure 17: Maximum and Minimum Control Forces and Torque [24] .....	40
Figure 18: Load Diagram of the Control Stick assembly .....	40
Figure 19: FBD of the Flight Control Bracket .....	41
Figure 20: Sheet Metal Bracket –Base Design - Design Parameters.....	46
Figure 21: Representative Cross-Section of Clevis Joint .....	50
Figure 22: Pin Shear Force, Bending Moment Diagram.....	51
Figure 23: Sheet Metal Bracket –Base Design - Manufacturing Parameters.....	56
Figure 24: Manufacturing Operations - 1 .....	57
Figure 25: Sheet Metal Bending using Gooseneck .....	58
Figure 26: Manufacturing Operations - 2 .....	58
Figure 27: Optimized Design of the Flight Control Bracket .....	60
Figure 28: Roll Frame on a Diamond DA40 Aircraft.....	61
Figure 29: Specific Strength vs. Specific Stiffness for Composite and Metallic Materials [29].....	68
Figure 30: Roll Frame Ply Stackup.....	70
Figure 31: Effect of Ply Stacking Sequence on Ply Deflection due to applied Axial Load [30].....	71
Figure 32: Buckling Coefficient of Hat Section Stiffeners [28] .....	72
Figure 33: Base Design – Roll Frame – Design Parameters.....	73
Figure 34: Roll Frame – Design Parameters – Strain Plot .....	74
Figure 35: Buckling Coefficient for Rectangular Section Stiffeners [28].....	76
Figure 36: Problems with Laminate Corners [30] .....	76
Figure 37: Composite Laminate Design Envelope.....	79
Figure 38: Roll Frame Ply Stackup.....	80
Figure 39: Composite Manufacturing using Vacuum Bagging [30].....	81
Figure 40: Comparison of Mold Types [30].....	81
Figure 41: Roll Frame – Manufacturing Parameters- Strain Plot.....	83
Figure 42: Roll Frame – Ply Regions .....	85
Figure 43: Roll Frame – Global Layup .....	85

Figure 44: Roll Frame – Base Reinforcement.....	86
Figure 45: Roll Frame – Base Bend Reinforcement .....	86
Figure 46: Roll Frame – Optimized Design - Strain Plot .....	87
Figure 47: Door Design Concepts.....	89
Figure 48: Ply Orientation, Stack-up Sequence and Number of Plies for the NLG Bay Door .....	95
Figure 49: Door – Base Design – Design Parameters .....	96
Figure 50: Door – Design Parameters - Deflection Plot .....	96
Figure 51: Door – Design Parameters - Strain Plot .....	97
Figure 52: Ply Orientation, Stack-up Sequence and Number of Plies for the NLG Bay Door .....	99
Figure 53: Composite Door Manufacturing Process.....	101
Figure 54: Door – Manufacturing Parameters - Deflection Plot .....	102
Figure 55: Door – Manufacturing Parameters - Max Principal Strain Plot .....	102

# 1 INTRODUCTION

## 1.1 PREAMBLE

In today's hyper competitive business environment, companies must deliver higher quality products at the cheapest cost, in the least amount of time while simultaneously exceeding environmental and labor standards; incorporate sustainable operations and continuously improve the level of customer service. These simultaneous and often conflicting objectives can be attributed to factors that are both internal and external to a company and place an onerous amount of pressure on the product developers. Product developers have to be familiar not only with the functional aspects of design but also be adept with existing, new and upcoming manufacturing techniques, supply chain logistics, business strategy and operations.

Before the dawn of the industrial revolution, product developers (craftsmen) would design, source, manufacture and sell their wares almost single handedly. As products became more complex, craftsmen had given way to separate design and manufacturing teams incorporating thousands of people often spread around geographies, working in conjunction to bring ideas from concept to realization to market. However, owing to their size, geography and diversity, product design and development functions are often separated from manufacturing and processing both physically and intellectually. This resulted in designers who are so focused on creating functional and optimized designs that they overlooked the manufacturing challenges that arose due to the inherent complexity of their designs. On the other hand, manufacturing engineers are obsessed with fabrication without regard to the functional aspects of the design.

To bridge the link between designers and manufacturers, concepts such as Design for Manufacturing and Assembly (DFMA) were developed. DFMA is a systematic procedure that helps companies to effectively utilize their existing manufacturing resources and keep the part count minimal. One such successful

implementation of Design for Manufacture and Assembly (DFMA) at GE on an accelerator pedal resulted in the number of parts dropping from 13 to 2, the number of assembly operations dropping from 24 to 2 and the cost reduced from \$1.28 to 9 cents [1].

The above example illustrates the importance of incorporating “Design for Manufacturing” (DFM) from the conceptual stage and how early incorporation of DFM can result in business survivability and long-term sustainability.

## 1.2 BACKGROUND

Any development process begins with identification of the functional requirements. Functional requirements typically detailed in a Technical Requirements Document (TRD) can incorporate performance parameters, load limits, weight targets, development timeframe and unit cost among other requisites. The goal of the development team is to translate these implicit and explicit requirements into a practical design that can be manufactured. The analysis teams work in conjunction with the design team to ensure that the proposed design meets the performance targets. The output from the design and analysis activities is an optimized design that is ready to be manufactured. During the manufacturing process, non-conformance due to manufacturing limitations, process changes/ improvements or errors may result in design changes and/or re-evaluation of the design/ analysis. The manufactured structure is subsequently examined for quality issues prior to testing. Any observations during the development process is incorporated in the design, analysis and manufacturing steps. Usually, a product goes through a few iterations of the above steps before serial production begins. The traditional product development model described is illustrated in Figure 1.

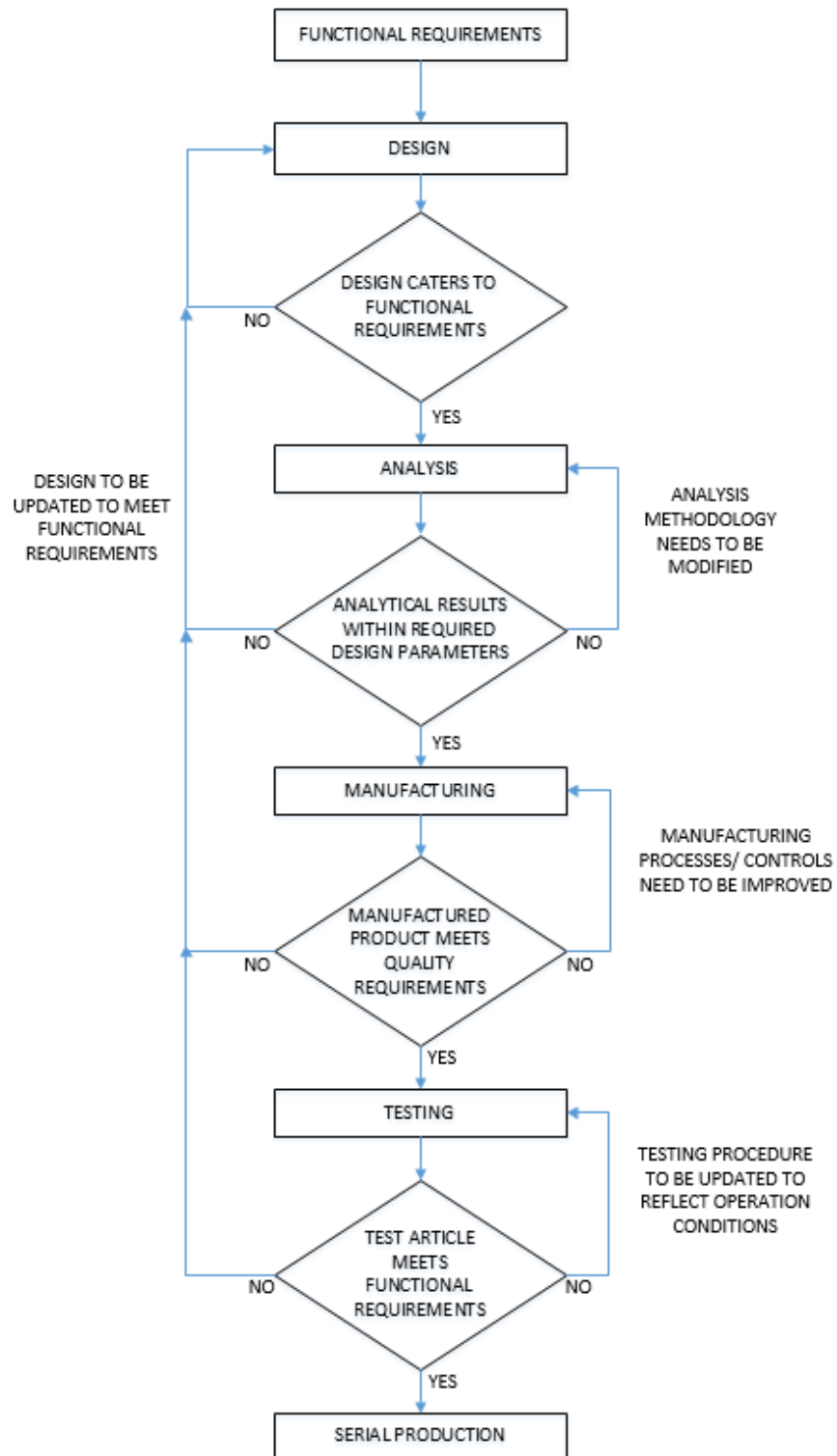


Figure 1: Traditional Product Development Model

Traditionally product development has followed a “Waterfall” approach (Figure 2) which is a model linking concept formulation to Entry into Service (EIS) through a series of sequential steps. Each step comprises of gates, whose requirements need to be fulfilled before proceeding to the next step.

The “waterfall” approach became popular since it gave structure to a program and had inherent features of program risk reduction as evidenced by its extensive use by the US Department of Defence [2] in all software development programs during the 1980’s.

Problems with the waterfall model emerged quickly when it was identified that the program cannot proceed to the next step, until the gate requirements have been cleared. Furthermore, any iteration, modification or feedback to the existing product required that all the previous gates have to be cleared again. This resulted in significant time and cost overruns making the development process unviable unless all challenges are anticipated in advance and are provisioned for.

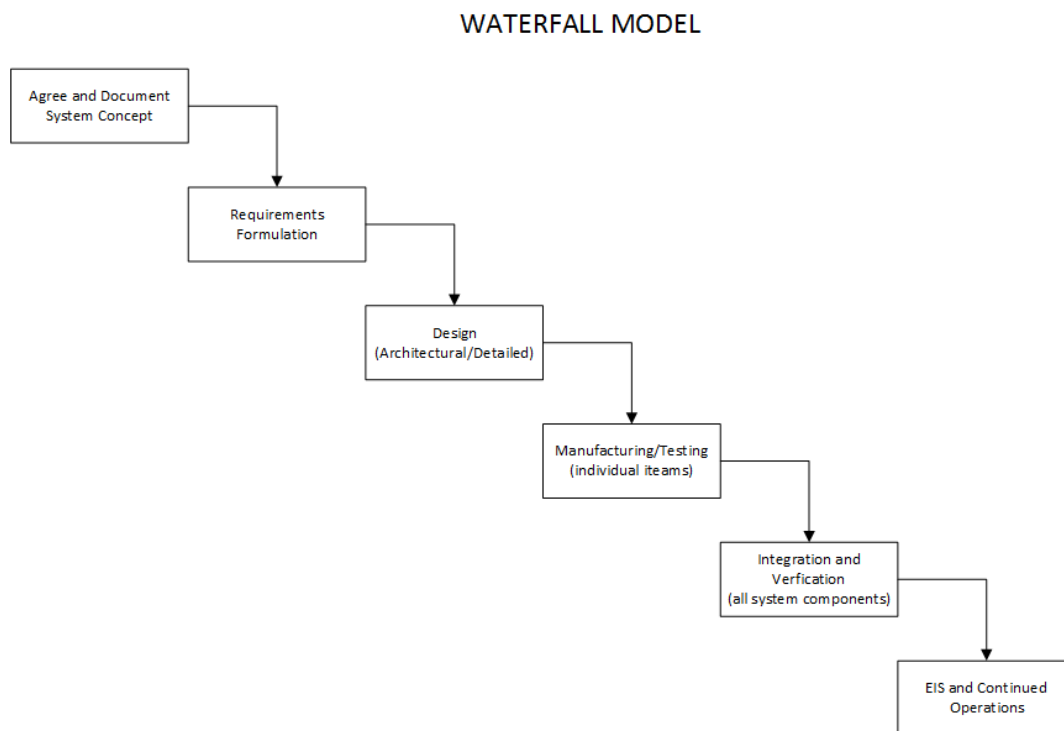


Figure 2: Waterfall Model [3]



The “waterfall” model of product development was replaced by the “concurrent” or “simultaneous” engineering model (Figure 3) which considered all product life cycle issues simultaneously and has been successfully implemented by businesses to bring their products to the market more quickly [4].

Use of concurrent engineering has given rise to Integrated Product Development Teams (IPDT) comprising of people from various disciplines involved in different aspects of the workflow (such as design, performance, analysis, testing, manufacturing and maintenance) working together to develop the product. Although, the initial states may require longer implementation times, the product comes out better, quicker and cheaper since there are less interruptions towards the end of the development cycle as all foreseeable risks are accounted for and downstream personnel are apprised of the design decisions from the beginning.

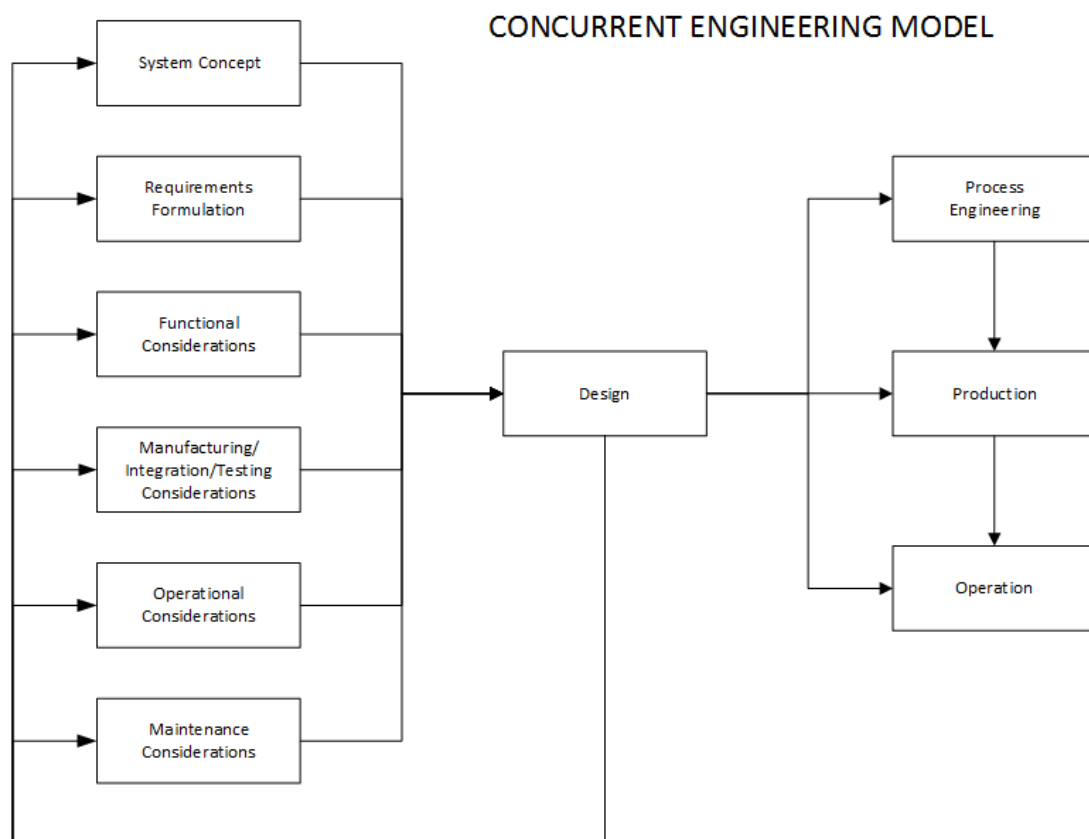


Figure 3: Concurrent Engineering [5]

### 1.3 PROBLEM DEFINITION AND SCOPE

The objective of this project is to establish a methodology right from the scope to the detailed design for developing manufacturable structures using the “Concurrent Engineering” approach.

Although, several methods exist (such as Classical Methods and Genetic Algorithms) for conceptual design optimization, there exists a disconnect between the conceptual design selection process and the detailed design optimization process for manufacturing.

The methodology presented in this document will enable rapid selection of a conceptual design from a huge set of designs based on a set of functional requirements. Subsequently, the conceptual design is optimized for a set of design and manufacturing parameters to develop a detailed design.

The concurrent development methodology presented will not only improve the communication between all stakeholders of the product but also ensure a smoother EIS and better support for continued operations.

### 1.4 REPORT STRUCTURE

The report is organized into five chapters; Introduction, Literature Review, Methodology followed by Case Studies and finally the Conclusion.

The report commences with the Introduction comprising of a preamble, background discussion of “linear” versus “concurrent” product development models, their advantages and disadvantages followed by problem definition and realization of scope.

The chapter on Literature Review explores several Product Development Models for both conceptual and detailed design.

The Methodology chapter illustrates the process of design for manufacturing through parameter space generation and parameter space integration.

Three Case Studies using three separate approaches are illustrated in the Case Studies chapter to substantiate the methodology described.

Finally, the Conclusion reinforces the results of the work performed and avenues for future progress.

An Appendix section is also included and substantiates the analysis that is presented in the case studies.

## 2 LITERATURE REVIEW

Chapter 2 presents a summary of traditional conceptual product development and detailed product optimization techniques in use today.

Three distinct methods have been discussed within the scope of conceptual product development:

- 1) Set Based Concurrent Engineering (SBCE)
- 2) Pugh Controlled Convergence (PuCC)
- 3) Quality Function Deployment (QFD)

The detailed product development methods comprise of:

- 1) Classical Methods
- 2) Vector Evaluated Genetic Algorithm (VEGA)
- 3) Nondominated Sorting Genetic Algorithm (NSGA)

### 2.1 CONCEPTUAL PRODUCT DEVELOPMENT METHODS

#### 2.1.1 SET BASED CONCURRENT ENGINEERING MODEL

The SBCE model is a combination of both the sequential and concurrent engineering (CE) models. Contrary to concurrent engineering, SBCE incorporates step-wise convergence towards a solution that is acceptable to all stakeholders. Similar to the traditional “Waterfall” approach, SBCE incorporates decision points which act like gates to remove unwanted solutions based on knowledge and experienced gained. Although, the initial steps take longer, the product is much more mature and technically sound. Toyota’s Total Production System (TPS) which uses the SBCE approach does not use many of the practices of Concurrent Engineering; rather it incorporates lean manufacturing principles resulting in a superior product [6].

Typically in CE, there are cross-functional teams often working on a single project till completion. The main objective is to reduce the time taken from product conceptual development to EIS while mitigating risks through involvement of downstream personnel right from the very beginning. In contrast, Toyota

does not co-locate development teams. Except a few key personnel, engineers are not tied to any single project at any given time. Cross-functional job rotation is extremely unusual for the first ten to twenty years of service. Furthermore, Toyota spends more time on finalizing designs than any of its competitors by considering a broader design set and delaying certain decisions which are contrary to the fast-moving automotive industry [6].

The SBCE approach revolves around three core principles (as illustrated in Figure 4) each with three different approaches to implementing the principle. Together they form the framework which allows parallel development of the product in the initial stages of development while arriving at the best solution towards the end. The three principles along with the different approaches are elaborated below:

- 1) Map the Design Space
  - a. Define feasible regions
  - b. Explore trade-offs by designing multiple alternatives
  - c. Communicate sets of possibilities
- 2) Integrate by Intersection of independent solutions
  - a. Look for intersection of feasible sets
  - b. Impose minimum constraints
  - c. Seek conceptual robustness
- 3) Establish feasibility before commitment
  - a. Narrow sets gradually while increasing detail
  - b. Stay within sets while committed
  - c. Control by managing uncertainty at process gates

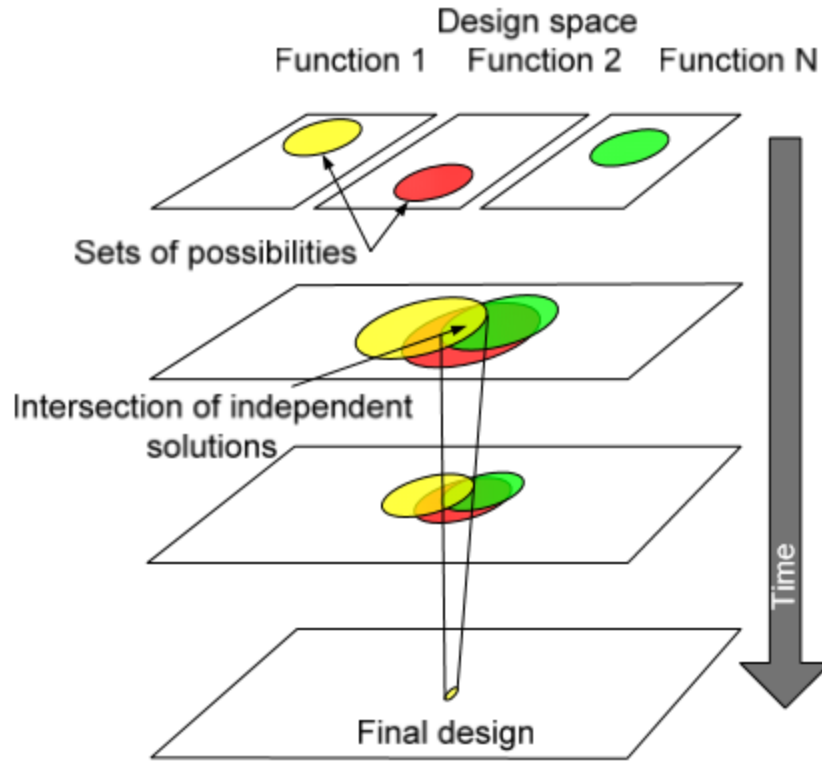


Figure 4: Principles of Set Based Concurrent Engineering [7]

#### 2.1.1.1 Map the Design Space

The design process begins with engineers exploring a range of alternative designs. This helps the developers “map out” several possible designs, along with the feasibility of each design with respect to the various systems and sub-systems pertaining to the vehicle and its production.

##### 2.1.1.1.1 Define Feasible Regions

Each functional department (fuselage, wing design) determines the primary constraints on the sub-systems that they are responsible for – what can or cannot be done, should or should not be done based on past experience, analysis and testing. The end goal is to develop design standards while liaising with other stakeholders.

#### 2.1.1.1.2 Explore Trade-offs by designing multiple alternatives

Trade-off studies are necessary to assess the impact of each design to subsequent systems and sub-systems. Although, the results of all the trade-studies are not used, this effort can lead to solutions that may be incorporated in other projects. For example, changing the wing sweep angle has broad implications on not only the aerodynamic characteristics of the vehicle but also structures, systems and other associated disciplines which must be explored.

#### 2.1.1.1.3 Communicate Sets of possibilities

The alternative found by each functional department are all listed as a set and communicated to other relevant departments. This is done in hindsight, as the best solution for one functional group might impede the implementation of a necessary feature of another functional group. The various sub-system alternatives are communicated using design matrices as illustrated in Table 1.

Table 1: Design Matrix for Communicating Alternatives

Alternative Designs	Evaluation Criteria			
	Criteria 1	Criteria 2	Criteria 3	Criteria 4 (e.g. cost)
Design Alternative 1	1	3	4	5
Design Alternative 2	3	3	2	4
Design Alternative 3	3	3	3	3
Design Alternative 4	3	3	3	3
Design Alternative 5	5	1	1	1

Legend	Unacceptable	Marginal	Average	Acceptable	Excellent
	1	2	3	4	5

#### 2.1.1.2 Integrate by Intersection

Once the alternatives are identified independently for each subsystem, the sub-system alternatives are integrated to form a workable system for all stakeholders. The three approaches used are listed below.

#### 2.1.1.2.1 Look for Intersection of Feasible Sets

Teams look for solutions that fulfill each criterion. Even at this stage multiple design alternatives may meet the evaluation criteria to various levels of conformance. The most promising ideas are retained while the least promising ideas are discarded.

#### 2.1.1.2.2 Impose Minimum Constraint

As an alternative to applying constraints to the design, sometimes it is better to constrain the design as little as possible. When working on large projects, the system integrator often specifies the interface points. All sub-systems have to be designed around those interface points. Although, this method of controlling interface points early in the program may reduce risk, it can sometimes prohibit the use of the best alternative design solution.

#### 2.1.1.2.3 Seek Conceptual Robustness

Robustness is built into the system right from the conceptual stage. As the systems change from one product to another, a robust system should be able to cater to all the varying system needs in the different products.

#### 2.1.1.3 *Establish Feasibility before Commitment*

This step acts as the final gateway for selecting the most mature design for production. The multiple alternatives that were identified in the second step are vetted down by the relevant stakeholders resulting in a final design that is chosen for further development.



#### 2.1.1.3.1 Narrow Sets Gradually While Increasing Detail

Elimination of alternative design ideas in stages allow for detailed introspection of the remaining concepts that are retained. However, to meet the product timelines this paring process must be concluded in a decisive, time bound manner.

#### 2.1.1.3.2 Stay within Sets once committed

It is imperative that there is no loopback to alternative designs with each down round of sets. The benefit of adopting a SBCE approach would be undone if loopbacks are allowed [8].

#### 2.1.1.3.3 Control by Managing Uncertainty at Process Gates

The level of uncertainty during each down round of sets must be agreed by the stakeholders beforehand. An example of managing uncertainty in an aircraft program managed through SBCE would be selection of the powerplant before some of the other details are frozen. If the powerplant is not defined while the aircraft configuration has been finalized the entire process may have to be revisited.

The approach of developing quality products in a time bound manner using SBCE has been proven to be effective. Companies such as Toyota and GE have successfully applied SBCE to develop state of the art products [8]. However, caution should be exercised when applying the SBCE approach, as the process is heavily dependent on communication between stakeholders and may not align with the company's culture of investing in design alternatives that will not work. Figure 5 provides an overview of the SBCE process as applied at Toyota.

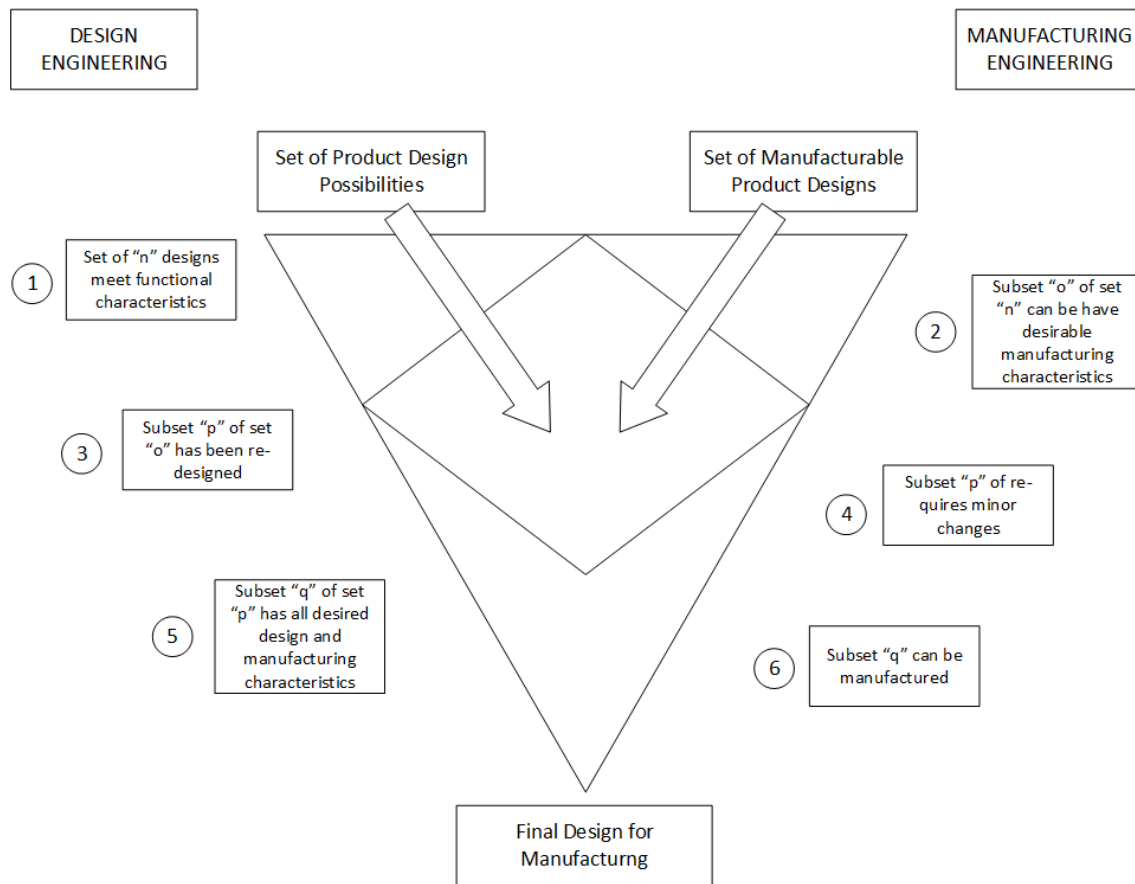


Figure 5: Set Based Concurrent Engineering Model [6]

### 2.1.2 PUGH CONTROLLED CONVERGENCE

Developed by Stuart Pugh in 1981, the Pugh Controlled Convergence (PuCC) is a structured but iterative process for product design and development [9].

The salient features of PuCC are:

- 1) Involvement of multiple stakeholders in the decision-making process
- 2) Consideration for multiple criteria
- 3) Separation of concerns into multiple criteria
- 4) Use of pair wise comparisons

The objective of PuCC is to converge on a few concepts out of many concepts that can out-compete the baseline (usually the current market leader).

Depicted as a matrix (Figure 6), PuCC is mostly used to evaluate concept designs. The various design concepts are listed in the columns of the matrix. The rows contain the various criteria that are used to judge the design concepts. A reference design (usually the market leader) which is well known and understood is selected as the datum. Each design is evaluated for each criteria by a panel of experts and the result is documented in the corresponding cell. There is no voting; only a discussion involving experts who either support or do not support the design for the evaluated criteria and their reasons for doing so. Often, this resolves any deadlock as discussion allows for facts to be presented that help in interpretation of the criteria and how the design fares against the criteria. If the discussion leads to an agreement among all the experts a “+” or “-” sign is recorded on the corresponding cell indicating that the design concept is better than or worse than the datum concept as judged according to the criteria of that row. If the experts cannot come to an agreement within a specified time, “S” is recorded in the corresponding cell. “S” can denote one of the following:

- 1) Experts agree that the design concept is similar as the datum concept
- 2) Differences between the design concept and datum concept are controversial and cannot be determined yet

For each design, the scores are added up and presented as a summary at the bottom of the evaluation matrix which facilitates comparison of the characteristics of each alternative design concept. The PuCC method was not developed to select a single winning design; rather it was developed to reduce the number of design alternatives under consideration. A single run of the matrix can lead to four possibilities:

- 1) Information gathering
- 2) Elimination of weak concepts
- 3) Further investigation and development of stronger concepts
- 4) Development of new design concepts that were not part of the original set

To get the best results, the process needs to be run iteratively while facilitating detailed discussion among all stakeholders on the criteria and the design alternatives. The end result should yield a handful of concepts that will facilitate development of a winning product.

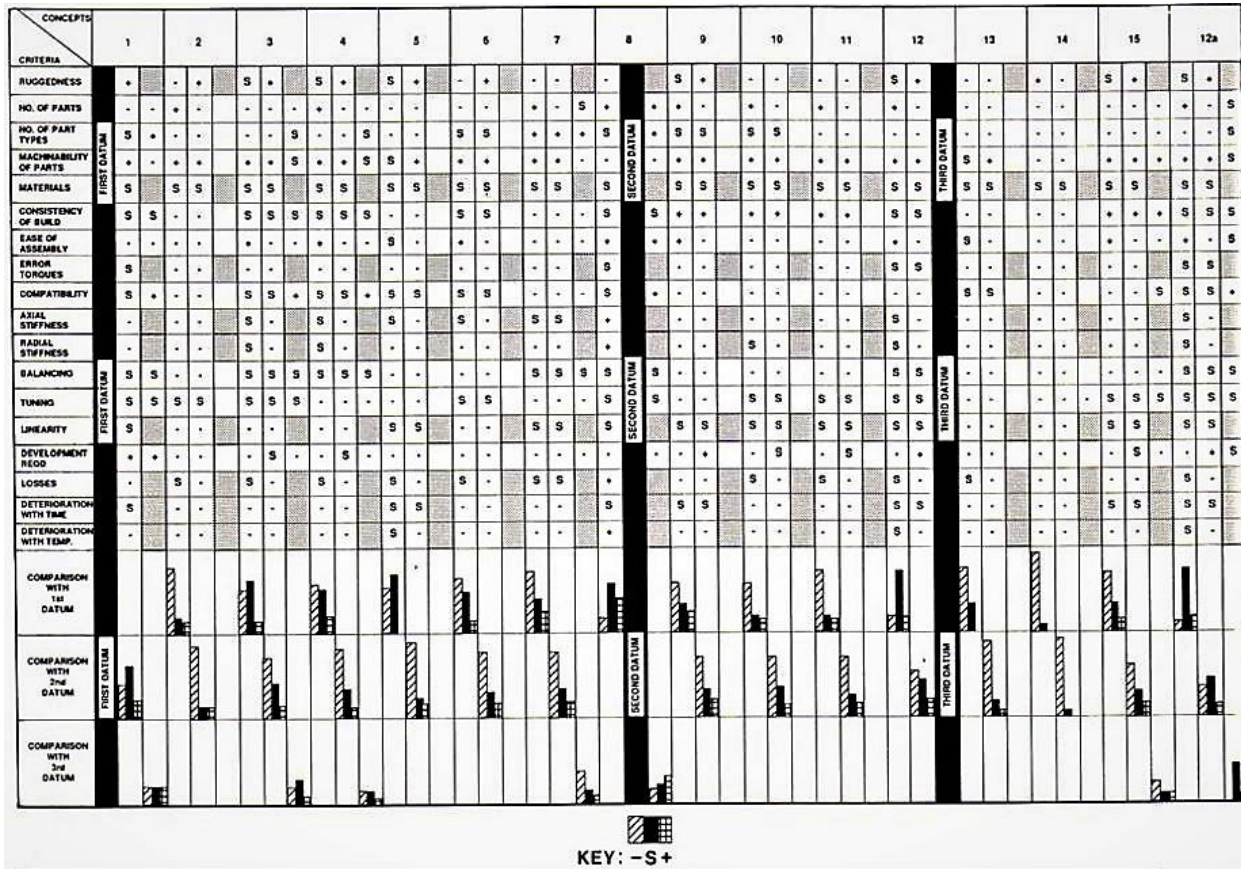


Figure 6: PuCC Matrix [10] [11]

### 2.1.3 QUALITY FUNCTION DEPLOYMENT

Quality Function Deployment (QFD) is a product and process development tool that guides product managers by transforming the voice of the customer into manufacturing operations through conceptualization, creation and realization of new products. It draws upon the expertise of domain experts to integrate the customer requirements into products, parts, processes and quality [12].

QFD primarily being a “people” approach, helps companies whose focus is either too “internal” or too “external” to develop a balanced product development process. “Internal” companies tend to focus more on the product without comprehending the requirements of the end user. “External” companies on the other hand tend to focus too much on the customer without consideration for the product. QFD helps companies make trade-offs resulting in shorter product development cycles.

Companies can leverage QFD to:

- 1) Develop knowledge about customer requirements
- 2) Competitive Analysis about competitor’s products
- 3) Develop priorities and directions of improvement
- 4) Relationship between customer requirements and design parameters
- 5) Study interdependencies between technologies and facilitate design trade-offs

The QFD process is divided into four phases as listed below (and shown in Figure 7):

- 1) Product Planning
- 2) Product Design
- 3) Process Planning
- 4) Process Control

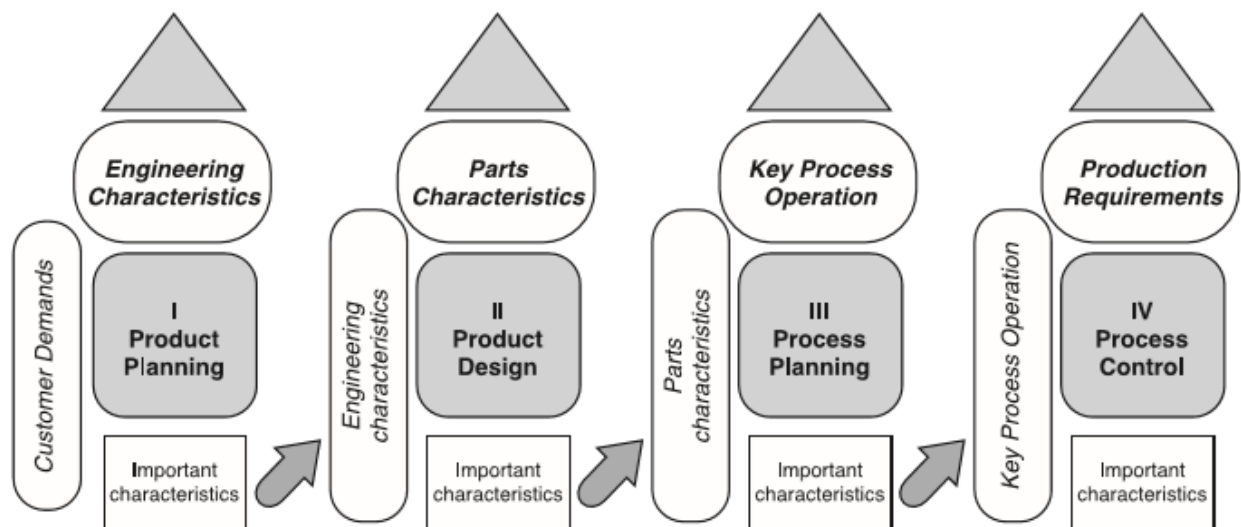


Figure 7: Four Phases of QFD [13]

#### *2.1.3.1 Product Planning: House of Quality*

Phase I of the QFD process involves building the House of Quality (HOQ) led by the marketing and sales department which establishes the relationship between the customer requirements and performance characteristics.

#### *2.1.3.2 Product Design*

The Product Design phase captures the relationship between performance characteristics and product specifications. Typically sphere headed by the engineering department, phase II of the QFD process evaluates various concept designs against the performance measures established in Phase I.

#### *2.1.3.3 Process Planning*

Process Planning relates the Product Specifications to Process Specifications. Manufacturing processes are established and critical process flows are determined. Critical process parameters are ascertained and equipment requirements are documented.

#### *2.1.3.4 Process Control*

The process control step is led by Manufacturing Engineering and Quality Assurance disciplines to determine critical process characteristics, establish process control methods and parameters. Risk assessment and control activities are undertaken to prevent failure. Inspection and test methods are finalized.

#### *2.1.3.5 House of Quality*

Phase I of the QFD process involves building the House of Quality (HOQ). The “House of Quality” (HOQ) is part of the QFD process which facilitates conceptual design of products through integration of the customer requirements and engineering parameters. In the absence of specific customer requirements (e.g. RFP, RFQ, TR), the requirements are obtained through extensive market research. Engineering

parameters are selected such that they can be easily measured and are typically independent of each other.

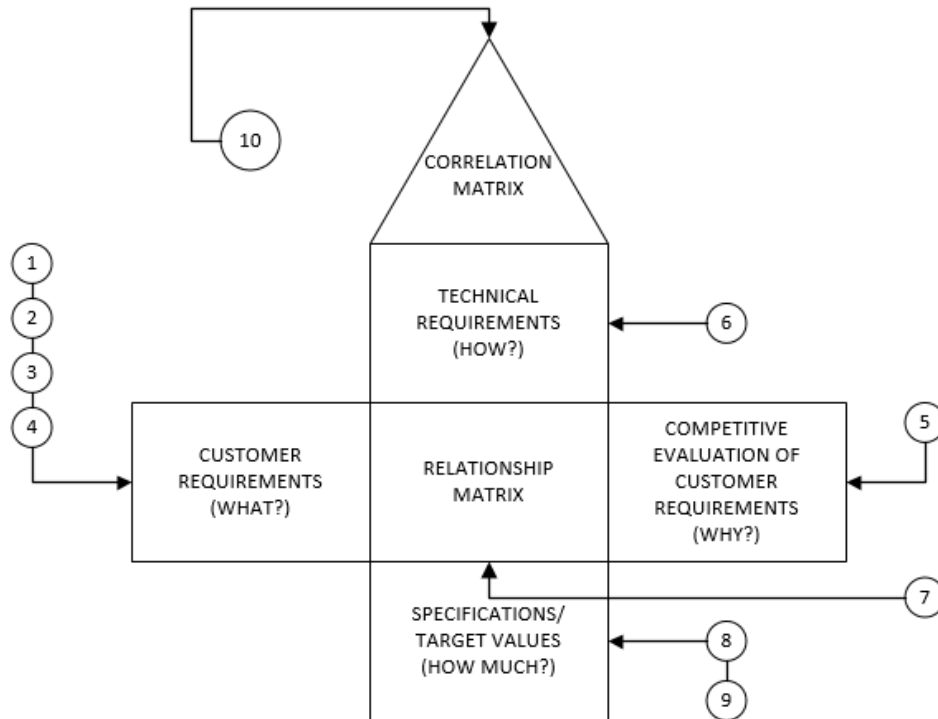


Figure 8: House of Quality Model [12]

INTERACTIONS:										RELATIONSHIPS:		
XX Strong negative relationship x Mild negative relationship ⊙ Mild positive relationship ○ Strong positive relationship												
										⊙ Strong relationship ○ Moderate relationship ▲ Weak relationship		
Product Design Reqs  Customer Reqs.		Priority	Competitive Evaluation									
			Bleed air ducting to interface p/c	Low AP U weight	Low turbine wheel weight	High equivalent shaft horsepower	Controlled turbine inlet temperature	Turbine assy. to hub containment	strong internal ring	Lightweight containment ring	1	5
Cust. envelope/interface		3	⊙						⊙		x	○
Max. Weight 160 lbs.		4	○	⊙	○				○	⊙	○	x
Bleed air 75 lbs/min		4	○			⊙					○	x
Turbine containment		5			○			○	⊙	⊙	⊙	
Elect pwr. 40 KVA		3				⊙					x	○
Reliable		5			○		⊙	○			○	x
Support oil-cooled gen.		5		○							○	x
...												
Technical Evaluation		5	x	○	x	x	○	x	○	x	○	
Target Value		Targ. Loc.	158lb	<6 lb	350hp	1850°	2.5 lb @ Pwr	3 lb @ Pwr			<6 lb	
Technical Difficulty			1	4	3	5	3	4	2	4		
Importance Rating			39	35	42	35	60	52	40	20		
EVALUATIONS: x We ○ XYZ Co.												

## 2.2 DETAILED PRODUCT OPTIMIZATION METHODS

### 2.2.1 CLASSICAL METHODS

Numerous studies have been undertaken to obtain optimized solutions with respect to single variable objective functions. Variables such as cost, weight and time feature amongst the most prominent parameters for optimization. In single variable optimization problems, the best design is achieved by taking the global minima or maxima of the objective function.

However, most problems that we encounter involve simultaneous optimization of multiple objectives. Therefore, most classical algorithms (such as weighted sum,  $\epsilon$ -constraint and the value function method) convert the multi objective problem to a single objective problem. For such problems, selecting the global minima or maxima of the objective function with respect to a single variable might not result in the best solution when considering all the other variables. These multi-objective problems require pareto-optimal solutions, which are a set of solutions that result in the best outcome when all variables are considered but the solutions are inferior when only one or some variables are considered. Although, there can be numerous pareto-optimal solutions, settling on a single solution is difficult. The suitability of one solution over another depends on a number of factors including human judgement and bias. Furthermore, there are often discontinuities or noise in some of the objectives; in such cases classical methods might not yield the best solution. In light of these problems, classical methods have given away to Genetic Algorithms (GA) such as Vector Evaluated Genetic Algorithm (VEGA) and Nondominated Sorting Genetic Algorithm (NSGA).



### 2.2.2 VECTOR EVALUATED GENETIC ALGORITHM (VEGA)

Vector Evaluated Genetic Algorithm (VEGA) is a multimodal Evolutionary Algorithm (EA) proposed by Schaffer [15] to evaluate an objective vector where each element of the vector represents a unique objective function. VEGA divides the population “N” for every generation into “M” equal sub-populations of  $N/M$ , where “M” is the number of objective functions. The sub-populations are then shuffled; crossover and mutation are performed in conjunction with fitness proportion selection [16] [17].

VEGA is easy to implement, requires only minor modifications to an existing Genetic Algorithm (GA) with no significant investment in computational resources. Although VEGA was intended to find pareto-optimal solutions of multiple non-linear objective functions, there seems to be a certain level of bias towards a particular set of solutions corresponding to the best individual solutions of each objective. Although Schaffer theorized that a crossover term would diversify the solutions thereby reducing the bias, solutions from VEGA are not diverse enough making them suitable only for specific problems [18].

### 2.2.3 NONDOMINATED SORTING GENETIC ALGORITHM (NSGA)

Nondominated Sorting Genetic Algorithm (NSGA) developed by Srinivas and Deb [19] is a multi-objective evolutionary algorithm (MOEA) designed to find multiple pareto-optimal solutions in one single run. In NSGA, the fitness assignment is carried out in several steps where in each step the nondominated solutions comprising of a nondominated front are assigned an identical but dummy fitness value. These solutions are shared with their dummy fitness values and ignored in the further classification process. Finally, the dummy fitness is set to a value less than the smallest shared fitness value in the current nondominated front from which the next front is extracted. This procedure is repeated until all individuals in the population are classified and assigned the same mock fitness value [16] [17].

Although, NSGA has been applied to many multi-objective problems, the requirement of high computational resources (especially for large population sizes) limits its widespread use. Furthermore, unlike other GAs, NSGA does not provide any consideration to elitism thereby limiting performance while not considering some potentially viable solutions. In traditional Gas, the presence of a sharing parameter ensures that there is diversity amongst the solutions; lack of which potentially reduces the solution diversity in NSGA [20].

The following figures illustrate examples of computer aided optimization of shapes using commercial packages and algorithms (similar to the methods described above).

Figure 10 illustrates a model of a support beam used in aircraft developed by MBB GmbH [21]. The beam is a machined structured manufactured from metallic materials with three equal sized and spaced lightening holes.

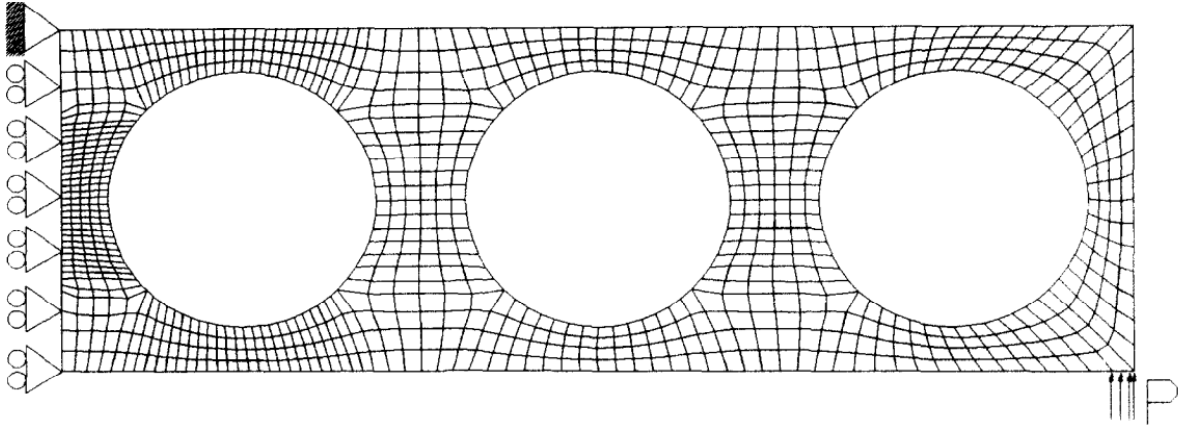


Figure 10: Initial Model before optimization [21]

Figure 11 shows the beam topology after optimization has been carried out for minimum weight. Although the overall size of the beam has remained the same, the cut-outs have undergone drastic transformation. Fabricating such a part will be both time consuming and costly because of the complex shapes involved. Additionally, the endurance of the part will be lower due to presence of stress concentration zones at the edges of the cut-outs undergoing a sudden change in area.

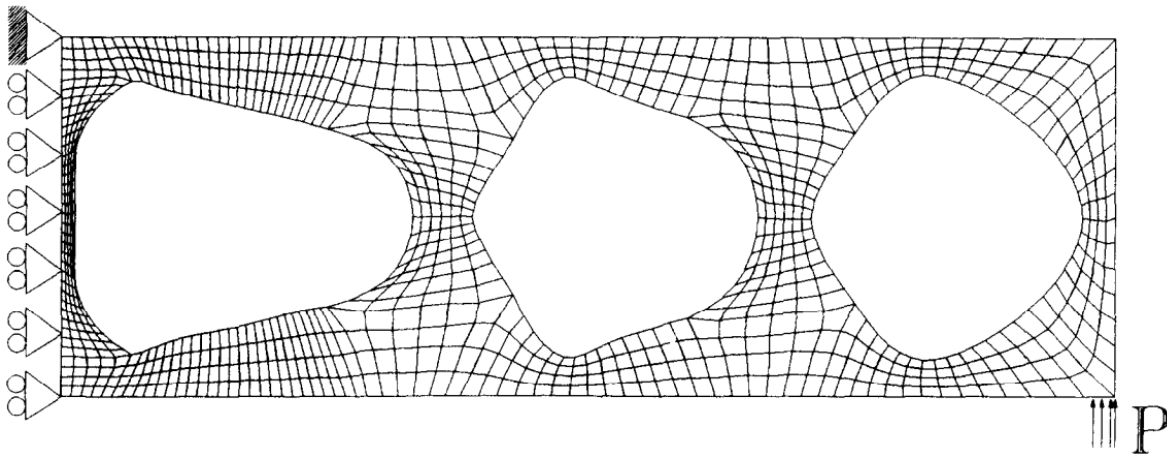


Figure 11: Final Model after optimization [21]

Figure 12 illustrates another example of a bracket designed for aerospace applications that has undergone optimization for weight reduction. Similar to Figure 11, the optimized bracket has a reduced weight, however it is not practical for EIS and continued operations.

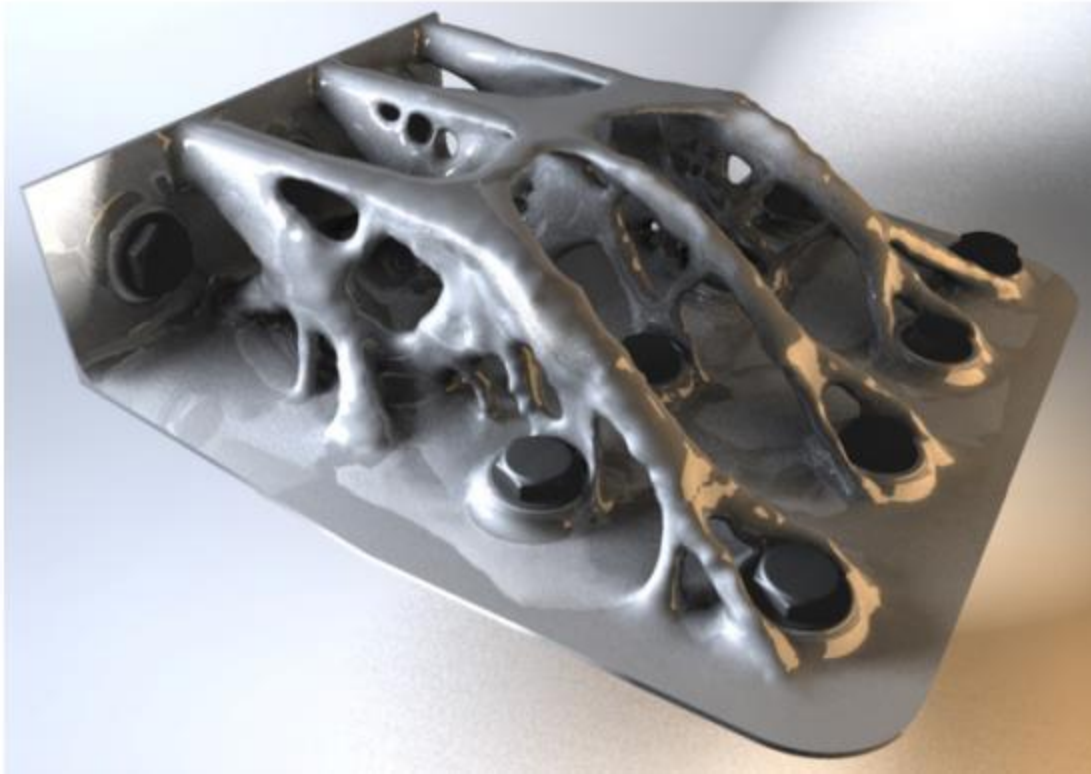


Figure 12: An optimized bracket [22]

Several conceptual product development approaches and detailed product optimization methods have been described in this chapter. Several of the conceptual product development models described, have been applied successfully in practical applications resulting in significant increase in operational efficiency. As for the detailed product optimization methods, real life applications have been mostly limited to experimental applications and secondary non-load carrying structures. A practical, time-sensitive methodology for designing manufacturable structures involving both conceptual and detailed design philosophies is proposed in the next chapter.

### 3 METHODOLOGY

This chapter presents the parametric, concurrent methodology used for manufacturing of metallic and composite structures. The methodology presented in this chapter will enable rapid selection of a conceptual design from a set of feasible designs based on a set of top level functional requirements. The selected concept would then be optimized to the functional requirements with design and manufacturing parameters acting as variables.

Although, several methods exist for design selection and optimization, there exists a disconnect between the conceptual design selection process and the detailed design optimization process for manufacturing. The concurrent development methodology presented will not only improve communication between all stakeholders of the product but also ensure a smoother EIS and better support for continued operations.

The methodology presented can be divided into two distinct parts:

1. Part I: Parameter Space Generation
2. Part II: Parameter Space Integration

Part I: Parameter Space Generation deals with the conceptual design phase of the project. In this phase, various design concepts are explored against a predetermined set of functional requirements and the most promising concept is chosen for detailed design.

Part II: Parameter Space Integration involves detailing the conceptual design selected in part I and carrying out design optimization based on an expanded set of functional requirements and variable parameters for design and manufacturing respectively.

The goal is to achieve a “first time right” product, where design deficiency prevention is more advantageous and cost effective than addressing design deficiencies and non-conformance reports (NCRs)

### 3.1 PART I: PARAMETER SPACE GENERATION

The following steps are involved in Parameter Space Generation:

#### **Step 1: Identify broad functional requirements that are most critical to the product**

These functional requirements are typically derived from the Technical Requirement Documents (TRD) and are traditionally non-negotiable; they are of absolute necessity for EIS. Examples of critical functional requirements include minimum load carrying capability, endurance limits, cost and maximum mass.

#### **Step 2: Rank functional requirements based on importance**

This is one of the most crucial steps in the conceptual design selection process, as the output of this step determines the overall product development strategy. The ranking of the functional requirements should ideally involve all stakeholders of the product; the developers, users, maintenance technicians etc. An alternative approach would be to use the results from an extensive survey of stakeholders familiar with a similar product category. No two functional requirements should have the same ranking. If the stakeholders are unable to come to agreement regarding the ranking of the functional requirements, they may re-visit the product objectives from the perspective of the end user. For example, for an interceptor (aircraft type) performance parameters such as speed and thrust to weight ratio are of the primary concern; therefore functional requirements related to thrust and weight will be ranked higher than cost. Alternatively, for a commuter jet, functional requirements relating to cost, time and reliability may be paramount.

#### **Step 3: Create conceptual designs of the product**

During this step, the design team should come up with several designs often with differing design philosophies and principles of operation. Each of the designs may vary in shape, size and materials among numerous other parameters. In safety critical products, often there are multiple independent design teams trying to solve the identical problem using dissimilar methods. This minimizes the occurrences of total system failure by eliminating common failure modes.

#### Step 4: Evaluate each conceptual design against the ranked functional requirements

A design selection matrix as shown in Table 2, is used to rank each conceptual design for each of the functional requirements determined in step 1. Each conceptual design is evaluated for each of the functional requirements, and how well each design fulfills the specifications documented in the TRD. The scale typically comprises of four symbols ( $\odot$ ,  $\circ$ ,  $\Delta$ ,  $-$ ) signifying a score of 3 (best option), 2 (mediocre option), 1 (least likely option) and 0 (does not meet the requirement). The total score used for selecting the winning conceptual design is determined by multiplying the ranking number with the respective score for each functional requirement and adding the results for each design concept.

Table 2: Conceptual Design Selection Matrix

FR \ Designs	Ranking	Design Concept 1	Design Concept 2	Design Concept 3
FR <sub>1</sub>	5	$\odot$	$\circ$	$\Delta$
FR <sub>2</sub>	4	$\odot$	$\circ$	$\odot$
FR <sub>3</sub>	3	$\Delta$	$\circ$	$\odot$
FR <sub>4</sub>	2	$\odot$	$\odot$	$\odot$
FR <sub>5</sub>	1	$\odot$	$\odot$	$\odot$
Score	---	39	33	35

#### Step 5: The conceptual design with the highest score is selected for detailed design

In the above example, Design Concept 1 is selected for detailed design.

### 3.2 PART II: PARAMETER SPACE INTEGRATION

By the end of Part I, a conceptual design that best caters to the TRD is been selected. Part II of the methodology concerns with detailed design and design optimization.

#### **Step 1: Determine the functional requirements for design**

The functional requirements for design are the parameters that can be measured to test the efficacy of the design over the course of the development process. The selection of the functional requirements for design is performed within the integrated product development team (IPDT) with the TRD as reference. Typical functional requirements for design include Weight, Deflection, Stress/ Strain and Endurance Limit.

#### **Step 2: Determine the variable design parameters**

The design parameters comprise of the variables that can be altered/ changed to affect the functional requirements. Typical design parameters include material strength, material stiffness, load and shape.

#### **Step 3: Develop a relationship matrix between the functional requirements for design and variable design parameters**

$$[FR_D] = [RM_D] * [DP_D] \quad \text{Equation 1}$$

where,

$[FR_D]$  is the functional requirement matrix for design and can be represented as

$$[FR_D] = \begin{bmatrix} FR_1 \\ FR_2 \\ \vdots \\ FR_n \end{bmatrix}_D \quad \text{Equation 2}$$

$[RM_D]$  is the relationship matrix for design and can be represented as

$$[RM_D] = \begin{bmatrix} RM_{D11} & RM_{D12} & \cdots & RM_{D1m} \\ RM_{D21} & RM_{D22} & \cdots & RM_{D2m} \\ \vdots & \vdots & \ddots & \vdots \\ RM_{Dn1} & RM_{Dn2} & \cdots & RM_{Dnm} \end{bmatrix}_D \quad \text{Equation 3}$$



$[DP_D]$  is the design parameter matrix and can be represented as

$$[DP_D] = \begin{bmatrix} DP_1 \\ DP_2 \\ \vdots \\ DP_n \end{bmatrix}_D \quad \text{Equation 4}$$

The relationship matrix assigns a score based on the impact of each variable parameter on the functional requirement. The scoring is based on the following methodology:

- 1) If  $[DP_n] \propto C[FR_n]$  and  $|C| > 1$  then  $[RM_{Dnm}]$  is assigned a score of 9.
- 2) If  $[DP_n] \propto C[FR_n]$  and  $|C| = 1$  then  $[RM_{Dnm}]$  is assigned a score of 3.
- 3) If  $[DP_n] \propto C[FR_n]$  and  $|C| < 1$  then  $[RM_{Dnm}]$  is assigned a score of 1.
- 4) If  $[DP_n]$  is not proportional  $C[FR_n]$  then  $[RM_{Dnm}]$  is assigned a score of 0.
- 5) If the value of  $C$  cannot be determined (without extensive analysis or testing) then a score of 1 is assigned.

The scoring methodology is illustrated using the following example. Consider three design parameters ( $DP_{n1}$ ,  $DP_{n2}$  and  $DP_{n3}$ ) as shown in Figure 13. From engineering trade studies, analyses, simulation and judgement, the impact of each design parameter  $[DP]_n$  on each functional requirement  $[FR]_n$  is determined. It can be seen that as parameter  $DP_{n1}$  is increased, the impact on the  $[FR]_n$  increases exponentially; therefore following the scoring methodology described,  $C$  is determined to be greater than 1 and a score of 9 is entered in the relationship matrix. Similarly, as parameter  $DP_{n2}$  is increased, the functional requirement increases linearly; therefore  $C$  is determined to be equal to 1 and a score of 3 is entered in the relationship matrix. For parameter  $DP_{n3}$ , the impact on the function requirement is positive but is a lot less significant than that of parameter  $DP_{n2}$  (which was linear); therefore  $C$  is determined to be less than 1 and a score of 1 is entered in the relationship matrix.

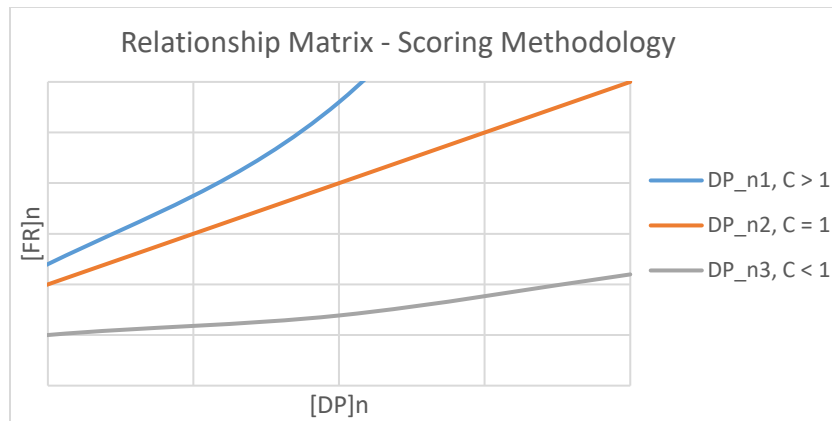


Figure 13: Relationship Matrix – Scoring Methodology

**Step 4: Develop the detailed design considering design parameters**

At this stage, the conceptual design selected in Phase I is detailed considering the design parameters, such that the functional requirements are either minimized or maximized. Several design solutions may be viable, some of which are the pareto-optimal solutions.

**Step 5: Determine the functional requirements for manufacturing**

Similar to the functional requirements for design, the functional requirements for manufacturing capture the parameters that can be measured to test the efficacy of the manufacturing process. Typical functional requirements for manufacturing include cost, lead time etc.

**Step 6: Determine the variable manufacturing parameters**

The manufacturing parameters comprise of all the variables that affect the functional requirements for manufacturing. The manufacturing parameters need not be mutually exclusive of the design parameters and can comprise of material hardness, machinability, curing time, processes etc.

**Step 7: Develop a relationship matrix between the manufacturing functional requirements and variable manufacturing parameters**

$$[FR_M] = [RM_M] * [DP_M] \quad \text{Equation 5}$$

where,

$[FR_M]$  is the functional requirement matrix for manufacturing and can be represented as

$$[FR_M] = \begin{bmatrix} FR_1 \\ FR_2 \\ \vdots \\ FR_n \end{bmatrix}_M$$

$[RM_M]$  is the relationship matrix for manufacturing and can be represented as

$$[RM_M] = \begin{bmatrix} RM_{M11} & RM_{M12} & \cdots & RM_{M1m} \\ RM_{M21} & RM_{M22} & \cdots & RM_{M2m} \\ \vdots & \vdots & \ddots & \vdots \\ RM_{Mn1} & RM_{Mn2} & \cdots & RM_{Mnm} \end{bmatrix}_D \quad \text{Equation 6}$$

$[DP_M]$  is the manufacturing parameter matrix and can be represented as

$$[DP_M] = \begin{bmatrix} DP_1 \\ DP_2 \\ \vdots \\ DP_n \end{bmatrix}_M \quad \text{Equation 7}$$

#### Step 8: Develop the detailed design considering manufacturing parameters

Once the manufacturing parameters are obtained, the design created in step 4 is modified further to maximize or minimize the functional requirements for both design and manufacturing. The number of viable solutions is reduced further to obtain pareto-optimal solutions that fulfill both the design and manufacturing requirements. The objective of developing the design and manufacturing relationship matrices is to identify the parameters which have the most significant impact on the functional requirements. The final design can then be represented by Equation 8 as follows:

$$[FR_C] = [RM_C] * [DP_C] \quad \text{Equation 8}$$

where,

$[FR_C]$  is the combined set of functional requirements represented as

$$[FR_C] = \{[FR_D]_n, [FR_M]_m\} = \begin{Bmatrix} [FR_D]_1 \\ \vdots \\ [FR_D]_n \\ [FR_M]_1 \\ \vdots \\ [FR_M]_m \end{Bmatrix} \quad \text{Equation 9}$$

$[DP_C]$  is the combined set of design and manufacturing parameters represented as

$$[DP_C] = \{[DP_D]_j, [DP_M]_k\} = \begin{Bmatrix} [DP_D]_1 \\ \vdots \\ [DP_D]_j \\ [DP_M]_1 \\ \vdots \\ [DP_M]_k \end{Bmatrix} \quad \text{Equation 10}$$

$[RM_C]$  is the combined relationship matrix for design and manufacturing

The combined functional requirements is obtained by combining the functional requirements for design and manufacturing. The combined set of functional requirements may be reduced by rationalizing the requirements in order of importance and selecting a subset comprising of the top requirements. Similarly, the design parameters may be rationalized based on the individual relationship matrix identified earlier in step 3 and step 7.

**Step 9: Once the impact of each of the parameters on the functional requirements are identified, the design may be optimized as per follows:**

$$\lim 1 < \frac{\partial [FR_C]}{\partial [DP_C]_i} < \lim 2 \quad \text{Equation 11}$$

where, the limits are set based on design, manufacturing, processing and other operational challenges and are often determined by standard guidelines e.g. if stress is the functional requirement, the lower limit is set to zero while the upper limit is set to the material yield strength.

**Step 10: The most optimized design can then be evaluated as follows:**

$$[A] \cap [B] \quad \text{Equation 12}$$

where

$[A]$  is the set of functional requirements for which a maximum value is desired

$[B]$  is the set of functional requirements for which a minimum value is desired

However, in reality it is very difficult to obtain an optimized solution for all the functional requirements. Algorithms are often employed to provide pareto-optimal solutions; however use of algorithms is not always possible for developing practical structures. Therefore a cut-off is established when all functional requirements are reasonably met and further optimization would result in diminishing returns.

### 3.3 LIMITATIONS OF THE METHOD

Although, the methodology described in the previous sections is fast and practical for developing complex structures, the following limitations should be considered:

**1) An implicit assumption of this methodology is that there is a certain level of domain knowledge on the structure that is being developed**

In the present form, the use of the above described methodology is limited to structures whose functions are well defined and fabrication processes are mature. Use of the methodology to design novel structures with new fabrication techniques might not yield the best design solution as the functional requirements to measure and variable parameters to modify might not be readily available, risking product development targets. Similarly, the cut-off point for design optimization is largely user dependant as the user decides the point of diminishing returns; hence, the optimization process can either drag on wasting valuable resources or finish too early resulting in a less optimized product.

**2) Limited number of variables can be modified**

Since there is significant human involvement in selecting the functional requirements to measure, the weights to assign, determine the scoring for the relationship matrix, the design can only be optimized for a limited number of parameters in a reasonable time frame with limited resources.

**3) The functional requirements must be defined such that the impact of changing the variable parameters can be clearly measured**

In cases where the relationship between functional requirements and variable parameters cannot be clearly established, the optimization methodology breaks down as the scoring is based on a relative criteria between the parameters and the requirements.

Figure 14 illustrates the standard product development approach, where each of the product development steps are sequential. Any design deficiencies that are identified in the manufacturing and testing phase requires the product developer to loop back to the design phase and repeat the development cycle. Figure 15 on the other hand, illustrates the methodology presented where design and manufacturing parameters are considered before freezing the final design, thereby reducing the probability of design deficiencies and approach a “first time right” design.

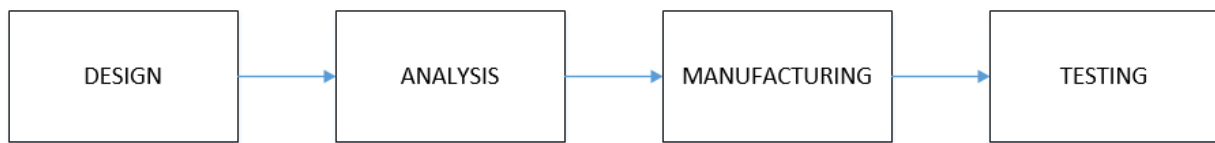


Figure 14: Standard Product Development Approach

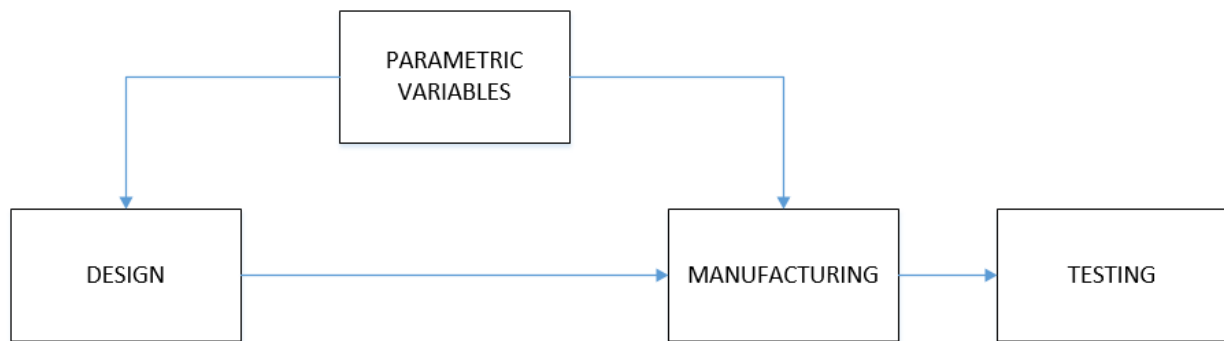


Figure 15:Proposed Product Development Approach

## 4 CASE STUDIES

This chapter documents the case studies that illustrate the product development methodology described in the previous chapter. The three case studies include:

1. Metallic Flight Control System Bracket
2. Composite Roll Frame
3. Composite Nose Landing Gear (NLG) Door

### 4.1 CASE STUDY 1: METALLIC FLIGHT CONTROL SYSTEM BRACKET

#### 4.1.1 DESIGN OBJECTIVE

The Flight Control Bracket is an indispensable component of the Aircraft Flight Control System and acts as an interface to transfer control inputs (forces) from one pushrod to a subsequent pushrod. This type of bracket is primarily used throughout the flight control system to change the direction and magnitude of the control forces.

The control bracket interfaces with the pushrod rod end by forming a double shear clevis joint. The control bracket is fastened directly or indirectly to the airframe structure.

The primary objective of the flight control bracket are listed as follows:

- 1) The bracket should be able to carry all operational loads without failure
- 2) The weight of the bracket shall be kept minimal with respect to the loads
- 3) The bracket shall be manufactured using commonly available aerospace grade materials
- 4) Since all flight control brackets in the flight control system are not identical, each bracket shall be designed for minimum cost
- 5) The lead time to manufacture the bracket shall be minimal

#### 4.1.2 PARAMETER SPACE GENERATION - CONCEPTUAL DESIGN SELECTION

The most critical functional requirements that will influence the final product are determined from the Technical Requirements Documents (TRD) as follows:

$$[FR] = \begin{bmatrix} \textit{Weight} \\ \textit{Cost} \\ \textit{Load} \\ \textit{Endurance} \\ \textit{Time} \end{bmatrix}$$

The functional requirements are ranked in order of importance to the customer. The ranking process is determined after extensive interaction among all stakeholders.

$$[FR] = \begin{bmatrix} \textit{Cost} \\ \textit{Time} \\ \textit{Weight} \\ \textit{Endurance} \\ \textit{Load} \end{bmatrix}$$

At this stage, several conceptual designs are generated. In this example, three distinct concepts have been explored:

- 1) A sheet metal bracket
- 2) A machined bracket
- 3) An additive manufactured bracket

Next, each concept is evaluated against the other concepts using the ranked functional criteria.

FR \ Designs	Ranking	Sheet Metal	Machined	Additive Manufactured
Cost	5	⊙	○	Δ
Time	4	⊙	Δ	⊙
Weight	3	○	○	⊙
Endurance	2	⊙	⊙	⊙
Load	1	⊙	⊙	⊙
Score		42	29	35



The conceptual design with the highest score is selected for detailed design.

The sheet metal bracket has the lowest cost and takes the least time to manufacture because of the simplicity of the processes involved. A machined bracket requires a trained CNC operator to program the cutting operations. Furthermore, complex machining operations are inherently more time consuming and require specialized tooling, making the entire operation prohibitive. Additive manufacturing techniques are not yet competitive on a cost per unit metric. Additive manufactured parts are used in high performance aerospace products where reducing weight and part count are of prime importance. From a static stress and endurance perspective, machined and sheet metal parts offer superior performance due to the familiarity, consistency and repeatability of the processes involved; however, all three designs are designed to sustain the static and fatigue loads. Therefore, the sheet metal bracket is selected for detailed design.

#### 4.1.3 PARAMETER SPACE INTEGRATION FOR DESIGN PARAMETERS

Phase II involves determining the functional requirements for design and manufacturing. The design and manufacturing parameters are identified, and a relationship matrix is used to establish the impact of each parameter on the final product. An optimization criteria of maximizing/ minimizing the functional requirements by modifying the parameters are used to arrive at the final design.

Figure 16, shows a partial schematic of the aircraft flight control system and the position of the control bracket.

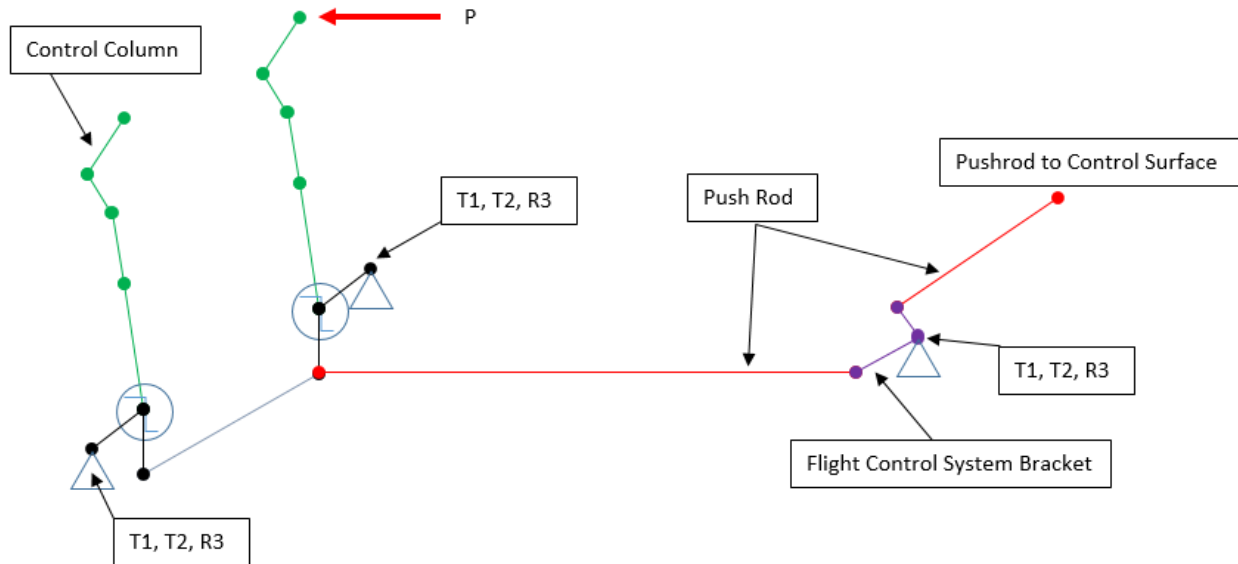


Figure 16: Partial schematic of the Flight Control System

The critical load case for the control bracket is determined to be the pilot input case. The maximum pilot input force for an aircraft with a Maximum Take-Off Weight (MTOW) of 5000 lbs is determined to be 167 lbs (ref. FAR 23.397 [23]) as shown in Figure 17. Furthermore, a factor of safety (F.S.) of 1.5 is applied to the limit load (ref. FAR 23.303 [23]).

$$P_{ult} = P_{lim} * F.S. \quad \text{Equation 13}$$

Therefore, the ultimate load that is applied on the control stick due to pilot input is 251 lbs.

Control	Maximum forces or torques for design weight, weight equal to or less than 5,000 pounds <sup>1</sup>	Minimum forces or torques <sup>2</sup>
Aileron:		
Stick	67 lbs	40 lbs.
Wheel <sup>3</sup>	50 D in.-lbs <sup>4</sup>	40 D in.-lbs. <sup>4</sup>
Elevator:		
Stick	167 lbs	100 lbs.
Wheel (symmetrical)	200 lbs	100 lbs.
Wheel (unsymmetrical) <sup>5</sup>		100 lbs.
Rudder	200 lbs	150 lbs.

Figure 17: Maximum and Minimum Control Forces and Torque [23]

Figure 18 shows an illustration of the forces acting on the Control Stick Assembly. The reaction (R) on the pushrod is calculated by balancing the moments about the hinge point according to the following equation:

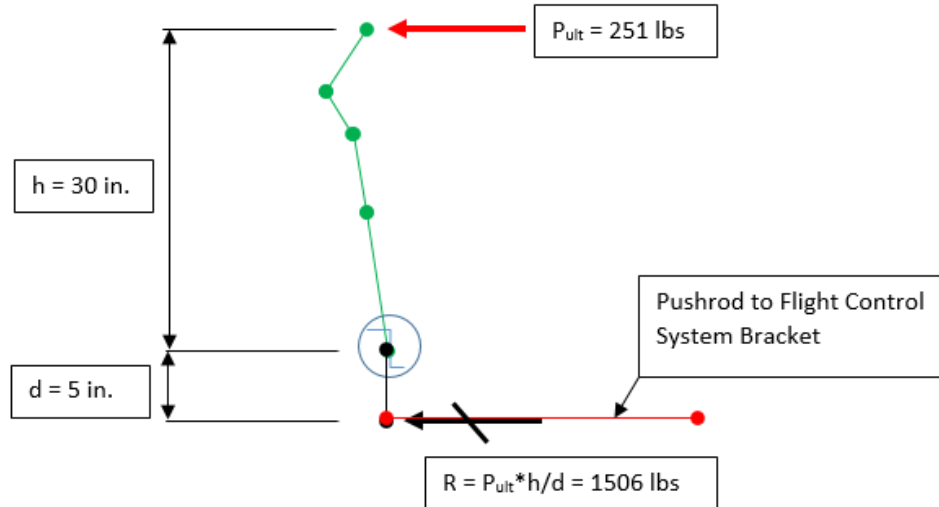


Figure 18: Load Diagram of the Control Stick assembly

$$\begin{aligned}
 \sum M &= 0 \\
 P_{ult} * h - R * d &= 0 \\
 R &= P_{ult} * \frac{h}{d}
 \end{aligned}
 \tag{Equation 14}$$

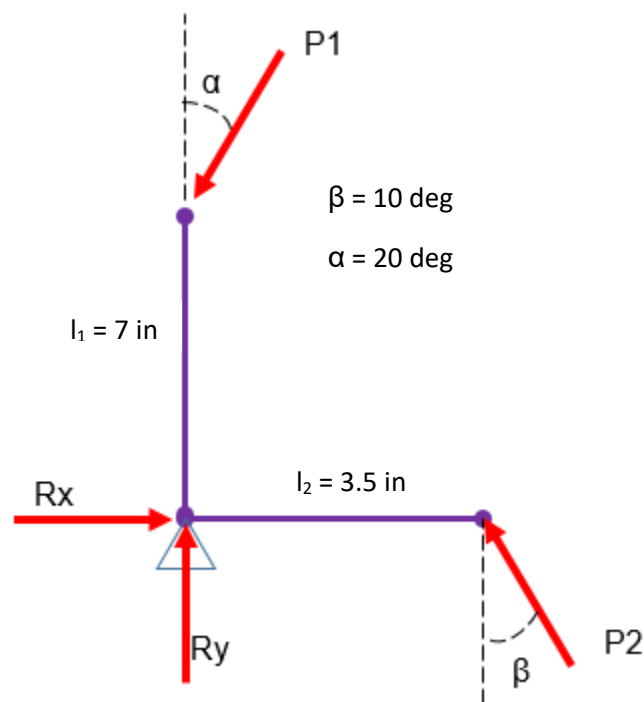
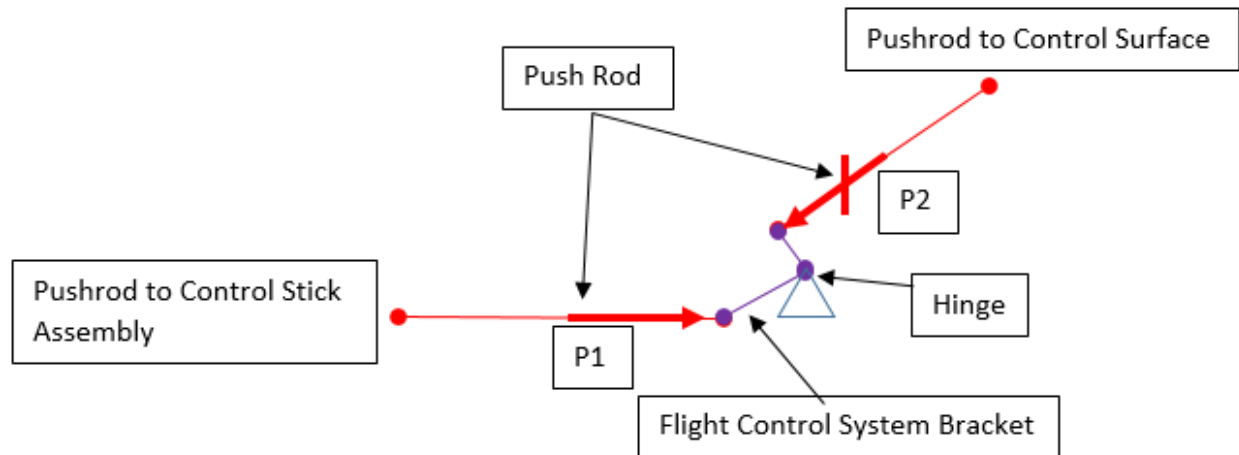


Figure 19: FBD of the Flight Control Bracket

Since,  $P_1 = R = 1506$  lbs,  $P_2$  can be determined by balancing the moments about the hinge point:

$$P_2 = P_1 * \frac{\sin \alpha * l_1}{\cos \beta * l_2} \quad \text{Equation 15}$$

$P_2 = 1046$  lb

For the Sheet Metal Bracket, the Functional Requirements and Parameters for Design are established as:

$$[FR_D] = [RM_D] * [DP_D]$$

where,

$$[FR_D] = \begin{bmatrix} Deflection \\ Stress \\ Endurance \\ Weight \end{bmatrix}_D$$

$$[DP_D] = \begin{bmatrix} Lug\ Radius \\ Bolt\ Diameter \\ Sheet\ Thickness \\ Material \\ Shape \end{bmatrix}_D$$

Influence of each of the design parameters are discussed and the relationship matrix for design is presented below.

#### 4.1.3.1 Material

Table 3 shows a comparative summary of material properties for traditional aluminum and steel sheets.

Aluminum (typically) has a higher strength to weight ratio than steel and almost comparable stiffness to weight ratio. Therefore aluminum 7075-T73 is chosen for initial design.

Table 3: Comparative Summary of Material Properties [24]

Property	4130 HT95	17-4PH H1150	7075-T73 (L)	6061-T62
FTU (ksi)	95	135	67	42
FTY (ksi)	75	105	55	33
FSU (ksi)	57	-	38	27
FBRU (ksi)	200	-	105	67
E (ksi)	29000	28500	10300	9900
el (in/in)	0.10	0.08	0.08	-
p (lb/in <sup>3</sup> )	0.283	0.284	0.101	0.098
$\sigma/\rho$	336	475	663	429
$E/\rho$	102473	100352	101980	101020

#### 4.1.3.2 Pin Diameter

The required pin diameter (assuming a standard steel bolt with FTU=160 ksi) is calculated from the following equations:

$$FTU = \frac{P * FF}{A_{net}} \quad \text{Equation 16}$$

where,

FTU      Ultimate material tensile strength  
FF      Fitting factor (FF = 1.15 from FAR 23.625)  
A<sub>net</sub>      Net cross section area of pin

$$A_{net} = \frac{\pi d^2}{4} \quad \text{Equation 17}$$

where,

d      Pin diameter

Therefore,

$$d = \sqrt{\frac{P * FF}{FTU * \frac{\pi}{4}}} \quad \text{Equation 18}$$

$$d = \sqrt{(1506 * 1.15) / (160000 * \pi * 0.25)}$$

$$d = 0.12 \text{ in. (assuming pin material FTU = 160 ksi)}$$

#### 4.1.3.3 Lug Radius

Lug analysis involves determining the lug loading from socket analysis and checking the lug for the following failure modes:

1. Shear Bearing Failure
2. Net-Section Tension Failure
3. Transverse Failure

As per industry guidelines, for aluminum lugs the ratio between the lug radius to pin diameter should be between 0.85 and 1.25 and is illustrated through the equation below:

$$0.85d \leq R \leq 1.25d \quad \text{Equation 19}$$

where,

R      Lug radius  
d      Pin diameter

Since the pin diameter was determined to be 0.12 in, the lug radius is  $0.12 * 1.25 = 0.15$  in.

#### 4.1.3.4 Sheet Thickness

The minimum required sheet thickness for adequate static margin can be determined using the following equation:

$$\sigma_{peak} = \frac{P * k_t}{A_{net}} \quad \text{Equation 20}$$

where,

$\sigma_{peak}$       Peak stress  
P      Applied load  
 $k_t$       Stress concentration factor ( $k_t = 3.0$  from Ref. [25]; flat plate with hole)  
 $A_{net}$       Net-cross-section area

$$A_{net} = w * t \quad \text{Equation 21}$$

where,

w      Section width  
t      Section thickness (material thickness)

The minimum sheet thickness required can be calculated through the following equations:

$$A_{net} = \frac{P * k_t}{FTU} \quad \text{Equation 22}$$

Since  $A_{net} = w * t$ , the equation can be rearranged as:

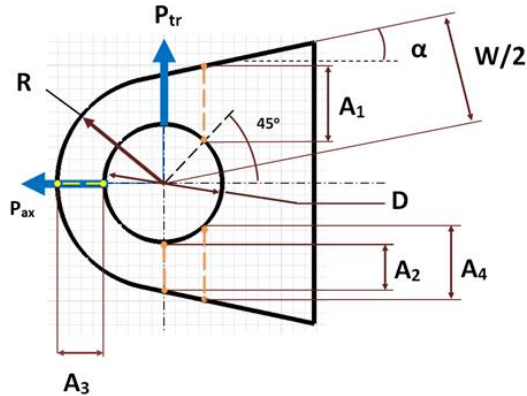
$$t = \frac{P * k_t}{FTU * w} \quad \text{Equation 23}$$

$$t = (1506 * 3 * 0.6) / (67000 * (0.3 - 0.12))$$

$$t = 0.225 \text{ in}$$

Note: Assume 60-40% load distribution on the clevis lugs.

Based on the above thickness, a bearing analysis is conducted. Bearing failure comprises of localized yielding of the lug bore diameter. A fitting factor of 1.15 is applied on the applied loads as per FAR 25.625 [23].

	SECTION: Clevis Joint MATERIAL: Rod End CASE: Jam Case	
<b>Applied Loads</b> $P_{br} = 1.506 \text{ kip}$		<b>Material Allowables</b> $FBR = 105 \text{ ksi}$
<b>Bearing Dimensions</b> $t = 0.225 \text{ in}$ $D = 0.120 \text{ in}$		
<b>Calculated Properties</b> $A_{net} = t * D = 0.027 \text{ in}^2$		<b>Bearing Factors</b> $F.F. = 1.15$
<b>Average Bearing Stress</b> $f_{br,avg} = \frac{FF * P_{br}}{A_{net}} = 64.144 \text{ ksi}$		<b>Margin of Safety</b> $MS_{ult} = \frac{FBR}{f_{br,avg}} - 1 = 0.64$

Since, the bearing margin is positive, the material thickness is adequate for design.

#### 4.1.3.5 Shape

The interface control points for the bracket to pushrod interface were finalized during the Flight Control System conceptual design phase. The exact size and shape of the bracket is variable within the constraints of the interface points.



The relationship matrix between the functional requirements for design and variable parameters is developed as illustrated in Table 4.

Table 4: Sheet Metal Bracket - Relationship Matrix - Design

	Lug Radius	Bolt Diameter	Sheet Thickness	Material	Shape
Deflection	0	0	3	0	1
Stress	1	1	3	0	1
Endurance	1	1	3	1	1
Weight	1	1	3	3	1

From the design relational matrix, it can be seen that sheet thickness and shape are the parameters that influence the design functional parameters the most, followed by lug radius, bolt diameter and material. Using the design parameters and relationship matrix, the base design was conceptualized having a “C” cross-section as shown in Figure 20.

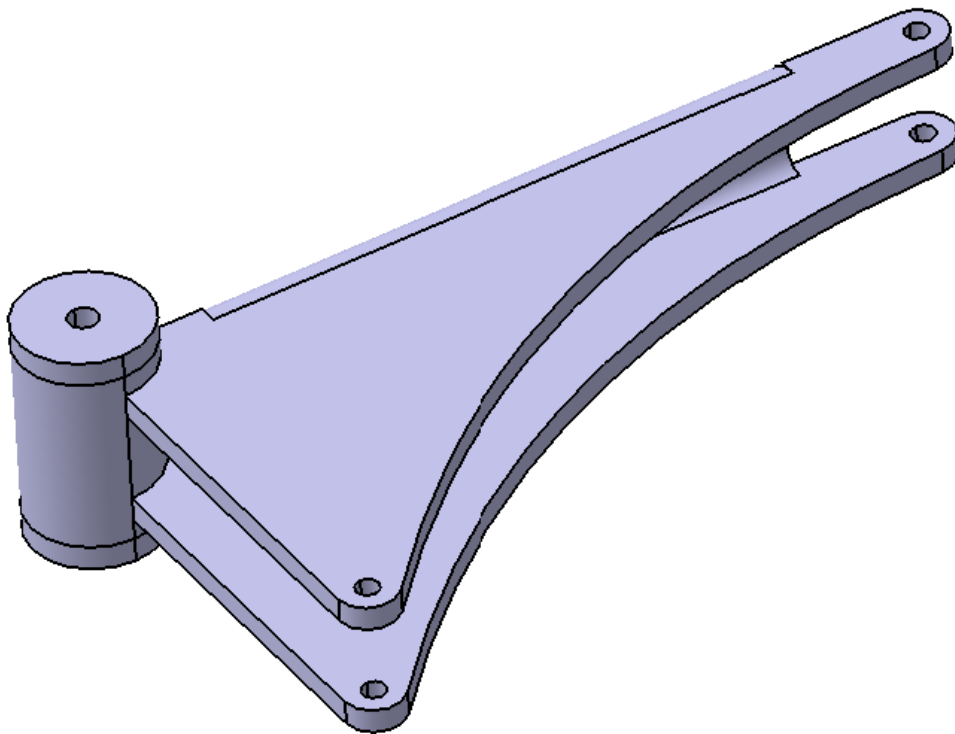


Figure 20: Sheet Metal Bracket –Base Design - Design Parameters

#### 4.1.4 PARAMETER SPACE INTEGRATION FOR MANUFACTURING PARAMETERS

For the Sheet Metal Bracket, the Functional Requirements and Parameters for manufacturing are established as:

$$[FR_M] = [RM_M] * [DP_M]$$

where,

$$[FR_M] = \begin{bmatrix} Cost \\ Time \\ Weight \end{bmatrix}_M$$

$$[DP_M] = \begin{bmatrix} Bolt Diameter \\ Sheet Thickness \\ Material \\ Shape \\ \#Manufacturing Operations \\ Processes \end{bmatrix}_M$$

Influence of each of the manufacturing parameters on the functional requirements are discussed below.

##### 4.1.4.1 Material

The material for the flight control bracket was changed from aluminum to steel to facilitate a weldable design. Most aluminum alloys are not readily weldable which presents fabrication challenges for this particular design. Furthermore, aluminum has vastly different properties depending on the grain direction eg: 7075-T651, thickness: 3.501-4.000 in, FTU = 66 ksi (L), 67 ksi (LT), 61 ksi (ST) [24].

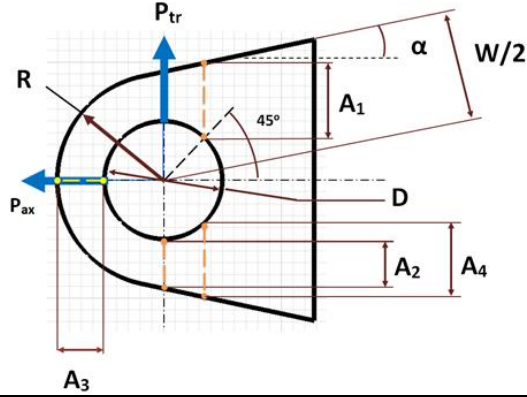
To simplify manufacturing controls and reduce costs, steel was used. Between the two steels shown in Table 3 (4130 and 17-4PH), 4130 has reasonable properties, is more widely available and is cheaper than 17-4PH.

#### 4.1.4.2 Sheet Thickness

The available sheet thicknesses for 4130 Steel are provided in the table below:

Material	Thickness (in)	Notes
4130 Steel	0.025	
	0.032	
	0.040	
	0.050	
	0.063	Commonly used
	0.071	
	0.080	
	0.090	
	0.100	
	0.125	Commonly used
	0.160	
	0.190	
	0.250	Commonly used

Since, steel is stronger and stiffer than aluminum, a sheet thickness of 0.125 in. (previously 0.225" thick aluminum sheet was selected) is selected for manufacturing the sheet metal bracket. Based on the above thickness, a bearing analysis is conducted below. Bearing failure comprises of localized yielding of the lug bore diameter. A fitting factor of 1.15 is applied on the applied loads as per FAR 25.625 [23].

	SECTION: Clevis Joint MATERIAL: Rod End CASE: Jam Case	
<b>Applied Loads</b> $P_{br} = 1.506 \text{ kip}$		<b>Material Allowables</b> $FBR = 200 \text{ ksi}$
<b>Bearing Dimensions</b> $t = 0.125 \text{ in}$ $D = 0.250 \text{ in}$		
<b>Calculated Properties</b> $A_{net} = t * D = 0.03125 \text{ in}^2$		<b>Bearing Factors</b> $F.F. = 1.15$
<b>Average Bearing Stress</b> $f_{br,avg} = \frac{FF * P_{br}}{A_{net}} = 55.421 \text{ ksi}$		<b>Margin of Safety</b> $MS_{ult} = \frac{FBR}{f_{br,avg}} - 1 = >2.000$

#### 4.1.4.3 Pin Diameter

The optimum pin diameter can be determined by evaluating the net pin cross section for the maximum shear and bending loads (obtained from a shear force – bending moment diagram). A representative cross-section of a clevis joint is illustrated in Figure 21.

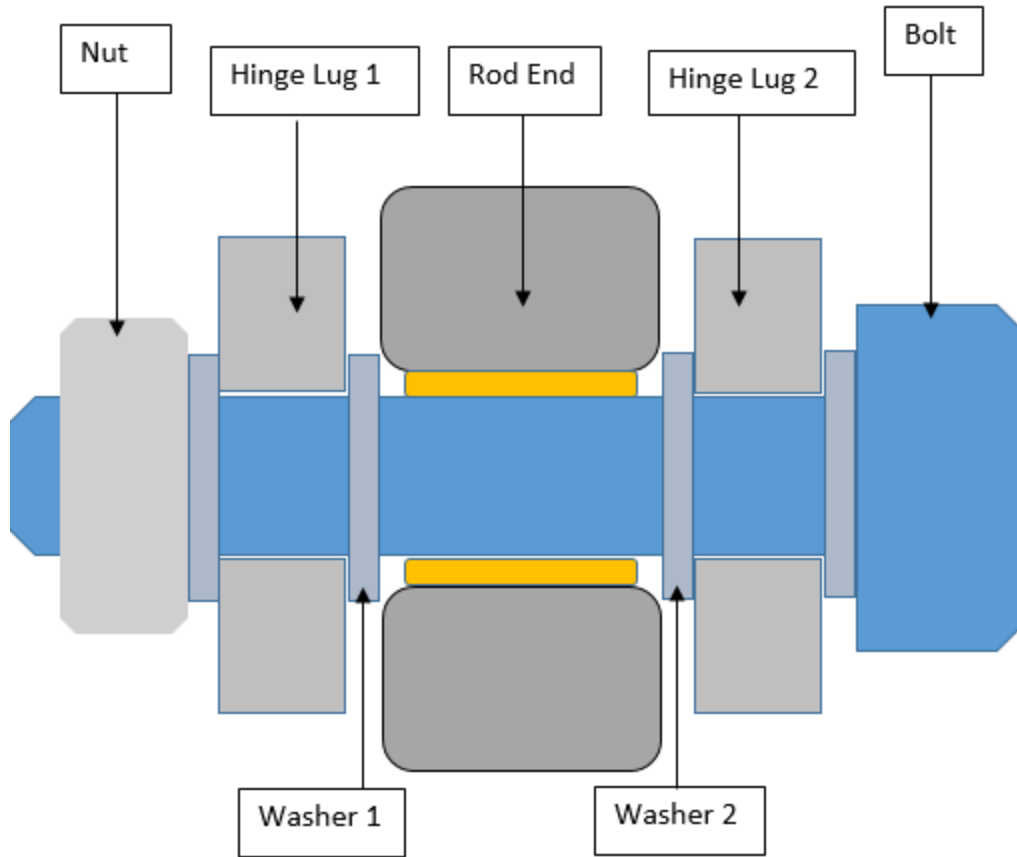


Figure 21: Representative Cross-Section of Clevis Joint

Rod End Width = 0.593 in (Ball Width, Ref. NHBB Catalogue [26])

Hinge Lug 1 Width = 0.125 in

Hinge Lug 2 Width = 0.125 in

Washer 1 Width = 0.064 in

Washer 2 Width = 0.064 in

The pin is assumed to be simply supported with the applied load acting in the middle of the socket. The shear force and bending moment distribution for the pin is illustrated in Figure 22. Based on the loading and support conditions, the maximum shear force and bending moment are determined to be 753 lb and 424 lb-in respectively.

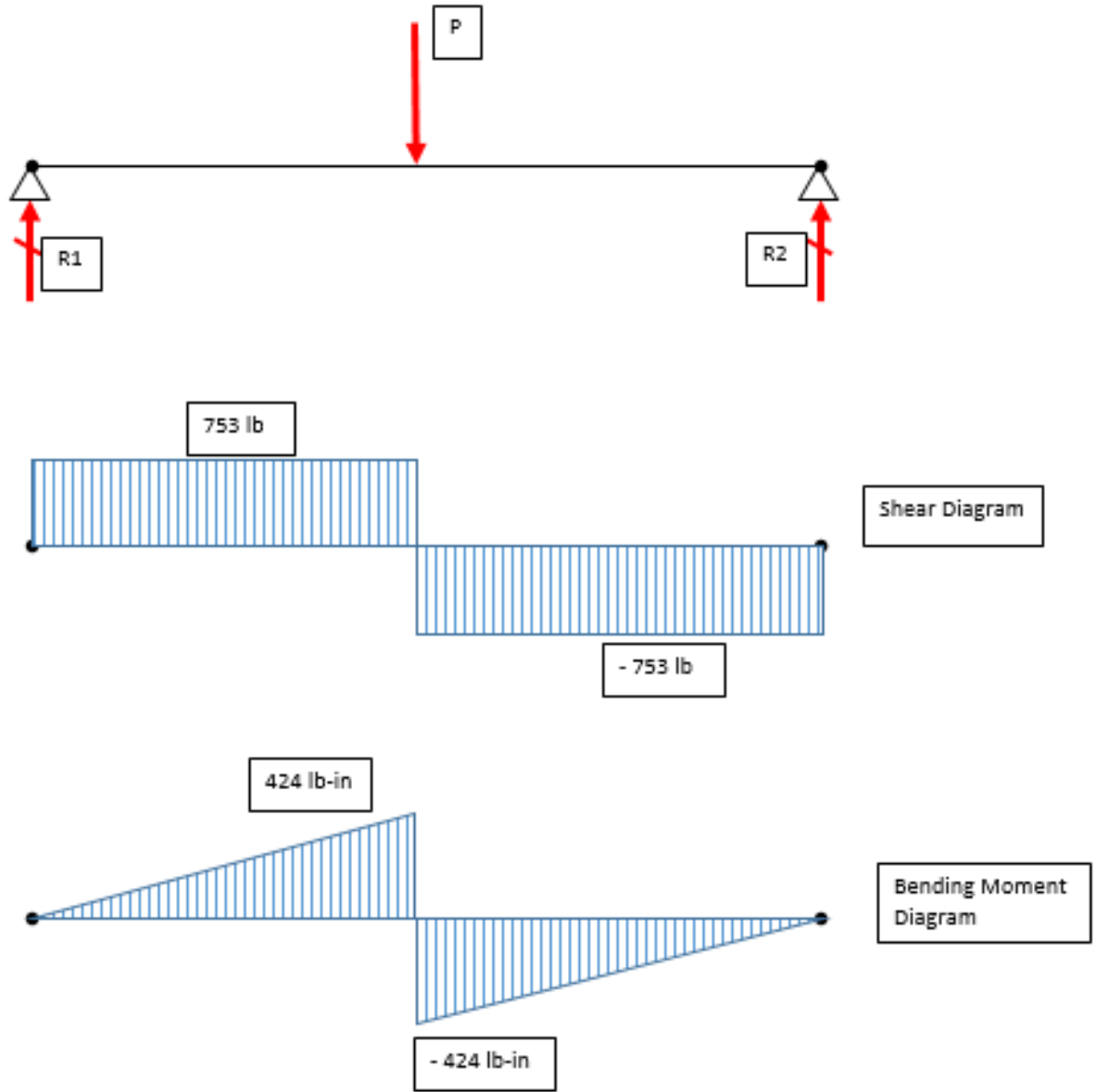


Figure 22: Pin Shear Force, Bending Moment Diagram

However, the maximum bending moment calculated from the shear force, bending moment diagram is overly conservative as the wide rod end provides support and prevents the pin from further bending. Equation 24 can be determined to provide a more realistic assessment of the maximum bending moment in the socket [27].

$$M_{max} = P_s * \left( \frac{t_{lug1}}{2} + g + \frac{t_{rodend}}{4} \right) \quad \text{Equation 24}$$

The section analysis of the pin is presented below. For conservatism, both max shear and max bending are assumed to occur at the same location.

**Part:** Bolt  
**Section:** A-A  
**Design Case:** Jam Case  
**Material:** Alloy Steel (FTU=160 ksi)

Tube, Version 1.1  
 MS Calculator  
 Tube, Version 1.1

#### Section Dimensions

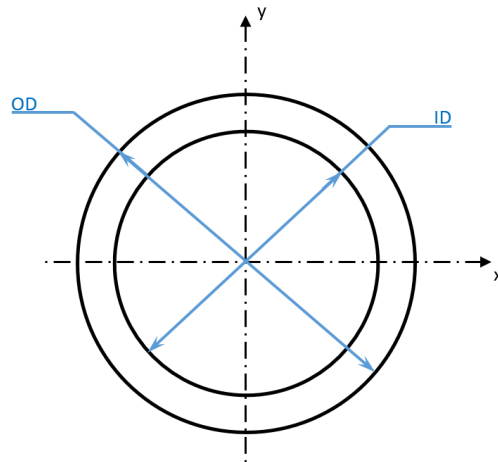
OD = 0.250 in  
 ID = 0.000 in

#### Internal Loads

Version:  
 Element :  
 Start Joint :  
 DX : in

#### Section Properties

OD/2 = 0.125 in  
 ID/2 = 0.000 in  
 t = 0.125 in  
 A = 0.049 in<sup>2</sup>  
 I<sub>yy</sub> = I<sub>xx</sub> = 0.000 in<sup>4</sup>  
 Z<sub>yy</sub> = Z<sub>xx</sub> = 0.002 in<sup>3</sup>  
 J<sub>zz</sub> = 0.000 in<sup>4</sup>  
 Q<sub>yy</sub> = Q<sub>xx</sub> = 0.001 in<sup>3</sup>  
 D/t = 2.000  
 K<sub>B</sub> = 1.698  
 K<sub>S</sub> = 1.333



#### Material Constants

E = 29000 ksi  
 e = 0.1

n = 9.8  
 μ = 0.32

#### Material Allowables

**Ultimate**  
 FTU = 160 ksi  
 FOU = 134.5 ksi  
 FBUX = 253.9 ksi  
 FBUY = 253.9 ksi  
 FSU = 96 ksi  
 FST = 96.0 ksi

**Yield**  
 FTY = 108 ksi  
 FCY = 108 ksi  
 FOY = 47.9 ksi  
 FBYX = 141.4 ksi  
 FBYY = 141.4 ksi  
 FSY = 64.8 ksi

**Part:** Bolt  
**Section:** A-A  
**Design Case:** Jam Case  
**Material:** Alloy Steel (FTU=160 ksi)

Tube, Version 1.1  
 MS Calculator  
 Tube, Version 1.1

#### Ultimate Applied Loads

Axial, P = 0.000 kip  
 Shear X, P<sub>Sx</sub> = 0.753 kip  
 Shear Y, P<sub>Sy</sub> = 0.000 kip  
 Bending X, M<sub>Bx</sub> = 0.000 kip\*in  
 Bending Y, M<sub>By</sub> = 0.218 kip\*in  
 Torsion, T = 0.000 kip\*in  
 Pressure, p = 0.000 ksi

#### Applied Stresses

f<sub>A</sub> = 0.000 ksi  
 f<sub>Smax,x</sub> = 20.453 ksi  
 f<sub>Smax,y</sub> = 0.000 ksi  
 f<sub>Savg,x</sub> = 15.340 ksi  
 f<sub>Savg,y</sub> = 0.000 ksi  
 f<sub>Bx</sub> = 0.000 ksi  
 f<sub>By</sub> = 142.114 ksi  
 f<sub>St</sub> = 0.000 ksi  
 f<sub>H</sub> = 0.000 ksi

#### Stress Ratios

	Ultimate	Limit
R <sub>A</sub> =	0.000	0.000
R <sub>Smax,x</sub> =	0.213	0.210
R <sub>Smax,y</sub> =	0.000	0.000
R <sub>Savg,x</sub> =	0.160	0.158
R <sub>Savg,y</sub> =	0.000	0.000
R <sub>Bx</sub> =	0.000	0.000
R <sub>By</sub> =	0.560	0.670
R <sub>St</sub> =	0.000	0.000
R <sub>H</sub> =	0.000	0.000
R <sub>Smax</sub> =	0.213	0.210
R <sub>Savg</sub> =	0.160	0.158
R <sub>B</sub> =	0.560	0.670

#### Utilization Factors

	Ultimate	Limit	
U <sub>1</sub> =	0.582	0.688	$U_1 = \sqrt{((R_A - R_B)^2 + R_H^2 - (R_A - R_B)R_H + (R_S + R_{ST})^2)}$
U <sub>2</sub> =	0.582	0.688	$U_2 = \sqrt{((R_A + R_B)^2 + R_H^2 - (R_A + R_B)R_H + (R_S + R_{ST})^2)}$
U <sub>3</sub> =	0.213	0.210	$U_3 = \sqrt{(R_A^2 + R_H^2 - R_A \cdot R_H + (R_{Smax} + R_{ST})^2)}$
<b>Max U =</b>	<b>0.582</b>	<b>0.688</b>	

Margin of Safety	Ultimate	Limit
M.S.	0.718	0.453

Since the MS > 0, a smaller diameter pin can be theoretically used. However, standard NAS bolt diameters are 3/16", 1/4", 5/16" and 3/8". A 3/16" dia. bolt is adequate in shear but is not capable of carrying both



shear and bending loads. Therefore, the next available bolt size i.e 1/4" dia. was selected. A customized bolt optimized for the loads can be fabricated but will add to lead time and consume resources.

#### 4.1.4.4 Lug Radius

The final lug size is determined from the calculation below:

**Part:** Hinge Lug  
**Lug Location:** Upper Hinge  
**Design Case:** Tension Case  
**Material:** 4130 HT-95 Steel

Lug Analysis  
Lug Analysis  
Version 1.0

#### Ultimate Applied Loads

**Material:** 4130

$P_{ax} = 0.708$  kip  
 $P_{tr} = 0.258$  kip

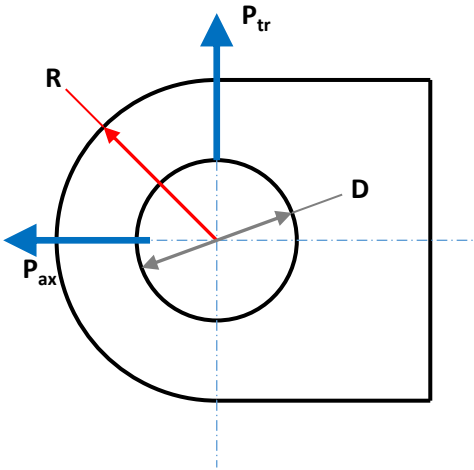
$F_{tu} = 95$  ksi  
 $F_{tux} = 95$  ksi  
 $F_{ty} = 75$  ksi  
 $F_{tyx} = 75$  ksi

#### Lug Dimensions

$R = 0.250$  in  
 $D = 0.250$  in  
 $t = 0.125$  in  
 $\alpha = 0.0$  °

#### Calculated Properties

$W = 0.500$  in  
 $A_1 = 0.020$  in<sup>2</sup>  
 $A_2 = 0.016$  in<sup>2</sup>  
 $A_3 = 0.016$  in<sup>2</sup>  
 $A_4 = 0.020$  in<sup>2</sup>  
 $A_{av} = 0.018$  in<sup>2</sup>  
 $A_{br} = 0.031$  in<sup>2</sup>  
 $A_t = 0.031$  in<sup>2</sup>



#### Lug Factors

$D/t = 2.000$   
 $R/D = 1.000$   
 $W/D = 2.000$   
 $A_{av}/A_{br} = 0.589$

→  
→  
→  
→

#### Efficiency Factors

$K_{br} = 0.766$   
 $K_t = 0.970$   
 $K_{tru} = 0.784$   
 $K_{try} = 0.712$

**Part:** Hinge Lug  
**Lug Location:** Upper Hinge  
**Design Case:** Tension Case  
**Material:** 4130 HT-95 Steel

Lug Analysis  
 Lug Analysis  
 Version 1.0

#### Allowable Ultimate Load for Shear Bearing

$$P_{bru} = K_{br} * A_{br} * F_{tu} = 2.274 \text{ kip}$$

#### Allowable Ultimate Load for Tension

$$P_{tu} = K_t * A_t * F_{tu} = 2.879 \text{ kip}$$

#### Allowable Ultimate Transverse Load

$$P_{tru} = K_{tru} * A_{br} * F_{tux} = 2.326 \text{ kip}$$

#### Allowable Axial Limit Load

$$P_{u,min} = \min(P_{bru}, P_{tu}) = 2.274 \text{ kip}$$

$$P_{u,min} / (A_{br} * F_{tux}) = 0.766 \rightarrow C = 1.1$$

$$P_{ya} = C * (F_{tyx} / F_{tux}) * P_{u,min} = 1.975 \text{ kip}$$

#### Allowable Transverse Limit Load

$$P_{try} = K_{try} * A_{br} * F_{tyx} = 1.669 \text{ kip}$$

#### Load Ratios

$$R_{a,lim} = P_{ax} / (1.5 * P_{ya}) = 0.239$$

$$R_{tr,lim} = P_{tr} / (1.5 * P_{try}) = 0.103$$

$$R_{a,ult} = P_{ax} / P_{u,min} = 0.311$$

$$R_{tr,ult} = P_{tr} / P_{tru} = 0.111$$

#### Margin of Safety

$MS_{lim} =$	$1 / (FF * (R_{a,lim}^{1.6} + R_{tr,lim}^{1.6})^{0.625}) - 1 =$	2.149
$MS_{ult} =$	$1 / (FF * (R_{a,ult}^{1.6} + R_{tr,ult}^{1.6})^{0.625}) - 1 =$	1.503

where, FF = 1.15

#### 4.1.4.5 Shape

There was limited scope of changing the overall shape of the flight control bracket from what was presented in Figure 23.

The bracket was reinforced with an additional flange as reducing the material thickness negatively impacts the bracket stiffness due to out-of-plane loads. The lug radius was also increased to account for the material lost due to the lug thickness reduction. The profile of the bracket was also modified to make the transition more gradual compared to before.

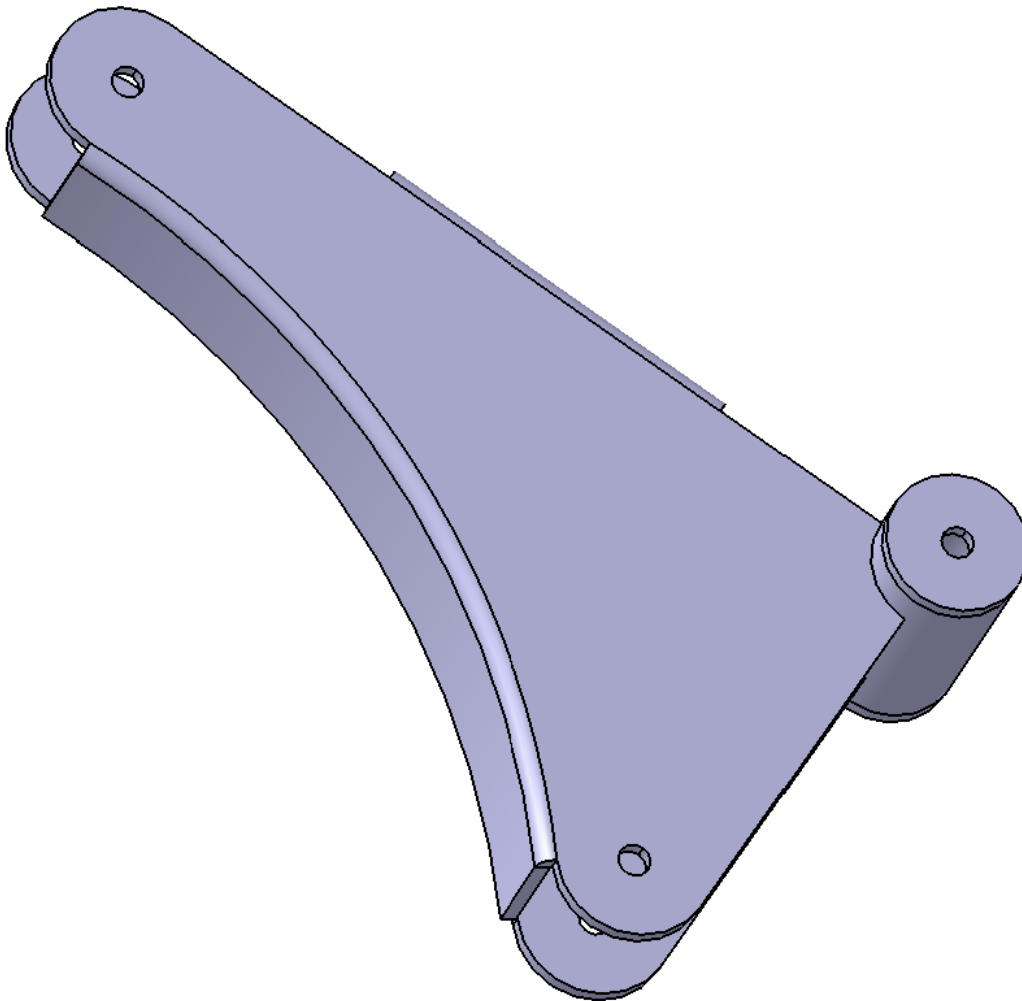


Figure 23: Sheet Metal Bracket –Base Design - Manufacturing Parameters

#### 4.1.4.6 Manufacturing Operations and Processes

The flight control bracket is designed to be manufactured from sheet steel. Standard sheet metal fabrication techniques (such as bending, stamping and punching) are preferred to keep manufacturing cost and lead times low. The first step in manufacturing the bracket is to cut the sheet to the broad contours of the shape of the bracket as illustrated in Figure 24. The steps can be performed in a single operation depending on the type of tooling used.

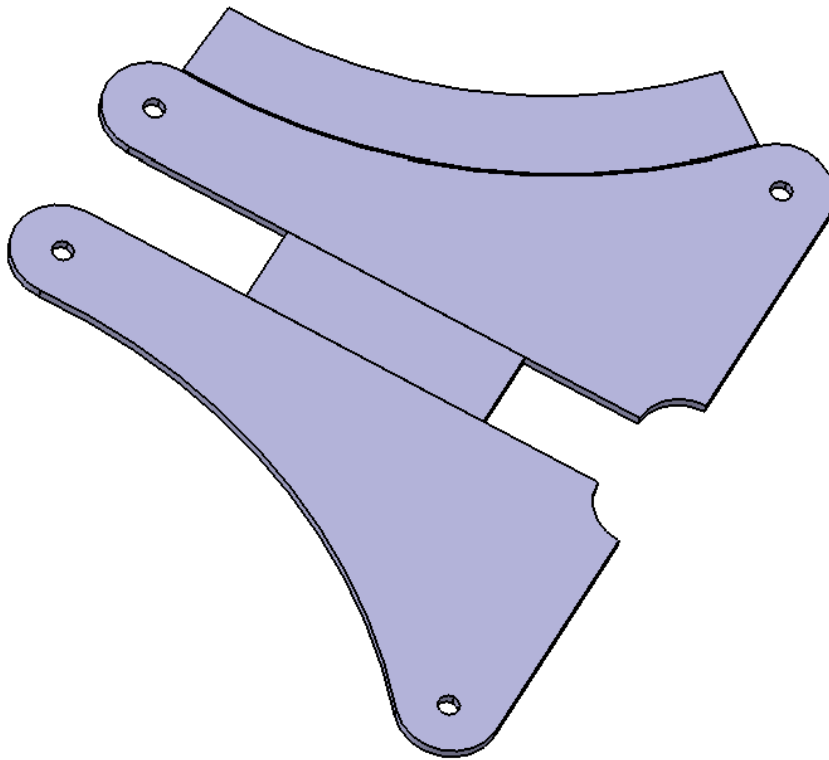


Figure 24: Manufacturing Operations - 1

The first 90-degree bend is carried out on a standard V-Block. However, for the subsequent 90 degree bends a gooseneck is required as shown in Figure 25. Custom tooling can be very expensive; therefore, the size of the bracket is limited by the gooseneck.

**90° bending/gooseneck type  
(sheet thickness: 0.4–3.2 mm)**

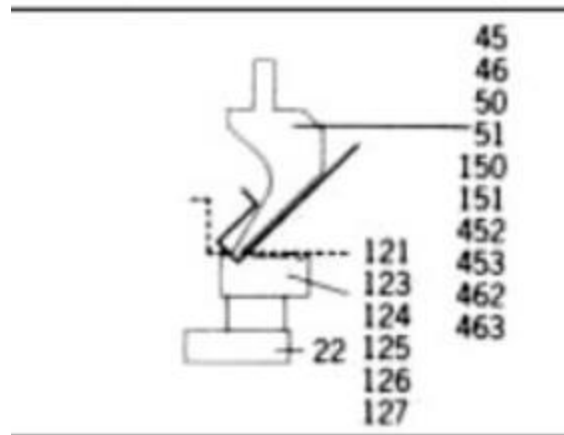


Figure 25: Sheet Metal Bending using Gooseneck

The base of the bracket is manufactured from a steel tube of standard thickness to which two pre-fabricated end pads get welded onto. The end pads are made from flat sheet steel stocks and feature a bolt hole at the center for the hinge bolt.

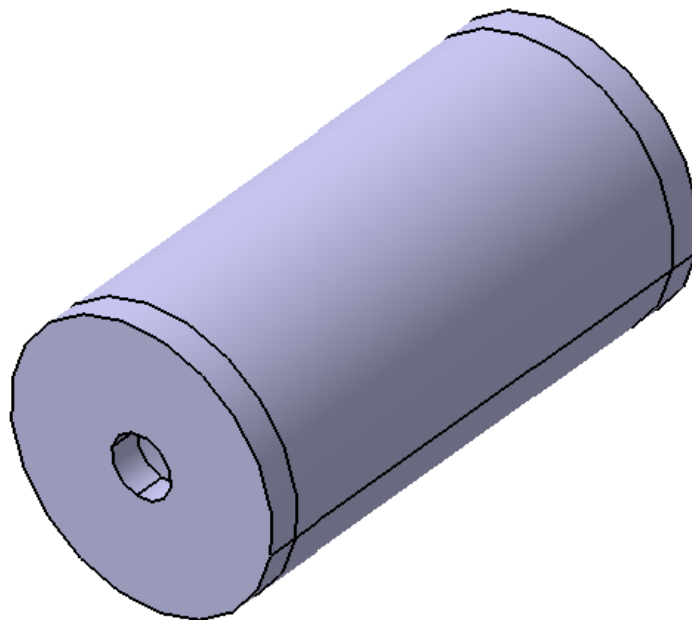


Figure 26: Manufacturing Operations - 2

Table 5: Sheet Metal Bracket - Relationship Matrix - Manufacturing

	Bolt Diameter	Sheet Thickness	Material	Shape	# Manufacturing Operations	Processes
Cost	0	9	3	1	1	3
Time	0	9	1	1	1	3
Weight	0	3	3	1	0	0

From the manufacturing relational matrix, it can be seen that sheet thickness, material and shape are the parameters that influence the manufacturing functional parameters the most, followed by number of manufacturing operations and processes.

The combined functional requirements and parameters are established to be:

$$[FR_C] = \{[FR_D]_n, [FR_M]_m\} = \left\{ \begin{array}{c} \textit{Deflection} \\ \textit{Strain} \\ \textit{Endurance} \\ \textit{Weight} \\ \textit{Cost} \\ \textit{Time} \end{array} \right\}$$

$$[DP_C] = \{[DP_D]_j, [DP_M]_k\} = \left\{ \begin{array}{c} \textit{Lug Radius} \\ \textit{Bolt Diameter} \\ \textit{Sheet Thickness} \\ \textit{Material} \\ \textit{Shape} \\ \textit{\#Manufacturing Operations} \end{array} \right\}$$

From the design and manufacturing relational matrices, sheet thickness, shape and material are the most influential parameters. The design was therefore optimized further for the above parameters resulting in the final design as shown in Figure 27.

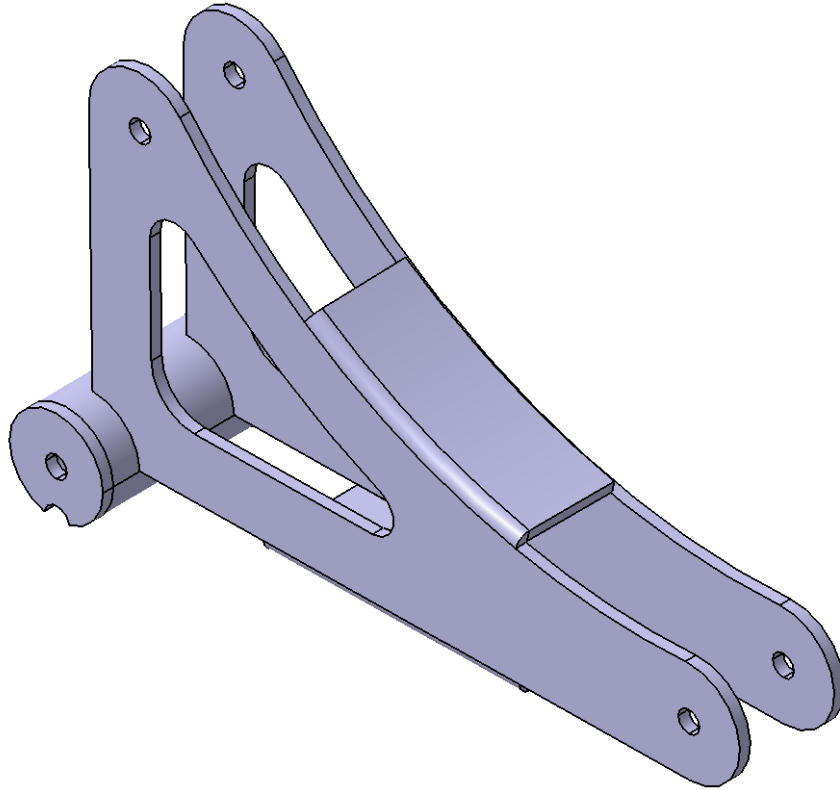


Figure 27: Optimized Design of the Flight Control Bracket

Sheet thickness and material were already optimized considering both the design and manufacturing parameters; however, the shape could still be varied. Cut-outs were introduced to the design to reduce weight (0.7 lb when considering design parameters, 1.8 lb when considering manufacturing parameters and 1.4 lb when considering both design and manufacturing parameters). Although the bracket weighed less when manufactured from aluminum, the complexity associated with bending increases exponentially with sheet thickness (factors such as residual stresses, increased bend tolerances and multi-step bending operations need to be considered). Furthermore, the steel design typically costs less than a third to manufacture compared to the aluminum design and can be fabricated in a single day with minimal tooling. Cut-outs were also introduced to the end-pads to facilitate drainage and prevent corrosion as evident in older designs with similar features. The end result is a superior product than that was achieved when each of the design and manufacturing parameters were considered in isolation.

## 4.2 CASE STUDY 2: ROLL FRAME FOR A LIGHT UNPRESSURIZED AIRCRAFT

### 4.2.1 DESIGN OBJECTIVE

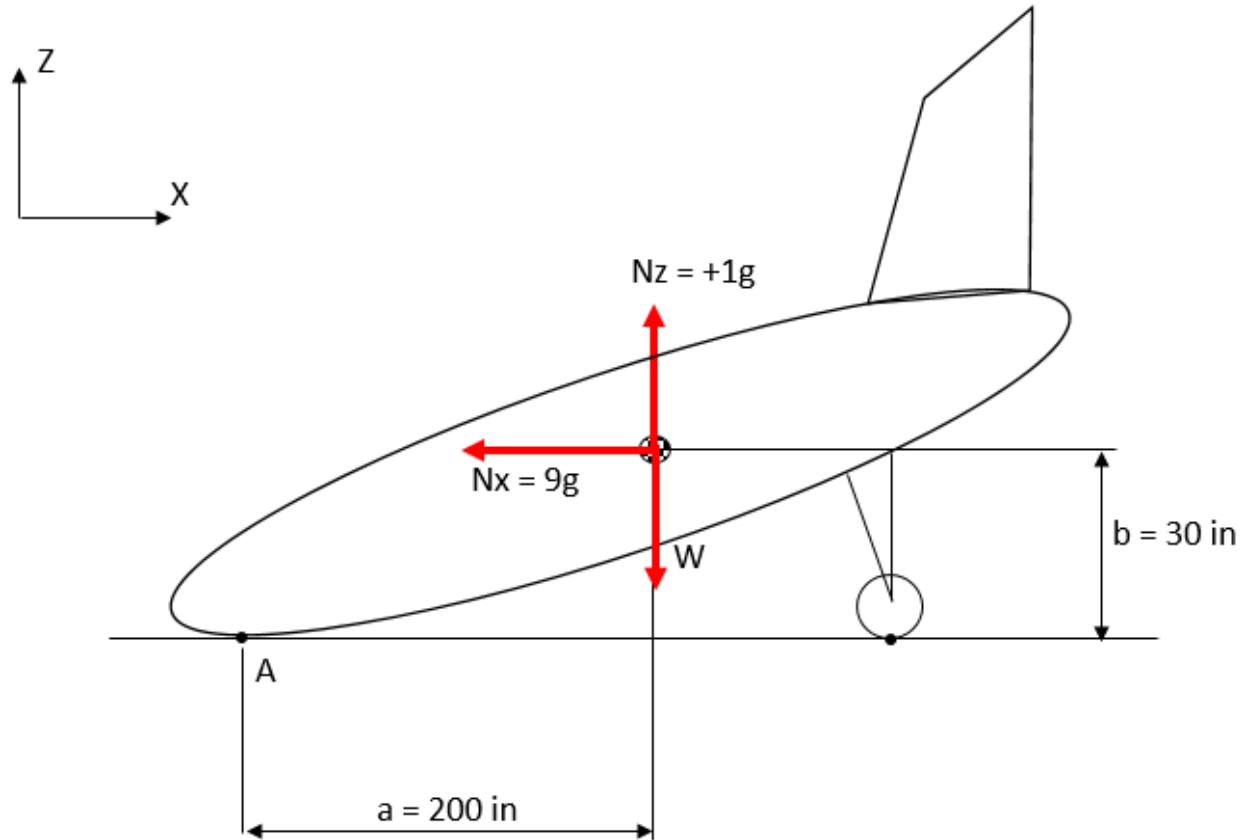
The Roll Frame is a safety critical structure designed to protect the occupants in the event of an aircraft turnover during emergency landing.



Figure 28: Roll Frame on a Diamond DA40 Aircraft

FAR 23.561 (d) [23] specifies that if it is not established that a turnover is unlikely during emergency landing, the structure must be designed to protect the occupants in a complete turnover. The likelihood of turnover is established as follows:





The aircraft can turn over if the following condition is met

$$M_{tipping} > M_{resisting} \quad \text{Equation 25}$$

where,

$$M_{tipping} = (N_x * b + N_z * a) * W \quad \text{Equation 26}$$

$$M_{resisting} = W * a \quad \text{Equation 27}$$

$$W = 5000 \text{ lb}$$

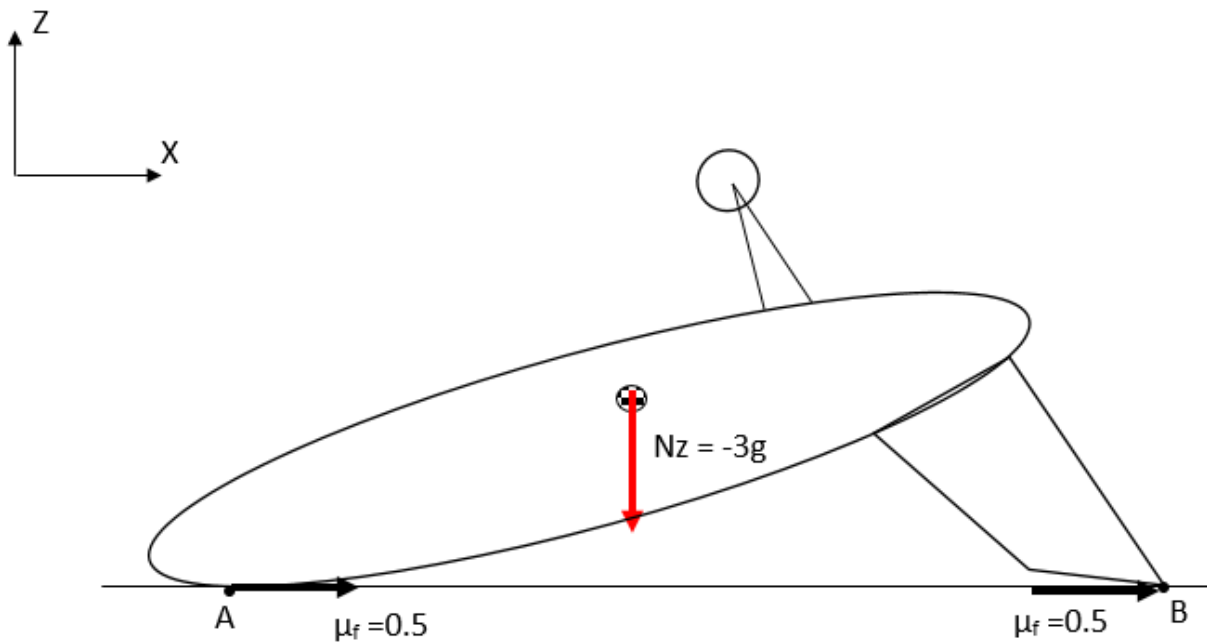
$$M_{tipping} = (1 * 30 + 9 * 200) * 5000 = 9,150,000 \text{ lb-in}$$

$$M_{resisting} = (5000 * 200) = 1,000,000 \text{ lb-in}$$

Therefore,  $M_{tipping} > M_{resisting}$ .

Since, it is established that the aircraft can potentially turn over, FAR 23.561 (d)(2) [23] specifies that loads applied to an inverted airplane after a turnover should be as follows:

- a) An upward ultimate inertia load factor of  $3.0g$
- b) A drag force corresponding to a coefficient of friction with the ground of  $0.5$



The primary objective of the roll frame is listed as follows:

- 1) The roll frame should be able to protect the occupants in the event of a turnover
- 2) The weight of the frame shall be kept minimal with respect to the loads
- 3) The frame shall be manufactured for minimum cost

#### 4.2.2 PARAMETER SPACE GENERATION - CONCEPTUAL DESIGN SELECTION

The most critical functional requirements that will influence the final product are determined from the Technical Requirements Documents (TRD) as follows:

$$[FR] = \begin{bmatrix} Weight \\ Cost \\ Load \end{bmatrix}$$

The functional requirements are ranked in the order of importance to the customer. The ranking process is determined after extensive interaction among all stakeholders.

$$[FR] = \begin{bmatrix} Load \\ Weight \\ Cost \end{bmatrix}$$

At this stage, several conceptual designs are generated. In this example, three distinct concepts have been explored:

- 1) A tubular metallic frame
- 2) A “C” shaped metallic frame
- 3) A “Omega” shaped composite frame

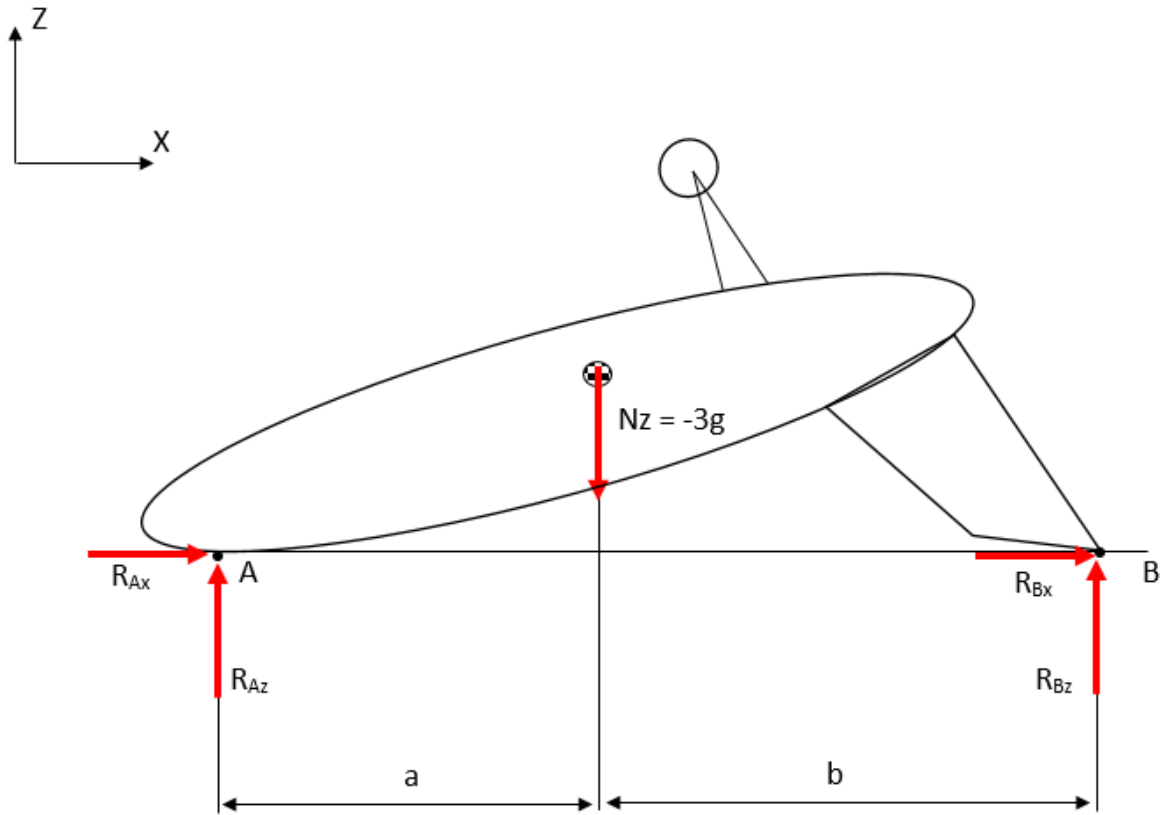
Next, each concept is evaluated against the other concepts.

FR \ Designs	Ranking	Tubular Metallic	“C” Shaped Metallic	“Omega” Shaped Composite
Load	3	⊙	⊙	⊙
Weight	2	○	Δ	⊙
Cost	1	⊙	○	○
Score	---	16	13	17

The applied loads are derived from regulations; hence all three designs are given the same score as all three designs have to sustain the same loads. In terms of weight, composites exhibit a higher strength to weight and stiffness to weight ratio over most metallic alloys; therefore, the composite roll frame is rated higher than the other designs. Finally, although cost is an important aspect of the conceptual design

selection process, safety and therefore performance of the roll frame is more important. The above exercise results in the composite roll frame to have the highest score, and is therefore selected for detailed design.

#### 4.2.3 PARAMETER SPACE INTEGRATION FOR DESIGN PARAMETERS



$$a = 180 \text{ in}$$

$$b = 220 \text{ in}$$

$$W = 5000 \text{ lb}$$

$$N_z = 150000 \text{ lb } (N_z = 3 * W)$$

$$R_{Az} = 8250 \text{ lb}$$

$$R_{Bz} = 6750 \text{ lb}$$

$$R_{Ax} = 0.5 * N_z * (R_{Az} / N_z) = 4125 \text{ lb}$$

$$R_{Bx} = 0.5 * N_z * (R_{Bz} / N_z) = 3375 \text{ lb}$$

The load in the x direction (drag load) acts on the outer surface of the aircraft and is not considered for the analysis of the roll frame. Only the vertical component of load ( $R_{Az} = 8250 \text{ lb}$ ) acts on the roll frame.

The load is not multiplied by a factor of 1.5 as per FAR 23.303 [23], since the structure is not designed to carry on flight operations after an overturn. Therefore, the limit load is equal to the ultimate load.

For the Roll Frame, the Functional Requirements and Parameters for Design are established as:

$$[FR_D] = [RM_D] * [DP_D]$$

where,

$$[FR_D] = \begin{bmatrix} \text{Weight} \\ \text{Stress} \\ \text{Deflection} \end{bmatrix}_D$$

$$[DP_D] = \begin{bmatrix} \text{Stacking Sequence} \\ \text{\#Plies} \\ \text{Material} \\ \text{Orientation} \\ \text{Shape} \end{bmatrix}_D$$

Influence of each of the design parameters are discussed and the relationship matrix for design is presented below.

#### 4.2.3.1 Material

The roll frame is a safety critical structure whose purpose is to protect the occupants in the event of a turnover. Since aircraft turnover is a failure case, the design philosophy for the roll frame is to have the frame absorb the maximum amount of energy resulting from the aircraft turnover.

Figure 29 illustrates the specific strength and stiffness of common aerospace materials. As illustrated in the figure, non-metallic materials such as Glass, Kevlar, Graphite and Boron exhibit superior properties compared to bulk metallic materials.

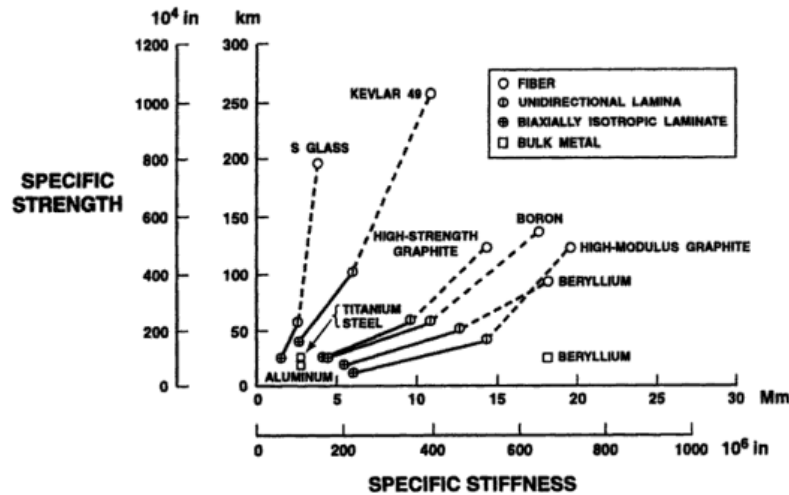


Figure 29: Specific Strength vs. Specific Stiffness for Composite and Metallic Materials [28]

Table 6 shows the value of weight savings (in dollars per kilogram) for various aerospace applications.

Table 6: Value of Weight Savings in Dollars [29]

Application	Value of Weight Savings in Dollars (\$/kg)
Small Aircraft	55
Helicopters	110
Aircraft Engines	440
Commercial Aircraft	880
Low Earth Orbit Satellites	2200
Geo Synchronous Satellites	22000
Space Shuttle	33000

Since composite materials inherently have higher strength to weight and stiffness to weight ratios than bulk metallic materials, there are significant weight advantages when fabricating structures from composite materials.

Table 7 shows a comparative summary of fibers used in aerospace applications. Although Polyethylene and Aramid fibers have a lower density, Carbon fibers possess the best overall combination of properties including high strength and modulus, low density, high service temperature and small cross-sectional diameter.

Table 7: Comparative Summary of Fiber Properties [29]

Fiber	Diameter (microns)	Density (lb/in <sup>3</sup> )	Tensile Strength (ksi)	Modulus (Msi)	Service Temperature (°F)
S-Glass	7	0.09	500-650	13	600-700
Aramid	12	0.052	400	10-25	500
Polyethylene	27-28	0.035	375-430	17-25	230
Carbon	7	0.06	350-450	33-55	1000
Quartz	9	0.079	500	10	2000
Silicon Carbide	10-20	0.083-0.094	400	28	2400
Alumina	20	0.141	200-300	55	1800
Boron	50-200	0.09	500	58	3500

Table 8 presents a comparative summary of thermosetting resin systems used in conjunction with the fibers presented in Table 7. As illustrated in Table 8, epoxy based resin systems are most widely used since they offer superior combination of properties.

Table 8: Comparative Summary of Thermosetting Resins [29]

Characteristics	Thermosetting Resins				
Property	Polyester	Epoxy	Phenolic	Bismaleimide	Polyimide
Processability	Good	Good	Fair	Good	Fair to Difficult
Mechanical Properties	Fair	Excellent	Fair	Good	Good
Heat Resistance (°F)	180	200	350	350	500-600
Price Range	Low-Medium	Low-Medium	Low-Medium	Low-Medium	High
Delamination Resistance	Fair	Good	Good	Good	Good
Toughness	Poor	Fair- Good	Poor	Fair	Fair
Remarks	Used in Secondary structures, cabin interiors, primarily with fiberglass	Most widely used, best properties for primary structures; principal resin type in current graphite production use	Used in secondary structures, primarily in fiberglass; good for cabin interiors; for low smoke generation	Good structural properties, intermediate temperature resistance; alternative to epoxy	Specialty use for high temperature applications

Therefore, carbon fiber with an epoxy resin system is selected for fabricating the roll frame.



#### 4.2.3.2 Ply Orientation and Stacking Sequence

Since composite materials can be tailored to have different properties in different directions, the orientation and stacking sequence of each lamina is of outmost importance.

If the design requirement is to sustain axial loads, a higher percentage of the lamina (in the laminate) should be oriented in the loading direction. Similarly, for sustaining shear loads, more lamina should be oriented at  $\pm 45$  degrees. However, to ensure adequate structural strength and stiffness in all directions, the laminate should incorporate a small percentage of lamina in the non-primary loading direction.

Since composite materials are anisotropic by nature, ply stacking sequence is critical in determining the overall stiffness and therefore response characteristics of the laminate to applied loads. Figure 31 illustrates the effect of various ply stacking sequences on the deflection of the laminate.

For the purposes of the base design, the laminate will be kept balanced and symmetric as shown in Figure 31.

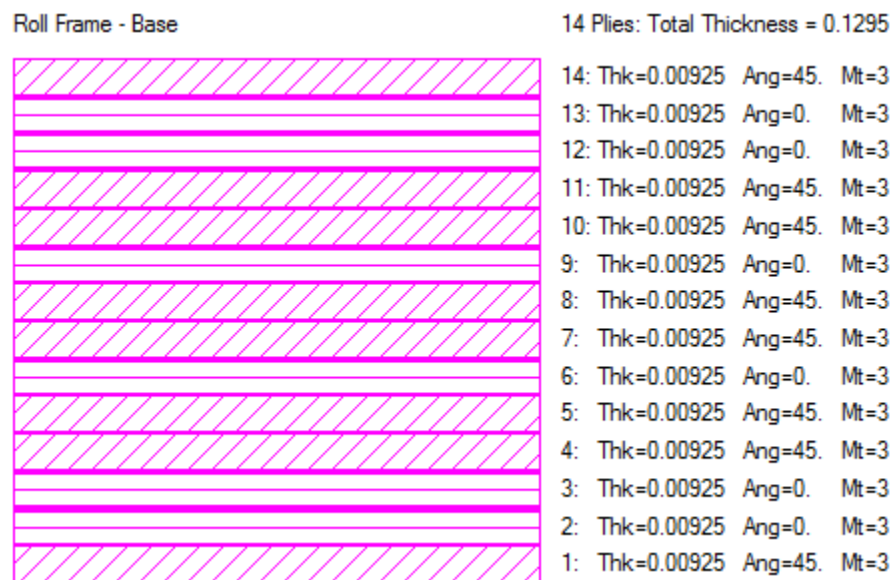


Figure 30: Roll Frame Ply Stackup

All plies at  $\theta^\circ$ . Axial load results in stretching-shearing behavior.



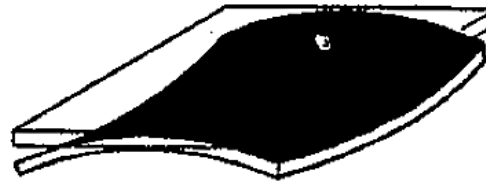
Two plies at  $\pm\theta$  (any angle). Opposing shear deformations in the plus and minus plies result in stretching-torsion interaction.



A  $0^\circ/90^\circ$  stacking. This arrangement bends under pure tension because the modulus-weighted centroid is not coincident with the geometric centroid, resulting in an offset load path.



Another  $0^\circ/90^\circ$  stacking. Because of different thermal expansion characteristics in each layer, this stacking deforms into a "saddle" when heated.



(sketches show how simple loads result in unusual deformations because of coupling action. With balance and symmetry present, these effects disappear)

Figure 31: Effect of Ply Stacking Sequence on Ply Deflection due to applied Axial Load [29]

#### 4.2.3.3 Shape

The roll frame is designed such that the buckling strength is maximized. Figure 32 shows, the buckling coefficient of hat section stiffeners for various ratios of side web to top web dimensions. From the figure, it can be interpreted that a wider hat (smaller  $b_w/b_T$ ) will result in a stiffer section that can carry higher loads. Following this philosophy, the roll frame section has been designed to be as wide as possible (large  $b_T$ ). The depth of the roll frame ( $b_w$ ) is determined by wiring and other associated components that are placed within the structure.

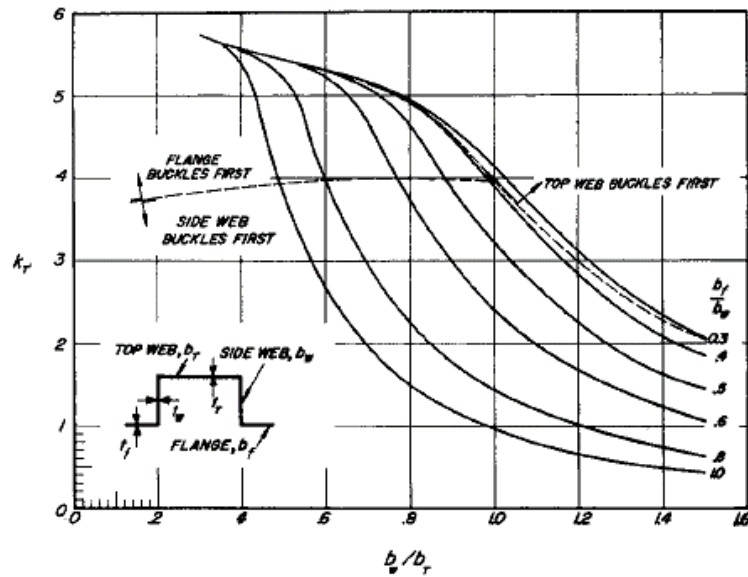


Figure 32: Buckling Coefficient of Hat Section Stiffeners [27]

#### 4.2.3.4 Number of Plies

In composite materials, each laminate can develop a different level of stress due to applied loads on the laminate, the lamina orientation and the stacking sequence. However, since strain varies linearly across the laminate, the laminate is analyzed for strain due to applied loads which are then compared to allowable strain to determine the corresponding margin of safety. The number of plies in the laminate is dependent on the following factors:

- Bearing Strength
- Pull Thru Strength
- Tensile Strength (incl. Open Hole Tension, Filled Hole Tension)
- Compression Strength (incl. Compression After Impact, Open Hole Compression)
- Shear Strength
- Modulus of Elasticity

Table 9: Roll Frame - Relationship Matrix - Design

	Stacking Sequence	# Plies	Material	Orientation	Shape
Weight	0	3	3	0	1
Strain	9	3	0	1	1
Deflection	9	1	0	1	9

From the design relational matrix, it can be observed that shape and stacking sequence are the parameters that influence the design functional parameters the most, followed by number of plies, material and orientation. The design of the roll frame after consideration of the design parameters is shown in Figure 33.

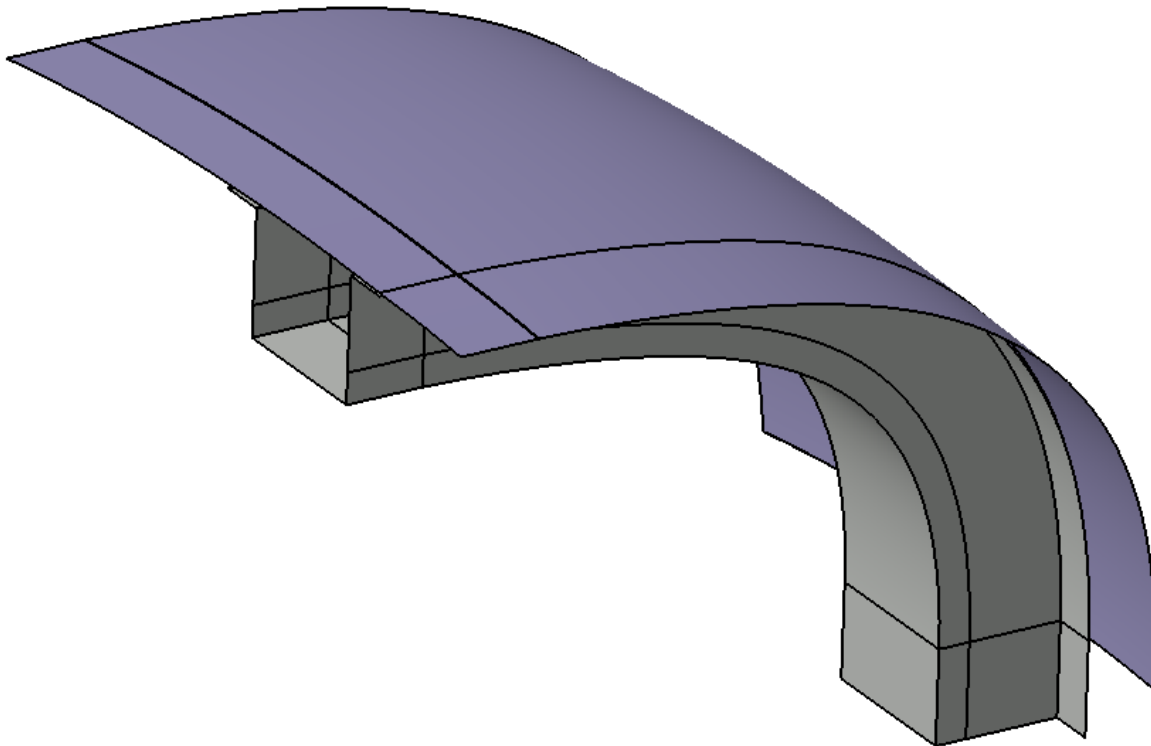


Figure 33: Base Design – Roll Frame – Design Parameters

The analysis results, comprising of a strain plot is shown in Figure 34.

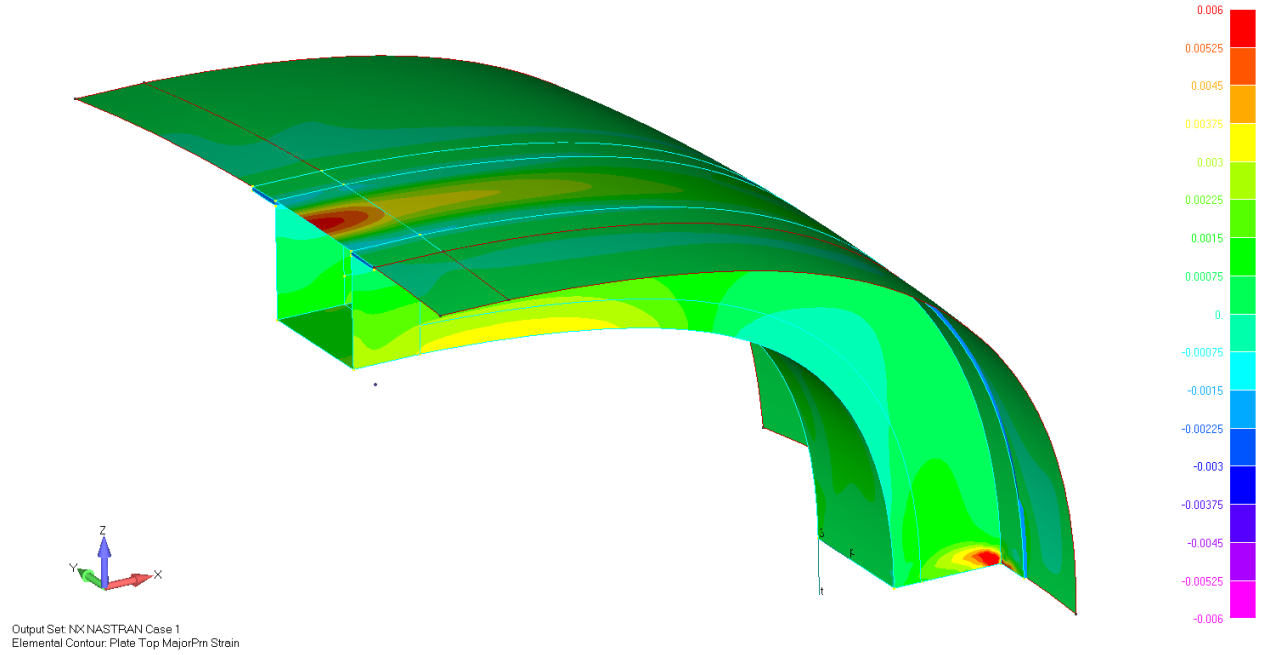


Figure 34: Roll Frame – Design Parameters – Strain Plot

#### 4.2.4 PARAMETER SPACE INTEGRATION FOR MANUFACTURING PARAMETERS

For the Roll Frame, the Functional Requirements and Parameters for Manufacturing are established as:

$$[FR_M] = [RM_M] * [DP_M]$$

where,

$$[FR_M] = \begin{bmatrix} \text{Weight} \\ \text{Cost} \\ \text{Time} \end{bmatrix}_M$$

$$[DP_M] = \begin{bmatrix} \text{\#Plies} \\ \text{Weave} \\ \text{Material} \\ \text{Orientation} \\ \text{Shape} \\ \text{Manufacturing Method} \end{bmatrix}_M$$

Influence of each of the manufacturing parameters on the functional requirements are discussed below.

#### 4.2.4.1 Shape

The shape of the roll frame was influenced by the available space and connecting interfaces. From a load and structures point of view, a bigger roll frame with the appropriate thickness provides a stiffer structure. However, the roll frame has to fit socket interfaces at the edges of the canopy which are of a predetermined size. In addition, the size of the frame is limited by the pilot's visibility requirements (depth limitations) and interfaces to other accessories on the side (width limitations).

The size of the roll frame has been reduced since the skin provides additional stiffness and stability to the roll frame, which should be considered as the entire structure reacts the load. Therefore, the effective section is a "Closed Box" as opposed to a "Hat Section". Figure 35 illustrates the buckling coefficient for "Box Section" stiffeners for various ratios of side web to top web lengths and top web to side web thicknesses. Comparing, Figure 35 to Figure 32, it can be seen that a closed "Box Section" is significantly stiffer than an open "Hat Section". Therefore, the size of the roll frame has been reduced without adversely affecting the structural stiffness. The cross-section of the frame has been tapered to ensure that demolding is easier after the curing phase.

In addition, the corners have been rounded off with generous bend radii to prevent issues such as fiber cracking and void generation as shown in Figure 36.

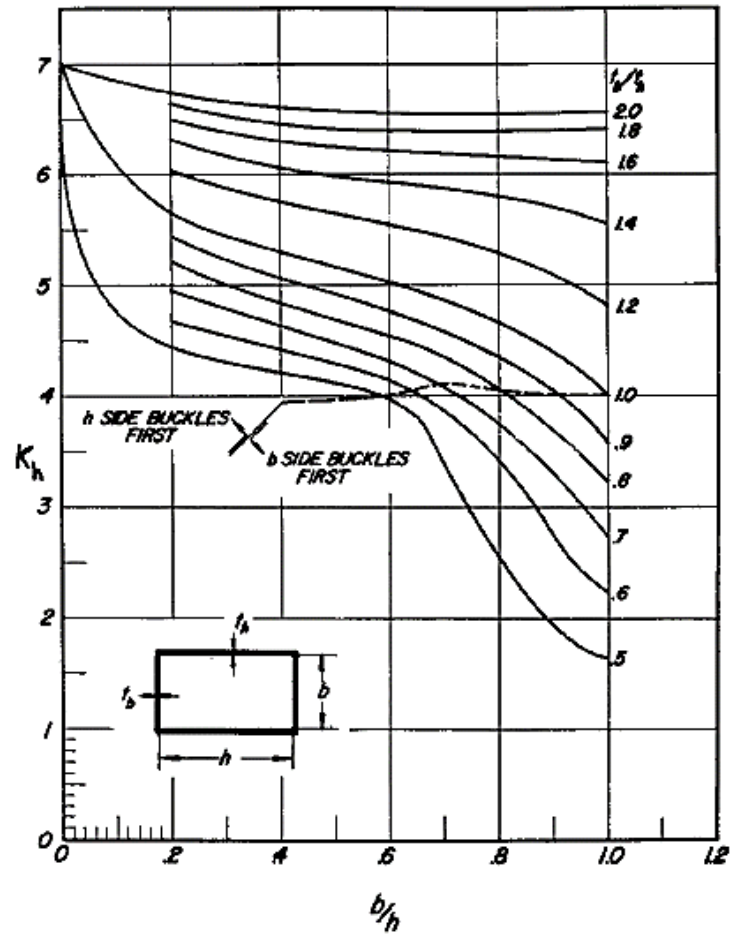


Figure 35: Buckling Coefficient for Rectangular Section Stiffeners [27]

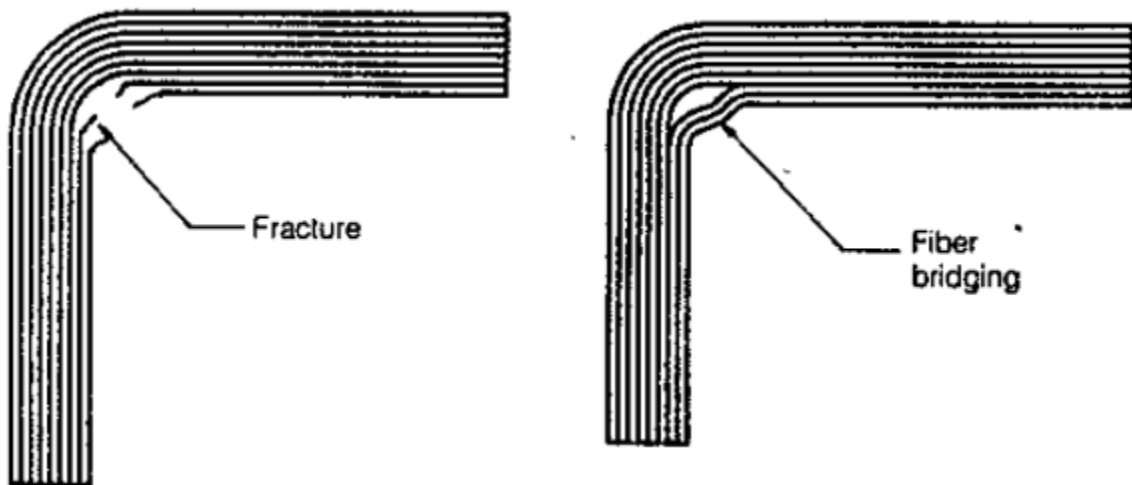


Figure 36: Problems with Laminate Corners [29]

#### 4.2.4.2 Material Forms and Weave

Although carbon fiber has been selected as the material of choice, the material form and weave have a substantial impact on the fabrication of the structure.

Table 11 presents a comparison of common composite material forms, namely uni-tape, uni-directional, woven and pre-formed fabrics. Uni-tape fabrics and uni-directional fabrics are typically employed in high performance applications where achieving performance objectives are more critical than other factors such as reducing cost. Woven fabrics on the other hand are more common in day to day applications as it provides a good balance of fiber properties, handleability and reduced cost.

Table 10: Comparison of various composite material forms [29]

Forms	Advantages	Disadvantages
Uni-tape	Maximum structural properties, design flexibility	Poor drapability, possible fiber misalignment
Woven fabrics	Good drapability, reduced lay-up costs	Some loss of properties due to fiber crimp, width limitations, less design flexibility
Unidirectional Fabrics	Improved drapability, fiber alignment, minimal reductions in fiber strength	Slight weight penalty
Pre-plyed fabrics Stitched fabrics, Pre-forms	Reduces lay-up costs Provides exceptional fiber stability needed for pultrusion, resin injection molding; some forms provide “Z” direction strength	Loss of design flexibility, weight penalty, increased cost

Table 11 presents the advantages and disadvantages of various composite fiber weaves. The most common fiber weaves are plain weave and unidirectional fabrics. Plain weaves are preferred in areas where the state of stress is lower and is biaxial in nature. Unidirectional fabrics are employed where the state of stress is higher and mostly in a principal direction.



Table 11: Comparison of composite fiber weaves [29]

Unidirectional Fabrics	Better drapability than tape Better properties in fiber longitudinal direction than plain weave and harness satin weave
Plain Weave Fabrics	Reduction in properties compared to uni-directional fabrics due to fiber crimping Better drapability than uni-directional Fabrics Less cost due to speedier layup Good damage tolerance properties compared to uni-directional or Harness Satin Weave Fabrics Easy to handle and produces reproducible laminate thickness Thicker than uni-directional fabric; hence heavier
Harness Satin Weave Fabrics	Reduction in properties compared to uni-directional and plain weave fabrics due to fiber crimping Better drapability than uni-directional and plain weave Fabrics Less damage tolerance than plain weave

Considering the various pros and cons, plain weave carbon fabrics have been used to fabricate the roll frame because of their ease of handling, all round properties and lower cost.

#### 4.2.4.3 Ply Orientation and Stacking Sequence

The following orientation and stacking rules should be followed when designing composite parts:

- 1) The laminate should be balanced and symmetric. If the laminate is asymmetric, the asymmetric plies should be located close to the mid plane.
- 2) The laminate should be enveloped with  $45^\circ$  plies on both sides to minimize free edge effects.
- 3) No more than 4 plies of the same orientation shall be stacked together in the laminate.
- 4) The lamina shall be oriented in the standard angles (i.e.  $0^\circ$ ,  $\pm 45^\circ$ ,  $90^\circ$ ).
- 5) Unidirectional tapes and core material should be enveloped with  $45^\circ$  plies.
- 6) The laminate should have at least 10% of the total number of plies in each direction

Figure 37 shows the composite laminate design envelope. Typically, the designer should try to design the structure such that the ply layup falls within the “yellow” design space. For “quasi-isotropic” structures, a ply sequence should be selected such that the layup falls with-in the “green” design space.

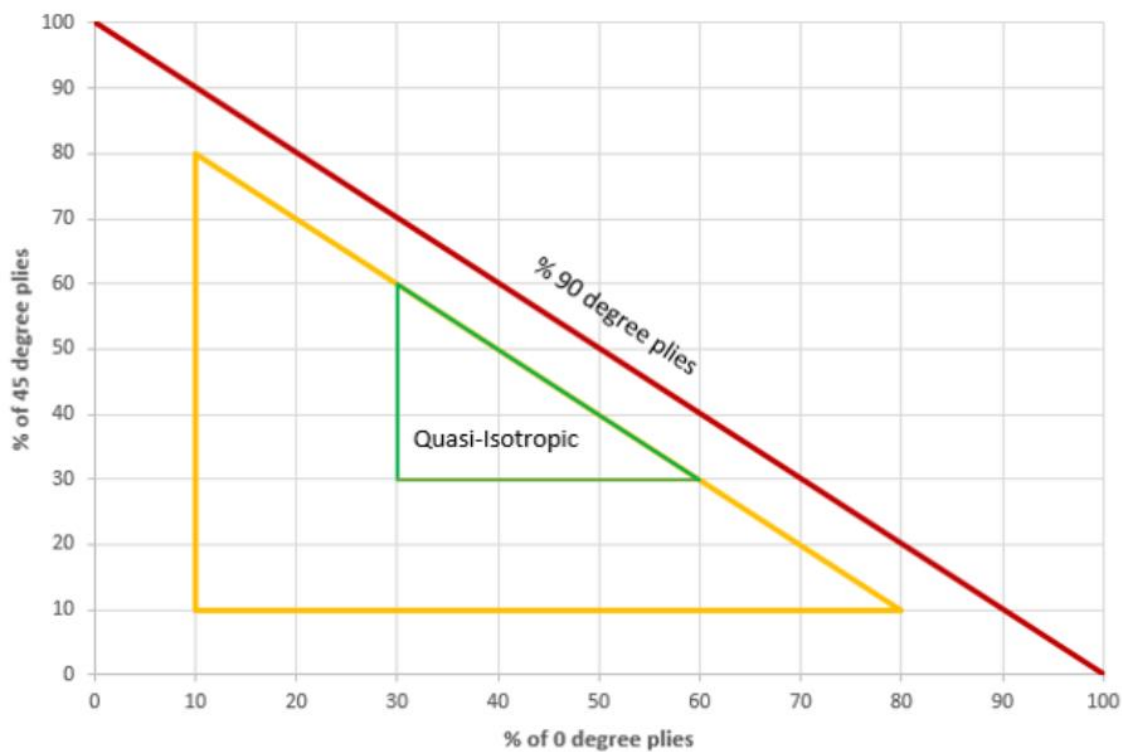


Figure 37: Composite Laminates Design Envelope

Following the above rules, the laminate stacking sequence is established to be as follows:

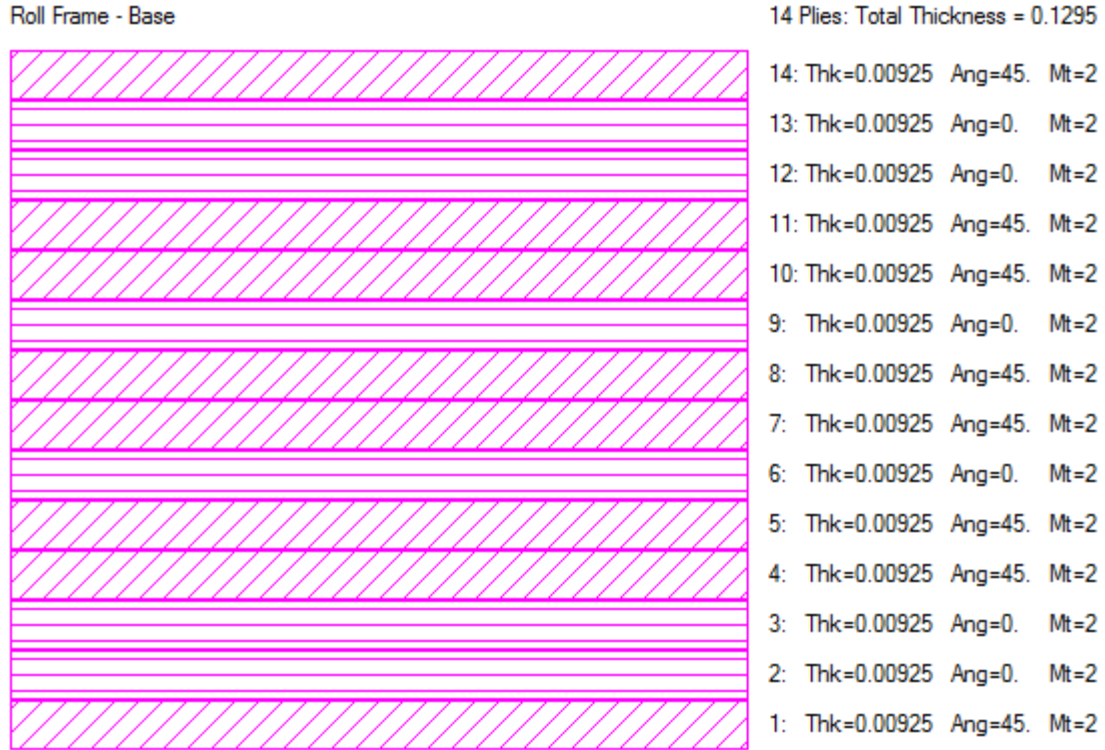


Figure 38: Roll Frame Ply Stackup

#### 4.2.4.4 Manufacturing Method

Manufacturing the roll frame involved employing the wet layup, vacuum bagging and curing approaches as illustrated in Figure 39. Once the ply layup and sequence were determined a female mold was used to give shape to the roll frame laminate structure. A female mold was used as the outer mold line (OML) of the roll frame acts as an interface for associated sub-structures and therefore needs a flat surface for mating interfacing components. Furthermore, the spring back after curing the part will be on the inside which will allow for easier integration saving cost and time. Finally, because the OML will be the surface that will be visible from the outside, a smoother finish is preferred for aesthetic considerations. The various mold types, their advantages/ disadvantages and materials are presented in Figure 40 and Table 12.

The mold was manufactured out of ceramics, since if the thermal expansion coefficient of the mold material is vastly different than the laminate, the dimensional accuracy of the part would not remain within prescribed tolerances.

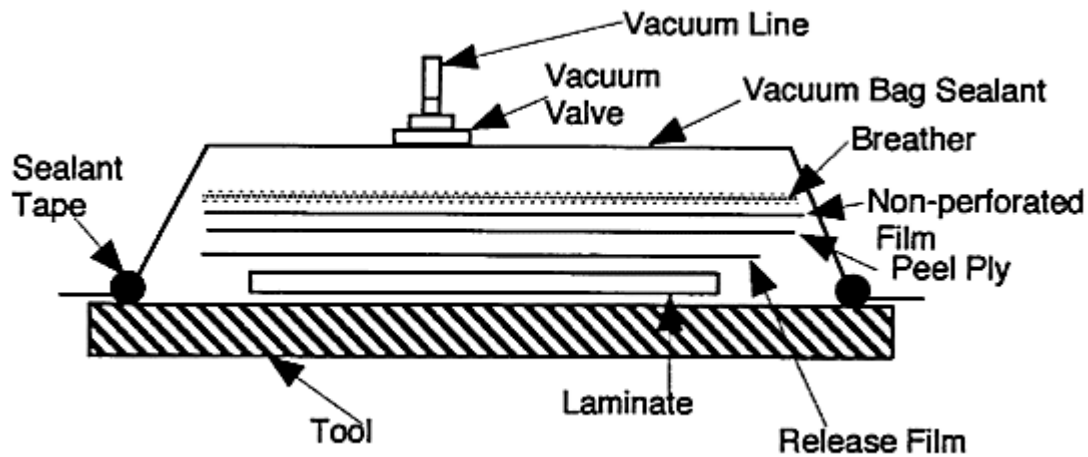


Figure 39: Composite Manufacturing using Vacuum Bagging [29]

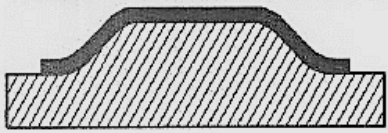
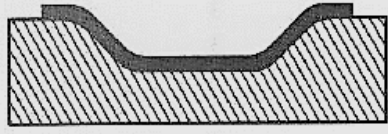
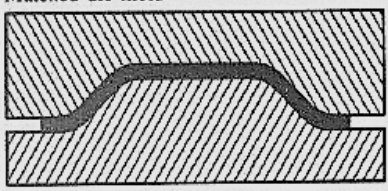
Type	Characteristics
(a) Male mold 	<ul style="list-style-type: none"> <li>• Most commonly used for aircraft parts because of its low cost</li> <li>• Lowest layup cost</li> <li>• Small radius producibility <math>\geq .05</math> inch</li> <li>• Baseline (non-aerodynamic surfaces)</li> <li>• Surface control one side only</li> <li>• Localized control of vacuum bag surface</li> </ul>
(b) Female mold 	<ul style="list-style-type: none"> <li>• Limited use in contour applications because of bend radius</li> <li>• Highest layup cost</li> <li>• Radius producibility <math>\geq .25</math> inch</li> <li>• Localized control of vacuum bag surface</li> <li>• Surface control one side only</li> </ul>
(c) Matched die mold 	<ul style="list-style-type: none"> <li>• Used male/female tooling to control laminate thickness and is very expensive</li> <li>• Best thickness control</li> <li>• Highest tooling cost</li> <li>• Moderate layup cost</li> <li>• OML/IML control (smooth surface both sides)</li> </ul>

Figure 40: Comparison of Mold Types [29]

Table 12: Comparison of common mold materials [29]

Tool Material	Coefficient of Thermal Expansion	Heat Conductivity	Material Cost	Fabrication Cost	Durability
Aluminum	Poor	Good	Good	Fair	Fair
Steel	Good	Good	Good	Poor	Good
Graphite	Excellent	Good	Good	Good	Poor
Ceramics	Excellent	Poor	Good	Fair	Fair
Fiberglass Resin Composite	Poor to Good	Fair	Good	Good	Poor
Graphite Epoxy Composite	Excellent	Fair	High	Fair	Poor

Table 13: Roll Frame - Relationship Matrix - Manufacturing

	Stacking Sequence	# Plies	Material	Orientation	Shape
Weight	0	3	1	0	1
Cost	3	3	1	1	9
Time	3	3	0	1	9

From the manufacturing relational matrix, it can be observed that shape and number of plies are the parameters that influence the manufacturing functional requirements the most, followed by stacking sequence, material and orientation. The design and analysis results of the roll frame after consideration of the manufacturing parameters is shown in Figure 41.

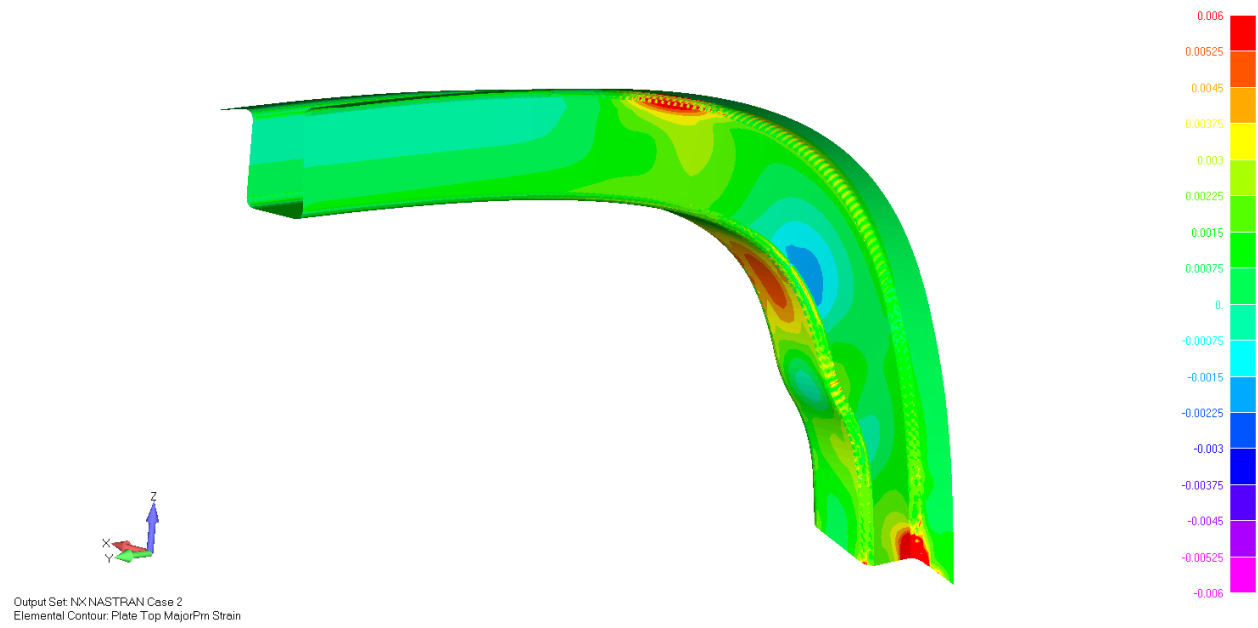


Figure 41: Roll Frame – Manufacturing Parameters- Strain Plot

The combined functional requirements and parameters are established to be:

$$[FR_C] = \{[FR_D]_n, [FR_M]_m\} = \left\{ \begin{array}{c} \textit{Weight} \\ \textit{Strain} \\ \textit{Deflection} \\ \textit{Cost} \\ \textit{Time} \end{array} \right\}$$

$$[DP_C] = \{[DP_D]_j, [DP_M]_k\} = \left\{ \begin{array}{c} \textit{\#Plies} \\ \textit{Stacking Sequence} \\ \textit{Weave} \\ \textit{Material} \\ \textit{Orientation} \\ \textit{Manufacturing Method} \\ \textit{Shape} \end{array} \right\}$$

From the design and manufacturing relational matrices, shape, stacking sequence and number of plies are found to be the most influential parameters. Since the shape of the roll frame was already extensively addressed, the design was therefore optimized further for stacking sequence and number of plies. The following figures show the revised ply layup of the roll frame:

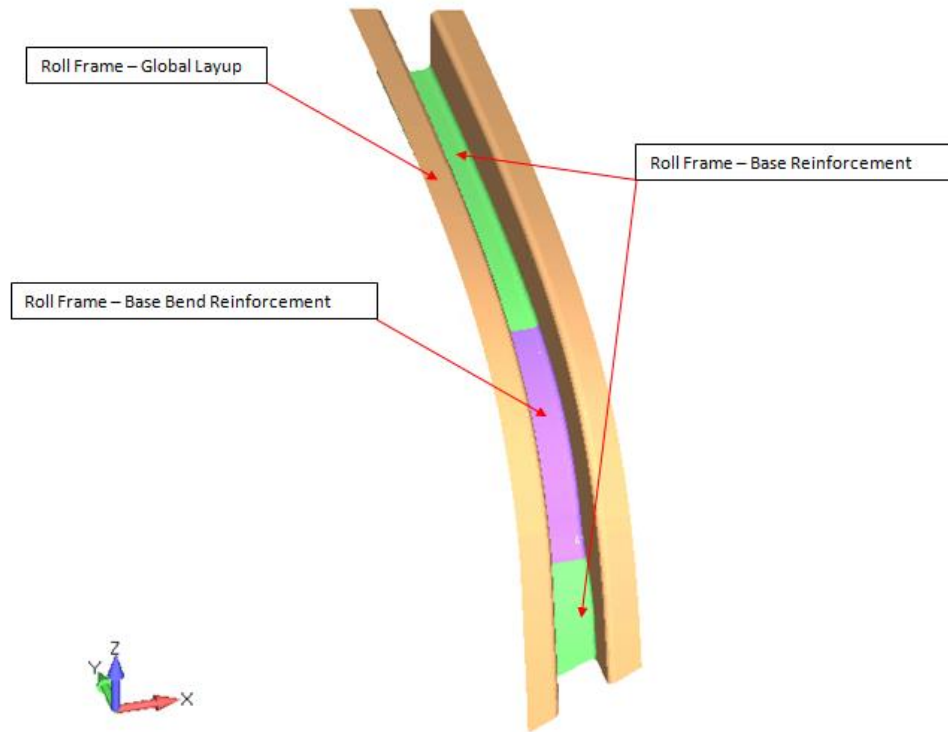


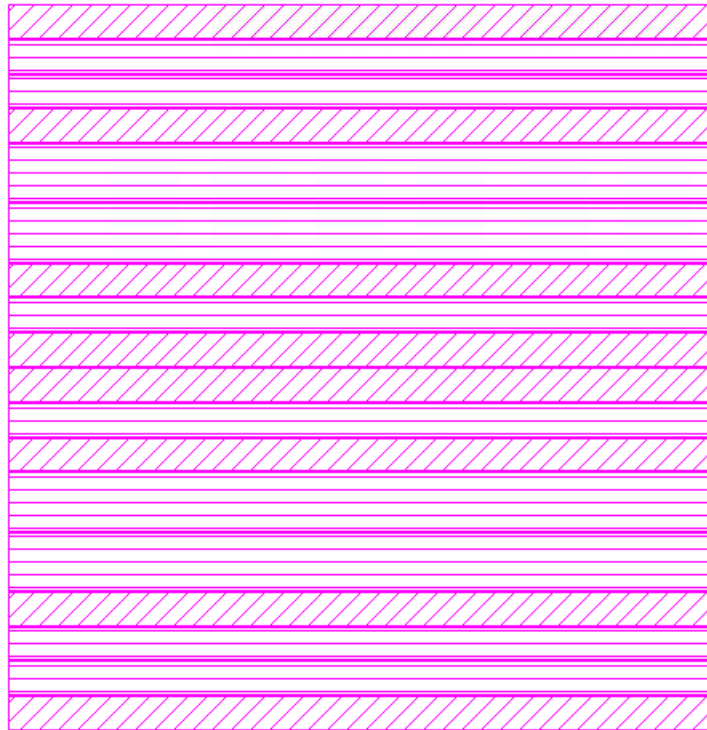
Figure 42: Roll Frame – Ply Regions

Roll Frame - Global Layup	14 Plies: Total Thickness = 0.1295
	14: Thk=0.00925 Ang=45. Mt=2
	13: Thk=0.00925 Ang=0. Mt=2
	12: Thk=0.00925 Ang=0. Mt=2
	11: Thk=0.00925 Ang=45. Mt=2
	10: Thk=0.00925 Ang=45. Mt=2
	9: Thk=0.00925 Ang=0. Mt=2
	8: Thk=0.00925 Ang=45. Mt=2
	7: Thk=0.00925 Ang=45. Mt=2
	6: Thk=0.00925 Ang=0. Mt=2
	5: Thk=0.00925 Ang=45. Mt=2
	4: Thk=0.00925 Ang=45. Mt=2
	3: Thk=0.00925 Ang=0. Mt=2
	2: Thk=0.00925 Ang=0. Mt=2
	1: Thk=0.00925 Ang=45. Mt=2

Figure 43: Roll Frame – Global Layup



Roll Frame - Base

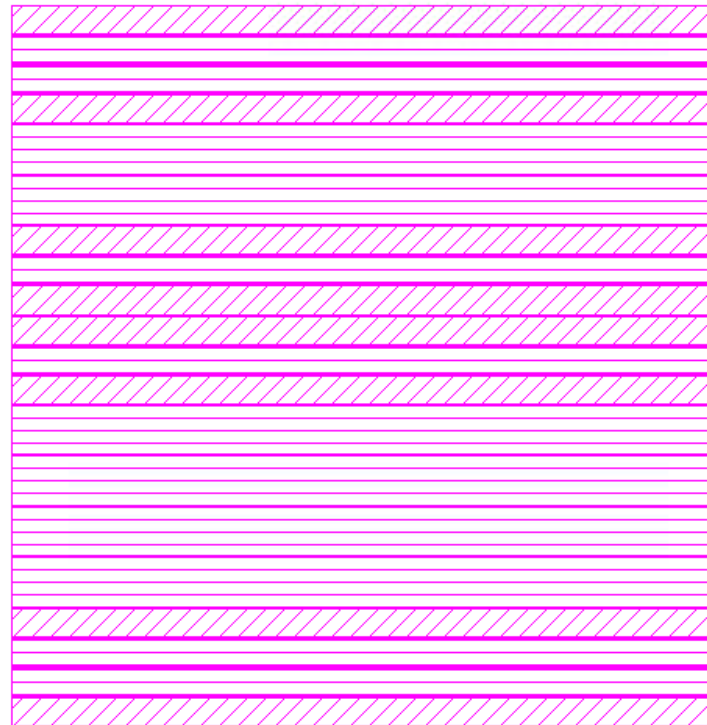


18 Plies: Total Thickness = 0.1925

18:	Thk=0.00925	Ang=45.	Mt=2
17:	Thk=0.00925	Ang=0.	Mt=2
16:	Thk=0.00925	Ang=0.	Mt=2
15:	Thk=0.00925	Ang=45.	Mt=2
14:	Thk=0.01575	Ang=0.	Mt=3
13:	Thk=0.01575	Ang=0.	Mt=3
12:	Thk=0.00925	Ang=45.	Mt=2
11:	Thk=0.00925	Ang=0.	Mt=2
10:	Thk=0.00925	Ang=45.	Mt=2
9:	Thk=0.00925	Ang=45.	Mt=2
8:	Thk=0.00925	Ang=0.	Mt=2
7:	Thk=0.00925	Ang=45.	Mt=2
6:	Thk=0.01575	Ang=0.	Mt=3
5:	Thk=0.01575	Ang=0.	Mt=3
4:	Thk=0.00925	Ang=45.	Mt=2
3:	Thk=0.00925	Ang=0.	Mt=2
2:	Thk=0.00925	Ang=0.	Mt=2
1:	Thk=0.00925	Ang=45.	Mt=2

Figure 44: Roll Frame – Base Reinforcement

Roll Frame - Base Bend



20 Plies: Total Thickness = 0.224

20:	Thk=0.00925	Ang=45.	Mt=2
19:	Thk=0.00925	Ang=0.	Mt=2
18:	Thk=0.00925	Ang=0.	Mt=2
17:	Thk=0.00925	Ang=45.	Mt=2
16:	Thk=0.01575	Ang=0.	Mt=3
15:	Thk=0.01575	Ang=0.	Mt=3
14:	Thk=0.00925	Ang=45.	Mt=2
13:	Thk=0.00925	Ang=0.	Mt=2
12:	Thk=0.00925	Ang=45.	Mt=2
11:	Thk=0.00925	Ang=45.	Mt=2
10:	Thk=0.00925	Ang=0.	Mt=2
9:	Thk=0.00925	Ang=45.	Mt=2
8:	Thk=0.01575	Ang=0.	Mt=3
7:	Thk=0.01575	Ang=0.	Mt=3
6:	Thk=0.01575	Ang=0.	Mt=3
5:	Thk=0.01575	Ang=0.	Mt=3
4:	Thk=0.00925	Ang=45.	Mt=2
3:	Thk=0.00925	Ang=0.	Mt=2
2:	Thk=0.00925	Ang=0.	Mt=2
1:	Thk=0.00925	Ang=45.	Mt=2

Figure 45: Roll Frame – Base Bend Reinforcement

The strain plot results for the optimized roll frame are illustrated in Figure 46.

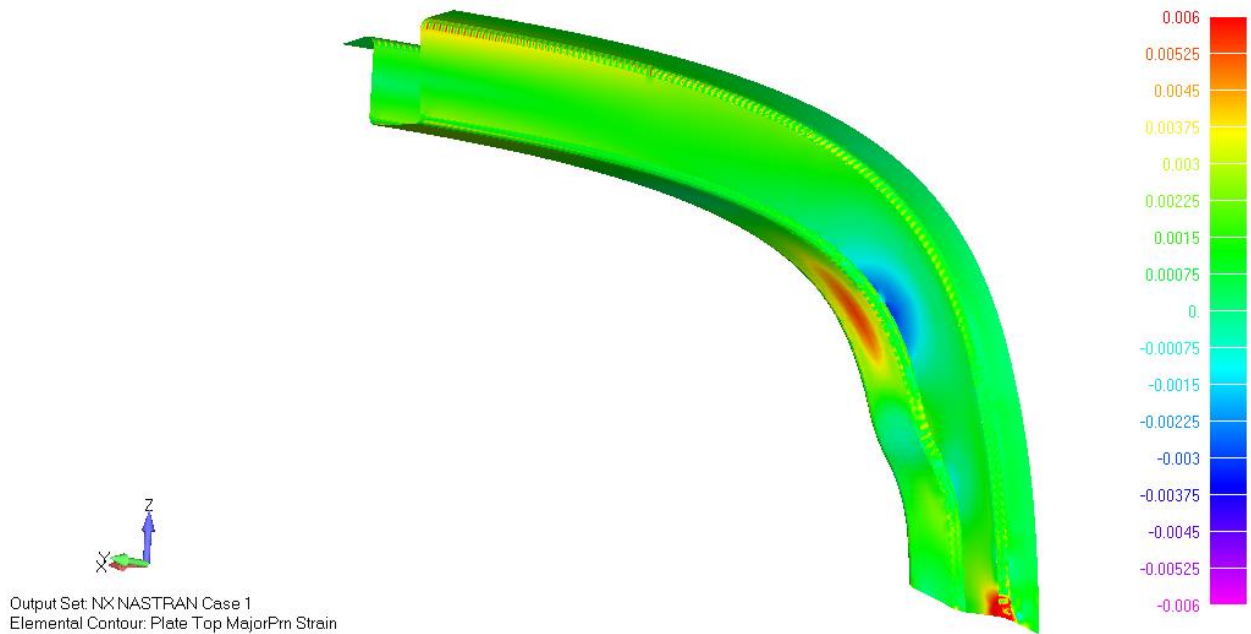


Figure 46: Roll Frame – Optimized Design - Strain Plot

The optimized roll frame design has at least 10% higher load carrying capabilities than the previous designs (when considering only the design or manufacturing parameters) at comparable or reduced weight. However, the lead time of the new frame design is more because of the complex layup involving various fiber types. Various design deficiencies that have been addressed (would not be potentially addressed if design and manufacturing parameters were considered separately) include fiber cracking and void generation due to improper bend radii, dimensional inadequacies due to springback, warping and dissimilar coefficient of thermal expansion.

### 4.3 CASE STUDY 3: COMPOSITE DOOR FOR A FAR 23 AIRCRAFT

#### 4.3.1 DESIGN OBJECTIVE

The Nose Landing Gear (NLG) Bay Door acts as a fairing to the NLG Bay where the NLG rests in a retracted position, held by the uplock. Typical design cases for aircraft doors range from differential pressure loads, gust loads, handling loads and aerodynamic loads.

For light aircraft designed to FAR 23 requirements [23], typical door mechanisms include hinged doors actuated through pushrods or links that interface with the NLG.

The requirements for the NLG bay door for this aircraft are stated as follows:

- 1) The door shall be designed to withstand limit loads without permanent damage
- 2) The deflection at design loads shall be minimal
- 3) The weight of the door shall be minimal
- 4) The door shall be manufactured at the least cost in the shortest time

#### 4.3.2 PARAMETER SPACE GENERATION - CONCEPTUAL DESIGN SELECTION

The most critical functional requirements that will influence the final product are determined from the Technical Requirements Documents (TRD) as follows:

$$[FR] = \begin{bmatrix} Weight \\ Cost \\ Strain \\ Time \\ Deflection \end{bmatrix}$$

The functional requirements are ranked in the order of importance to the customer. The ranking process is determined after extensive interaction among all stakeholders.

$$[FR] = \begin{bmatrix} Deflection \\ Weight \\ Cost \\ Time \\ Load \end{bmatrix}$$

At this stage, several conceptual designs are generated. In this example, three distinct concepts have been explored (illustrated in Figure 47):

- 1) A sandwich design
- 2) A hollow “clamshell” design
- 3) A semi-monocoque design

Concept (a) is of a sandwich construction, comprising of a foam core encapsulated by carbon plies on both sides. Concept (b) is a hollow “clamshell” design where the door is made from two laminated bodies; the lower laminate acts as the external surface and sits flush with the aircraft OML, while the upper laminate with a raised feature is bonded to the lower laminate. Concept (c) is typical for metallic doors with multiple lateral and transverse ribs fastened to a metallic skin; or can be manufactured as a one-piece machined structure.

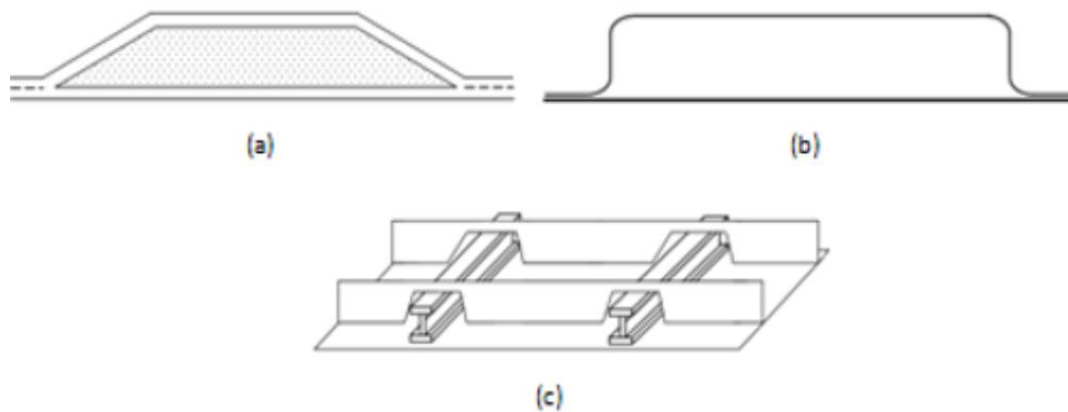


Figure 47: Door Design Concepts

FR \ Designs	Ranking	Sandwich	Hollow	Semi-Monocoque
Deflection	5	⊙	○	⊙
Weight	4	○	⊙	○
Cost	3	⊙	○	Δ
Time	2	⊙	○	Δ
Load	1	⊙	⊙	⊙
Score		41	35	31

Based on the evaluation criteria, Concept (a) was selected for detailed design. By design all three concepts must sustain the design loads and therefore meet the strength criteria. Concept (a) and (c) exhibit higher bending and torsional stiffness due to the use of core material and semi-monocoque design respectively; however, concept (b) sports a lower weight due to its inherent design. Concept (a) scores over the other concepts due to its ease of manufacturing, lower cost and lead time. Concept (a) could be manufactured from a single mold representative of the aircraft door OML, unlike concept design (b) which necessitates a die mold. Furthermore, prior experience with door structures similar to Concept (b) has shown that moisture trapped inside the clamshell can cause structural damage due to repeated freezing and thawing cycles. Concept (c) involves preparing multiple metallic stiffeners and fastening the stiffeners onto the skin or complex machining in case it is manufactured as a one-piece structure.

#### 4.3.3 PARAMETER SPACE INTEGRATION FOR DESIGN PARAMETERS

Since the aircraft in this case is a light, unpressurized aircraft, the door is to be sized for positive and negative pressure cases arising from aerodynamic effects when the aircraft is in flight. Equation 28 has been used to determine the net load acting on the door. The normal force coefficient has been obtained from NACA TM 738 [4].

$$N = \frac{1}{2} \rho V^2 S C_N \quad \text{Equation 28}$$

Using the above equation, the critical load case for the NLG Bay Door was determined to occur when the aircraft flew at a speed of 150 kts (TAS) with an AoA of 30 degrees, producing 38 lbf of force (limit) on the door surface. As per FAR 23.303, the ultimate load is determined by incorporating a safety factor of 1.5 on top of the limit load to obtain 57 lbf.

For the NLG Bay Door, the Functional Requirements and Parameters for Design are established as:

$$[FR_D] = [RM_D] * [DP_D]$$

where,

$$[FR_D] = \begin{bmatrix} \text{Weight} \\ \text{Strain} \\ \text{Deflection} \end{bmatrix}_D$$

$$[DP_D] = \begin{bmatrix} \text{Stacking Sequence} \\ \text{\#Plies} \\ \text{Material} \\ \text{Orientation} \\ \text{Shape} \end{bmatrix}_D$$

##### 4.3.3.1 Material

The material system selected for the composite door was carbon fiber with epoxy resin. The choice of the fiber and resin system is substantiated in Section 4.2.3.1.

Table 14 provides a comparative summary of the common core types used in fabricating composite structures. From the summary, it can be seen that honeycomb core offers the best rigidity to the door structure with the least weight penalty. Therefore, a honeycomb core has been selected for preliminary design.

Table 14: Comparison of common core types [29]

Core Type	Properties
Honeycomb Core	Can be made from any thin sheet material (both metallic and non-metallic) Low weight High Rigidity High Strength Suffers from moisture ingress problems Suffers from facesheet delamination and wrinkling issues Used to manufacture very thick panels Common uses: Aircraft Nose Radome, Wing Leading and Training Edges, Fuselage Floor Panels
Syntactic Core	Easily moldable High compressive, transverse tensile and lateral strength Denser than honeycomb core No facesheet wrinkling problems Provides continuous support to facesheets No moisture ingress issues Lower costs than honeycomb cores Not usually used for constructing thick panels
Foam Core	Easily moldable and processable Less dense than syntactic core High compressive, transverse tensile and lateral strength No moisture ingress issues Lower costs than honeycomb and syntactic cores

#### 4.3.3.2 Shape

The door is sized to resist torsion and bending loads arising from the differential pressure loads during flight. The inclusion of the core serves to provide bending as well as torsional rigidity to the structure while the panels carry the in-plane loads. The bigger the core (especially dimension  $b$ ), the greater the bending and torsional stiffness as given by Equation 29 and Equation 30 [30].

$$K = ab^3 \left[ \frac{16}{3} - \frac{3.36b}{a} \left( 1 - \frac{b^4}{12a^4} \right) \right] \quad \text{Equation 29}$$

$$I = \frac{2a(2b)^3}{12} \quad \text{Equation 30}$$

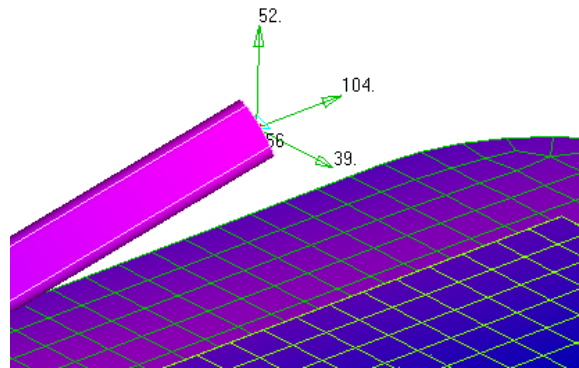
where,

- K Factor dependant on form and cross-section dimensions (for circular sections  $K = J$ )
- I Moment of Inertia
- a Half the distance of the base of the cross-section [30]
- b Half the distance of the height of the cross-section [30]

For the base design, a standard 0.5-inch-thick core is used. Cut-outs to the core are necessary to facilitate installation of the rod end bracket and accommodate the NLG tire envelope.

#### 4.3.3.3 Number of Plies

Similar to the roll frame, the number of plies in the laminate is dependent on the strength and stiffness requirements of the structure. A composite bearing and pull-thru analysis is presented below to determine if the number of plies shown in Figure 48 are adequate.





**Part Name:** Composite Door Panel  
**Section:** Attachment Fasteners  
**Design Case:** Max. Differential Pressure  
**Material:** Carbon Q-I

## Composite Bearing and Pull Thru V0.1

### Geometric Parameters

$d = 0.085$  in  
 $t = 0.056$  in  
 $d_w = 0.085$  in

### Composite Material

Matl. Name = Carbon Q-I  
 $F_{br,allowable} = 34.800$  ksi  
 $F_{s,allowable} = 3.625$  ksi

### Applied Loads (Ultimate)

$P_{shear} = 0.111$  kip  
 $P_{axial} = 0.052$  kip

Material	Bearing Allowables	Units
Glass Q-I	21.800	ksi
Glass non Q-I	14.500	ksi
Carbon Q-I	34.800	ksi
Carbon non Q-I	21.800	ksi

### Bearing Check

$f_{br} = 23.418$  ksi  
 $F_{br,allowable} = 34.800$  ksi  
 $MS_{ult} = 0.486$

### Pull Thru Check

$f_s = 3.490$  ksi  
 $F_{s,allowable} = 3.625$  ksi  
 $MS_{ult} = 0.039$

Material	Pull Thru Allowables	Units
All materials	3.625	ksi

Based on the interface loads shown and assuming a six ply layup, the diameter of the interfacing pins (door bracket to pushrod) required is 0.085 inch.

#### 4.3.3.4 Ply Orientation and Stacking Sequence

The ply orientation and stacking rules listed in section 4.2.4.3 have been followed to arrive at the door configuration illustrated in Figure 48.



Figure 48: Ply Orientation, Stack-up Sequence and Number of Plies for the NLG Bay Door

Table 15: Door - Relationship Matrix - Design

	Stacking Sequence	# Plies	Material	Orientation	Shape
Weight	0	3	3	0	1
Strain	9	3	0	1	1
Deflection	9	1	0	1	1

From the design relational matrix, it can be observed that stacking sequence and number of plies are the parameters that influence the design functional requirements the most, followed by material, orientation and shape. The design of the roll frame after consideration of the design parameters is shown in Figure 49.

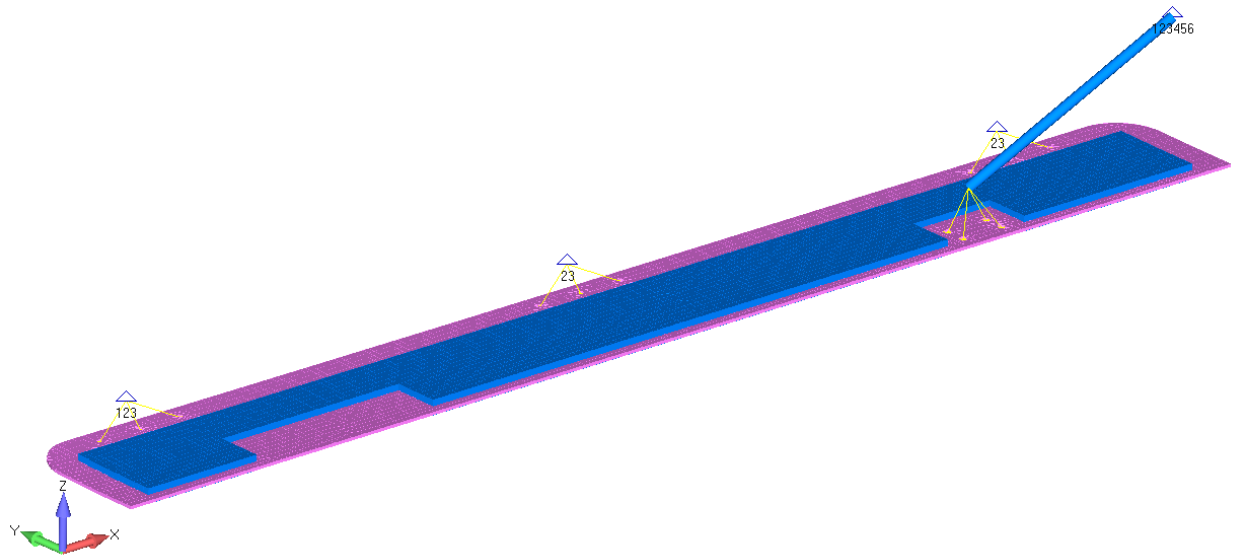


Figure 49: Door – Base Design – Design Parameters

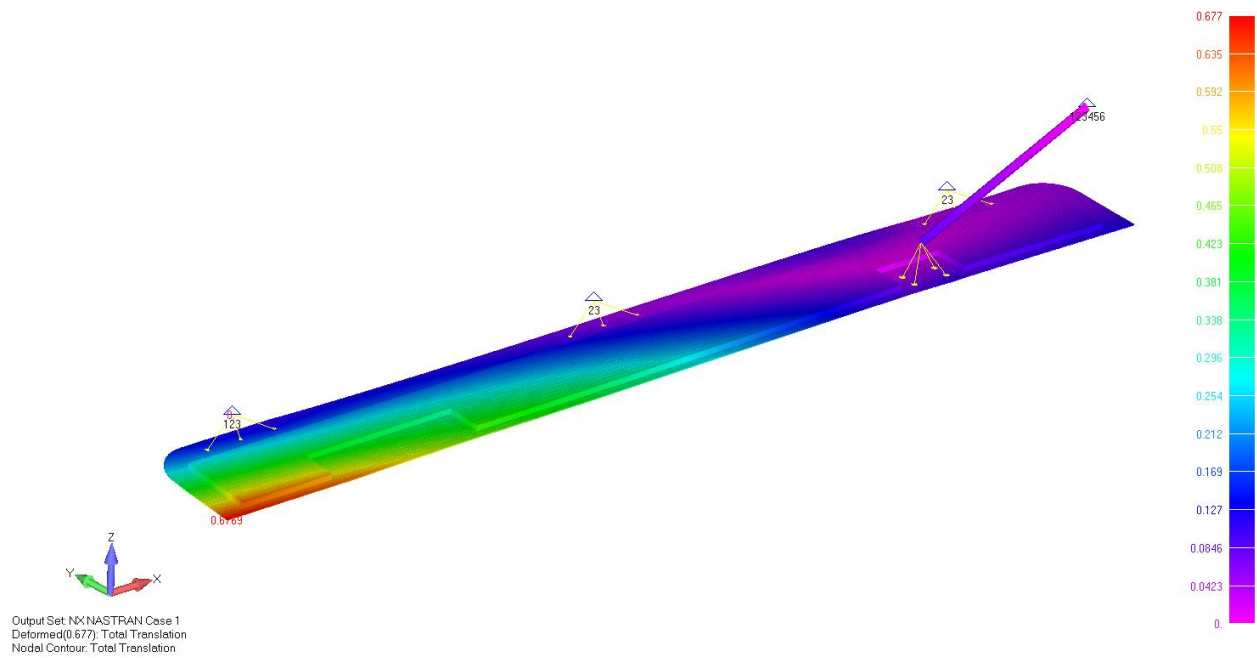


Figure 50: Door – Design Parameters - Deflection Plot

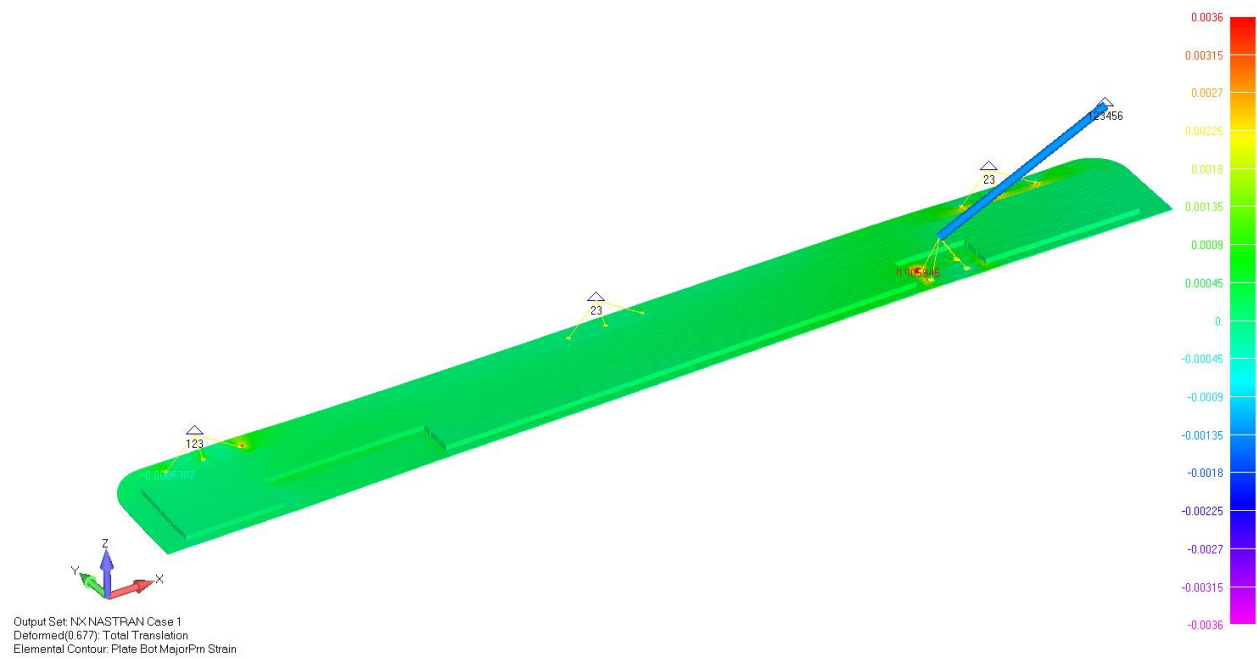


Figure 51: Door – Design Parameters - Strain Plot

#### 4.3.4 PARAMETER SPACE INTEGRATION FOR MANUFACTURING PARAMETERS

For the NLG Bay Door, the Functional Requirements and Parameters for Manufacturing are established as:

$$[FR_M] = [RM_M] * [DP_M]$$

where,

$$[FR_M] = \begin{bmatrix} Weight \\ Cost \\ Time \end{bmatrix}_M$$

$$[DP_M] = \begin{bmatrix} \#Plies \\ Stacking Sequence \\ Material \\ Orientation \\ Shape \\ Manufacturing Method \end{bmatrix}_M$$

Influence of each of the manufacturing parameters on the functional requirements are discussed below.

##### 4.3.4.1 Material

Although Honeycomb cores typically present the best combination of properties and are used extensively, in this particular application the honeycomb core has been replaced with a foam core. Foam cores are simpler, easy to handle and have lower costs. Use of honeycomb cores in panels which are susceptible to FOD (Foreign Object Damage) and moisture ingress presents significant maintainability challenges for in-service personnel. Foam cores on the other hand have much higher compressive strength, are typically more resilient to external damages and do not present moisture ingress challenges.

##### 4.3.4.2 Shape

Since the size of the door is fixed, the only variable that can be optimized is the shape of the core and the ply layup. The core depth has been reduced from the 0.5 in to 0.315 in, to accommodate for the tire grown envelope, which is the maximum tire volume. Furthermore, the core has been shaped such that there is

a gradual increase in the depth (“trapezoidal cross-section”) rather than a sudden increase (“box cross-section”). This has been done to prevent fiber fracture, ply delamination and void generation at the transition zones.

#### 4.3.4.3 Ply Orientation, Stacking Sequence and Number of Plies

The number of plies overlapping the core have been increased with several plies added locally over the core transition zone to mitigate the loss of bending and torsional stiffness resulting from core thickness reduction and shaping. The modified stacking sequence of the door laminate is illustrated in Figure 52.

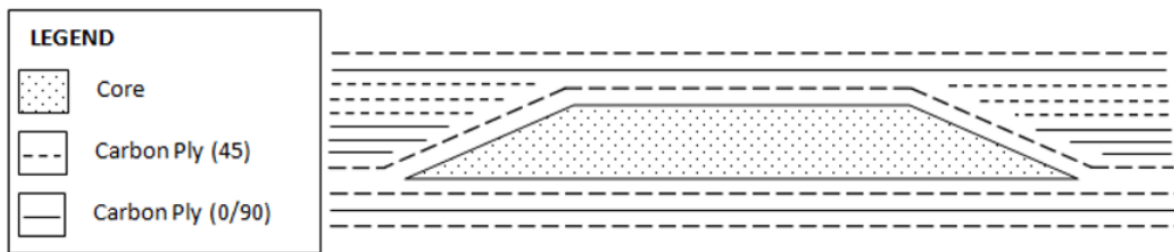


Figure 52: Ply Orientation, Stack-up Sequence and Number of Plies for the NLG Bay Door

The bearing and pull-thru check at the fastener locations are shown below.

**Part Name:** Composite Door Panel  
**Section:** Attachment Fasteners  
**Design Case:** Max. Differential Pressure  
**Material:** Carbon Q-I

Composite Bearing and Pull Thru V0.1

<b>Geometric Parameters</b>	<b>Composite Material</b>
d = 0.188 in	Matl. Name = Carbon Q-I
t = 0.056 in	F <sub>br,allowable</sub> = 34.800 ksi
d <sub>w</sub> = 0.188 in	F <sub>s,allowable</sub> = 3.625 ksi

#### Applied Loads (Ultimate)

P <sub>shear</sub> = 0.111 ki		
P <sub>axial</sub> = 0.052 ki		
Material	Bearing Allowables	Units
Glass Q-I	21.800	ksi
Glass non Q-I	14.500	ksi
Carbon Q-I	34.800	ksi
Carbon non Q-I	21.800	ksi

#### Bearing Check

f<sub>br</sub> = 10.616 ksi  
 F<sub>br,allowable</sub> = 34.800 ksi  
 MS<sub>ult</sub> = **2.278**

#### Pull Thru Check

Material	Pull Thru Allowables	Units
All materials	3.625	ksi

f<sub>s</sub> = 1.582 ksi  
 F<sub>s,allowable</sub> = 3.625 ksi  
 MS<sub>ult</sub> = **1.291**

A standard 3/16" dia. fastener has been used to keep costs low.

#### 4.3.4.4 Manufacturing Method

The door is manufactured using the wet layup, vacuum bagging and curing approach similar to the roll frame described in Case II. The mold used is a male mold and is manufactured from ceramic materials. Since the door structure is exposed to the elements and falls within a pre-defined lightning zone, copper mesh has been incorporated into the laminate to protect the structure from lightning strikes.

The manufacturing process starts with preparing the mold with application of release agent and primer, followed by the copper mesh; the OML or Bottom Face plies are laid thereafter. The machined foam core, sized to the correct thickness is subsequently bonded onto the plies using an adhesive paste. The core is positioned with help of tooling fabricated prior to the build. Thereafter the inner mold line (IML) or Top face plies are laid up; the breather cloth is placed and the entire mold along with the laminate is vacuum bagged and cured. Figure 53 illustrates the manufacturing process.

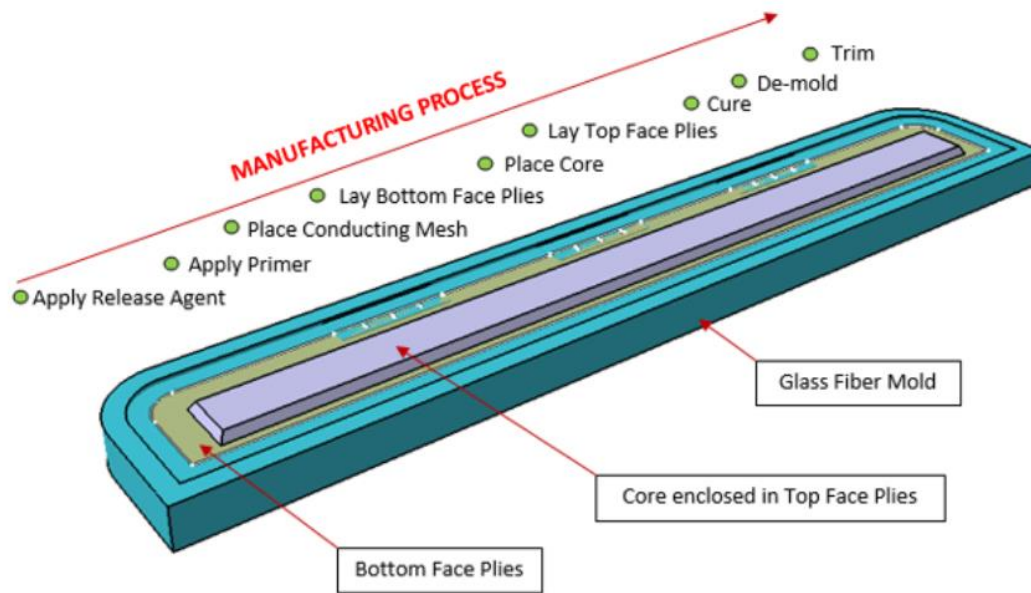


Figure 53: Composite Door Manufacturing Process

Table 16: Door - Relationship Matrix - Manufacturing [29]

	Stacking Sequence	# Plies	Material	Orientation	Shape	Manufacturing Method
Weight	0	3	1	0	1	1
Cost	3	3	1	1	1	3
Time	3	3	0	1	1	1

From the manufacturing relational matrix, it can be observed that number of plies and stacking sequence are the parameters that influence the manufacturing functional requirements the most, followed by



material, orientation, shape and manufacturing method. The design and analysis results of the roll frame after consideration of the manufacturing parameters is shown in Figure 54.

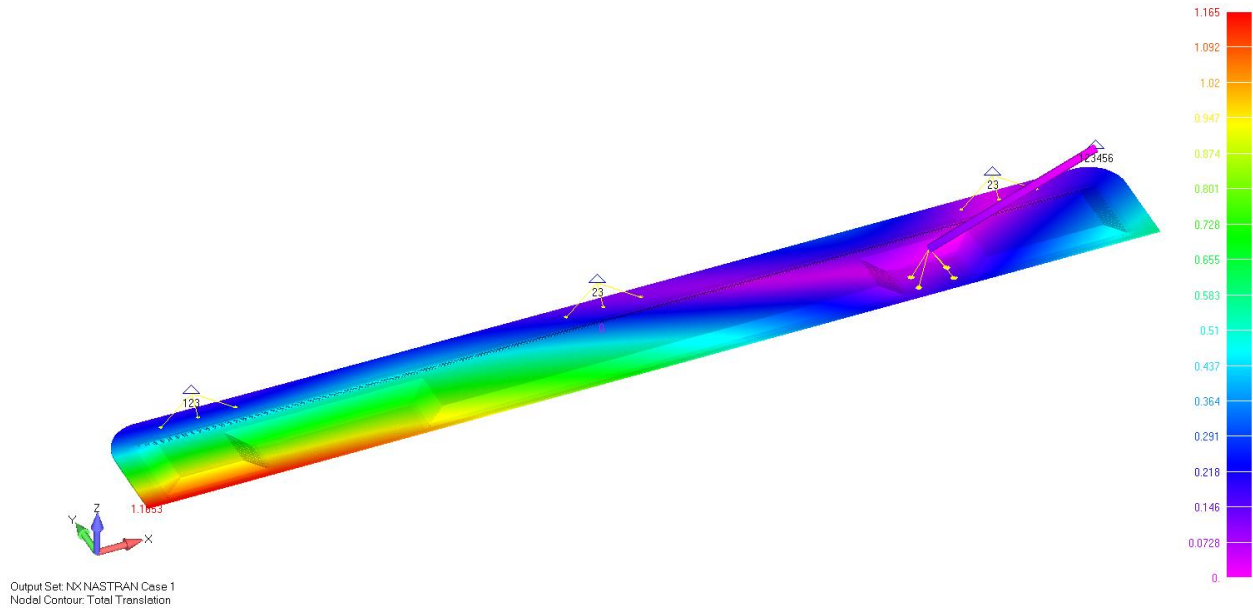


Figure 54: Door – Manufacturing Parameters - Deflection Plot

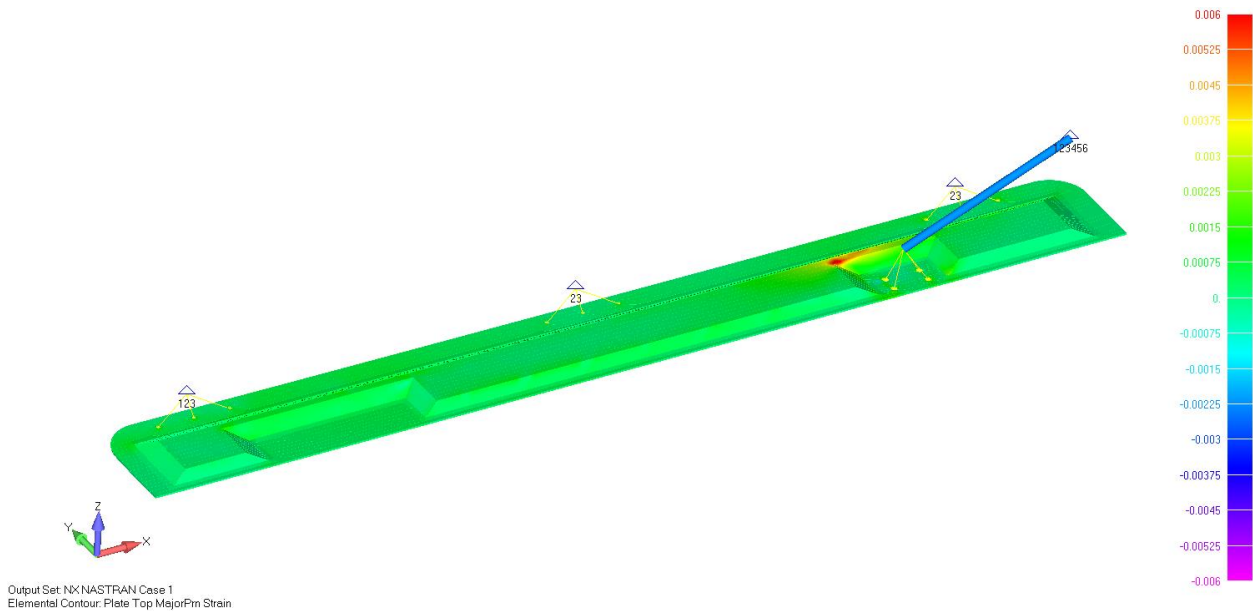


Figure 55: Door – Manufacturing Parameters - Max Principal Strain Plot

The combined functional requirements and parameters are established to be:

$$[FR_C] = \{[FR_D]_n, [FR_M]_m\} = \left\{ \begin{array}{c} \textit{Weight} \\ \textit{Strain} \\ \textit{Deflection} \\ \textit{Cost} \\ \textit{Time} \end{array} \right\}$$

$$[DP_C] = \{[DP_D]_j, [DP_M]_k\} = \left\{ \begin{array}{c} \textit{\#Plies} \\ \textit{Material} \\ \textit{Orientation} \\ \textit{Manufacturing Method} \\ \textit{Shape} \\ \textit{Stacking Sequence} \end{array} \right\}$$

From the design and manufacturing relational matrices, shape, stacking sequence and number of plies are found to be the most influential parameters. However, there is limited room for further optimization and it is determined that further optimization results in diminishing returns. Therefore the stacking sequence illustrated in Figure 52 and the result plots in Figure 54/Figure 55 are considered optimized for this application.

However, when compared to the base design, the optimized design is lighter by almost 20% on account of the core thickness reduction; furthermore, the cost and lead time of the optimized design is significantly less because of the use of a foam core compared to a honeycomb core.

## 5 CONCLUSION AND FUTURE WORK

A parametric, concurrent design methodology for manufacturing of metallic and composite structures is established. The methodology has been developed with the intent to bring down production costs, reduce product development times without sacrificing design functions by incorporating Design for Manufacturing (DFM) principles. The methodology bridges the gap between designers and manufacturers such that all aspects of the design right from functionality to in-service issues that might arise during service are considered before the design is frozen resulting in a “first time right” product.

Knowledge from existing product development models such as SBCE, PuCC and QFD has been drawn upon extensively to develop the process described in this study. Literature on “Design Optimization for Manufacturing” and “Multivariable Design Optimization” have also been referenced.

Three case studies have been presented to reinforce the methodology presented. Case I documents the design of a sheet metal bracket used in the flight control system of a FAR 23 class of aircraft. Case II illustrates the use of 2D composite structures to fabricate a roll frame. Case III involves the development of a 3D composite door for a light unpressurized aircraft. Although, the methodology has been applied on aircraft structures, the principles can be applied to all structures regardless of the application.

For each of the three case studies a separate optimization method has been employed. Case I uses an analytical approach, Case II uses FEM while CASE III employs a hybrid approach comprising of both FEM and analytical calculations.

Currently, many commercial optimization packages are available such as Abaqus Topology Optimization and Altair Inspire; however, the biggest challenge facing their widespread use is their inability to produce manufacturable designs for complex structures. Although the designs produced using commercial packages can be manufactured using additive manufacturing techniques, the structure may not meet all other functional requirements such as reduced lead time and cost.

Areas of future work include use of existing multi variable algorithms to compare pareto-optimal designs with in-service products. Specific refinements can be made to the sharing parameter and fitness parameter within evolutionary algorithms based on specific functional requirements to make the results from evolutionary algorithms more manufacturable.

Knowledge based engineering using deep learning and artificial intelligence is another area that needs to be explored, especially since certain structures require prior domain knowledge to be optimized for both design and manufacturing requirements.

However, despite advances in computing by leaps and bounds and development of technologies such as artificial intelligence, there will always be a requirement for human involvement in some form or another to truly ensure that designs meet their intended objectives while being easy to manufacture, service and dispose off. Therefore, it is imperative that designers and manufacturers with expertise on the various aspects of product development work together while utilizing advanced tools to develop products that can stand the test of time.

## 6 APPENDICES

### 6.1 APPENDIX-I: ROD END BEARINGS

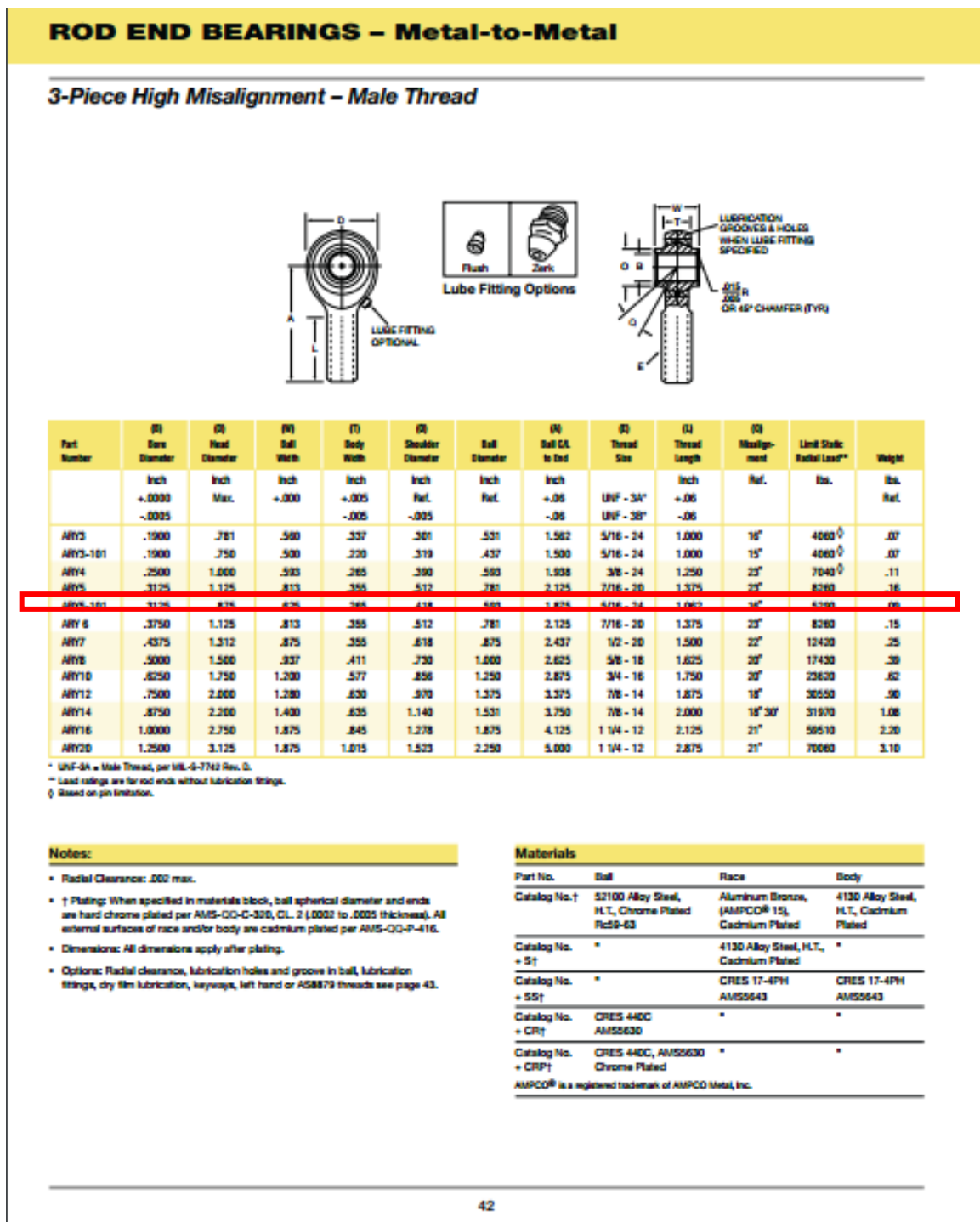


Figure 56: 3 Piece High Misalignment Rod End from NHBB

## 6.2 APPENDIX-II: ANALYSIS OF CLEVIS JOINTS

Clevis Joints are typical in aerospace structures and comprise of two interfacing components held by a pin. The interface is provided with a male lug on one component and female lugs on the other component. The most common type of clevis joint are double shear clevis joints characterized by two female lugs and one male lug.

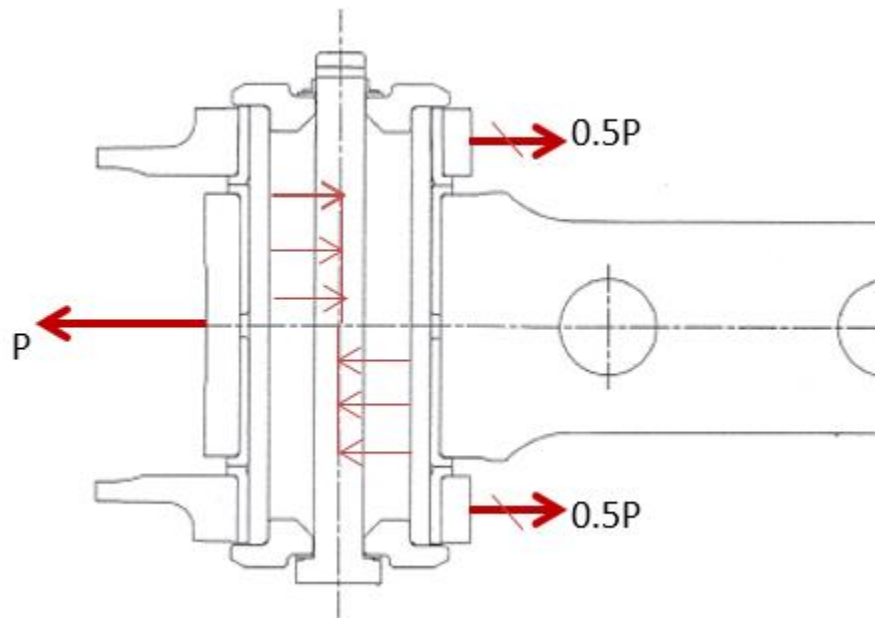


Figure 57: Example of a Clevis Joint

Analysis of clevis joints involves the following steps:

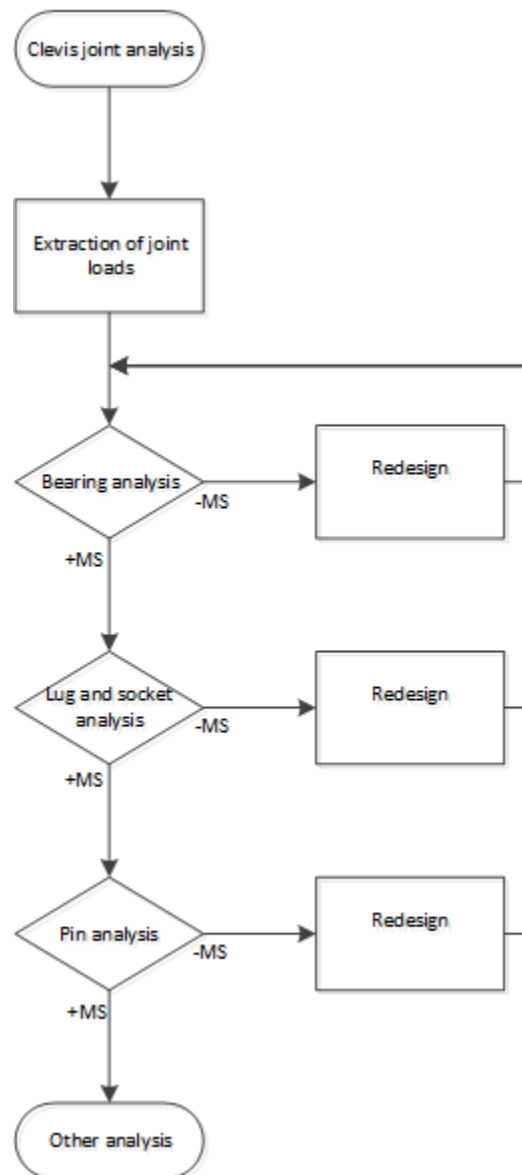


Figure 58: Clevis Joint Analysis Methodology

For transition and interference fit joints, and for joints where the stiffness between the lugs and the pin is not significant, a uniform load distribution is assumed to be acting on the joint. A 50:50 joint load distribution is considered on the female lugs of the double shear clevis joints. The male lug is analyzed using the full joint load.

### 6.2.1 BEARING ANALYSIS

Once the loads on the lugs are determined, a bearing check is conducted. Average bearing stresses are determined using Equation 31. For components that are coated, after plating component dimensions shall be used for bearing stress calculations.

$$f_{br} = \frac{FF * P_{br}}{A_{net}} \quad \text{Equation 31}$$

where,

- $f_{br}$  = Average bearing stress
- $P_{br}$  = Load applied on the bearing (working, limit/ ultimate)
- $A_{net}$  = Projected net bearing area
- $FF$  = Fitting factor ( $FF=1.15$ )

A fitting factor of 1.15 is used as per FAR 23.625 [23] in the average bearing stress calculation to account for uncertainties such as variations in the bearing load distribution and material properties.

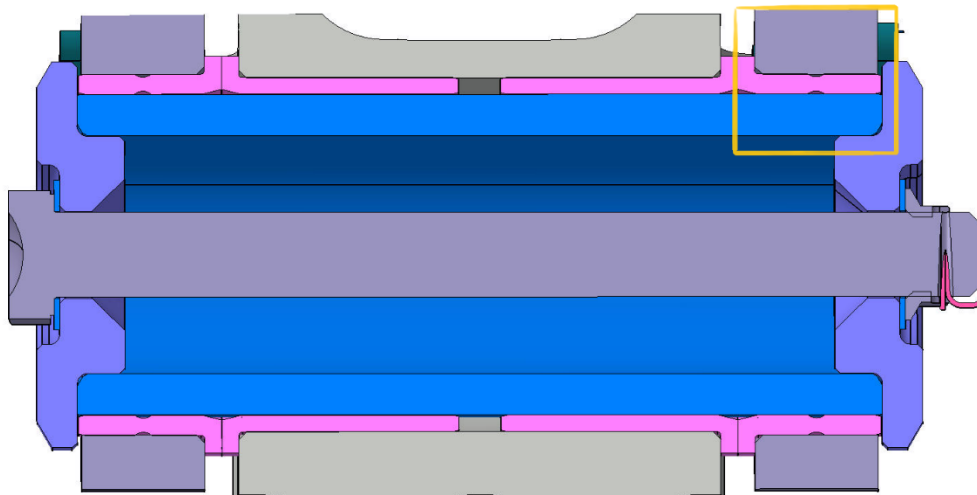


Figure 59: Cross Section of a Double Shear Clevis Joint



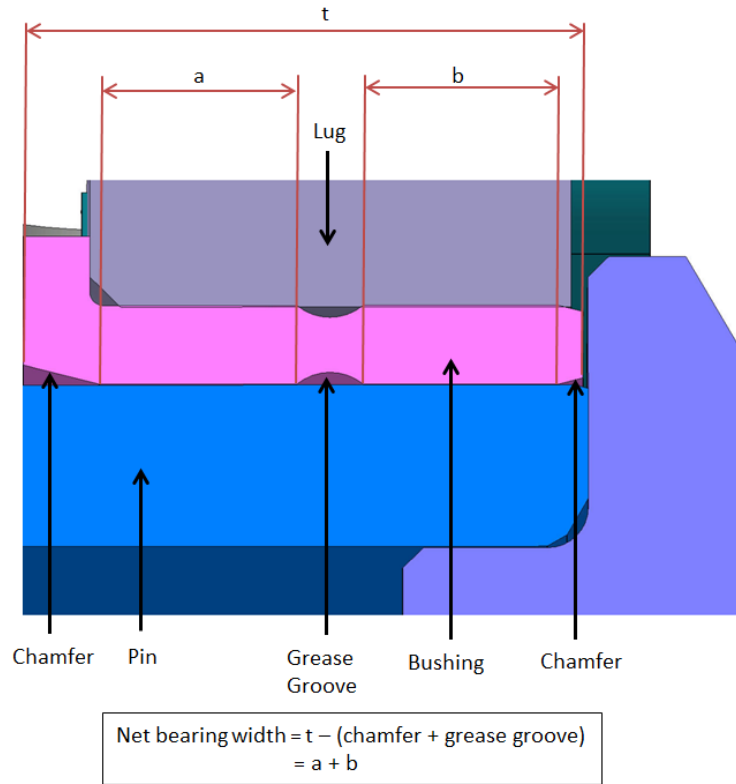


Figure 60: Bearing Area

$$A_{\text{net}} = D_{\text{min}} * (t_{\text{min}} - \text{grease grooves} - \text{chamfers})$$

Equation 32

The bearing margin of safety is then determined using:

$$MS = \frac{F_{br}}{f_{br}} - 1$$

Equation 33

where,

$f_{br}$  = Average bearing stress  
 $F_{br}$  = Allowable bearing strength  
 $MS$  = Margin of safety

## 6.2.2 LUG ANALYSIS

Lug Analysis involves determining the magnitude and orientation of the applied loads, determining the lug geometry and checking to ensure that the stresses for each mode of failure are below the allowable strength.

The primary checks that are conducted on the lug are as follows:

1. Shear Bearing Check
2. Net-Section Tension Check
3. Transverse Check

### 6.2.2.1 Lugs Loaded Axially

For lugs loaded axially, failure can occur by either shear-bearing failure or tension failure.

#### 6.2.2.1.1 Shear-Bearing Check

The allowable ultimate load to avoid shear-bearing failure is:

$$P_{bru} = K_{br} A_{br} F_{tu} \quad \text{Equation 34}$$

Where

$P_{bru}$  = Allowable ultimate load to avoid shear-bearing failure

$K_{br}$  = Shear-bearing efficiency factor

$A_{br}$  = Projected bearing area ( $A_{br} = D \cdot t$ )

$F_{tu}$  = Ultimate tensile strength of lug material

The allowable axial load attributed to shear-bearing yield strength

$$P_{ya} = C \frac{F_{tyx}}{F_{tux}} P_{u,min} \quad \text{Equation 35}$$

where

$P_{ya}$  = Allowable yield load on lug for axial loading

$C$  = Yield factor

$F_{tux}$  = Ultimate tensile strength of lug material in cross grain direction

$F_{tyx}$  = Tensile yield strength of lug material in cross grain direction

$P_{u,min}$  = Smaller of  $P_{bru}$  or  $P_{tu}$

#### 6.2.2.1.2 Net-Section Tension Check

The allowable ultimate load to avoid tension failure is:

$$P_{tu} = K_t A_t F_{tu} \quad \text{Equation 36}$$

where

$P_{tu}$  = Allowable ultimate load to avoid tension failure  
 $K_t$  = Tension efficiency factor which accounts for stress concentration  
 $A_t$  = Minimum net-section area for tension ( $A_t = t * (W-D)$ )  
 $F_{tu}$  = Ultimate tensile strength of lug material

#### 6.2.2.2 Lugs Loaded Transversely

A transversely loaded lug is checked for failure for ultimate and limit transverse loads.

##### 6.2.2.2.1 Allowable Ultimate Load to Avoid Transverse Failure

For lugs loaded transversely, the average area ( $A_{av}$ ) is defined as:

$$A_{av} = \frac{6}{\left(\frac{3}{A_1}\right) + \left(\frac{1}{A_2}\right) + \left(\frac{1}{A_3}\right) + \left(\frac{1}{A_4}\right)} \quad \text{Equation 37}$$

Where

$$A_1 = A_4 = \left( \frac{D}{2 * \sqrt{2}} (\tan \alpha - 1) + \frac{R}{\cos \alpha} \right) * t \quad \text{Equation 38}$$

$$A_2 = \left( \frac{R}{\cos \alpha} - \frac{D}{2} \right) * t \quad \text{Equation 39}$$

$$A_3 = \left( R - \frac{D}{2} \right) * t \quad \text{Equation 40}$$

The allowable ultimate load to avoid transverse failure is determined by:

$$P_{tru} = K_{tru} A_{br} F_{tux} \quad \text{Equation 41}$$

where

$P_{tru}$  = Allowable ultimate load to avoid transverse failure  
 $K_{tru}$  = Transverse load (ultimate) efficiency factor (use Figure 14 for hand calculations)  
 $A_{br}$  = Projected bearing area ( $A_{br} = D * t$ )  
 $F_{tux}$  = Ultimate tensile strength of lug material in cross grain direction

#### 6.2.2.2.2 Allowable Transverse Yield Load

The allowable yield load on the lug is:

$$P_{ytr} = K_{try} A_{br} F_{tyx} \quad \text{Equation 42}$$

where

$P_{ytr}$  = Allowable yield load on lug for transverse loading

$K_{try}$  = Transverse load (yield) efficiency factor (use Figure 14 for hand calculations)

$A_{br}$  = Projected bearing area ( $A_{br} = D \cdot t$ )

$F_{tyx}$  = Tensile yield strength of lug material in cross grain direction

#### 6.2.2.3 Lugs Loaded Obliquely

For obliquely loaded lugs the applied load is resolved into axial and transverse components and the allowable loads for each direction is calculated separately.

#### 6.2.2.4 Lug Margin of Safety Calculation

Margin of safety is the percentage by which the ultimate strength of a member exceeds the design load.

An interaction equation is used to determine the margin of safety for lugs:

$$(R_a^{1.6} + R_{tr}^{1.6}) = 1 \quad \text{Equation 43}$$

$$M.S. = \frac{1}{FF(R_a^{1.6} + R_{tr}^{1.6})^{0.625}} - 1 \quad \text{Equation 44}$$

where

MS = Margin of safety

FF = Fitting factor (FF = 1.15)

For limit load (the maximum load a structure is expected to be subjected to during operational life):

$R_a = R_{a,lim} = (\text{Axial component of applied load}) / (P_{ya})$

$R_{tr} = R_{tr,lim} = (\text{Transverse component of applied load}) / (P_{ytr})$

For ultimate load (1.5 \* limit load):

$R_a = R_{a,ult} = (\text{Axial component of applied load}) / (\text{Smaller of } P_{bru} \text{ and } P_{tu})$

$R_{tr} = R_{tr,ult} = (\text{Transverse component of applied load}) / (P_{tru})$

The efficiency factors used to determine the lug margin of safety are illustrated in the following figures:

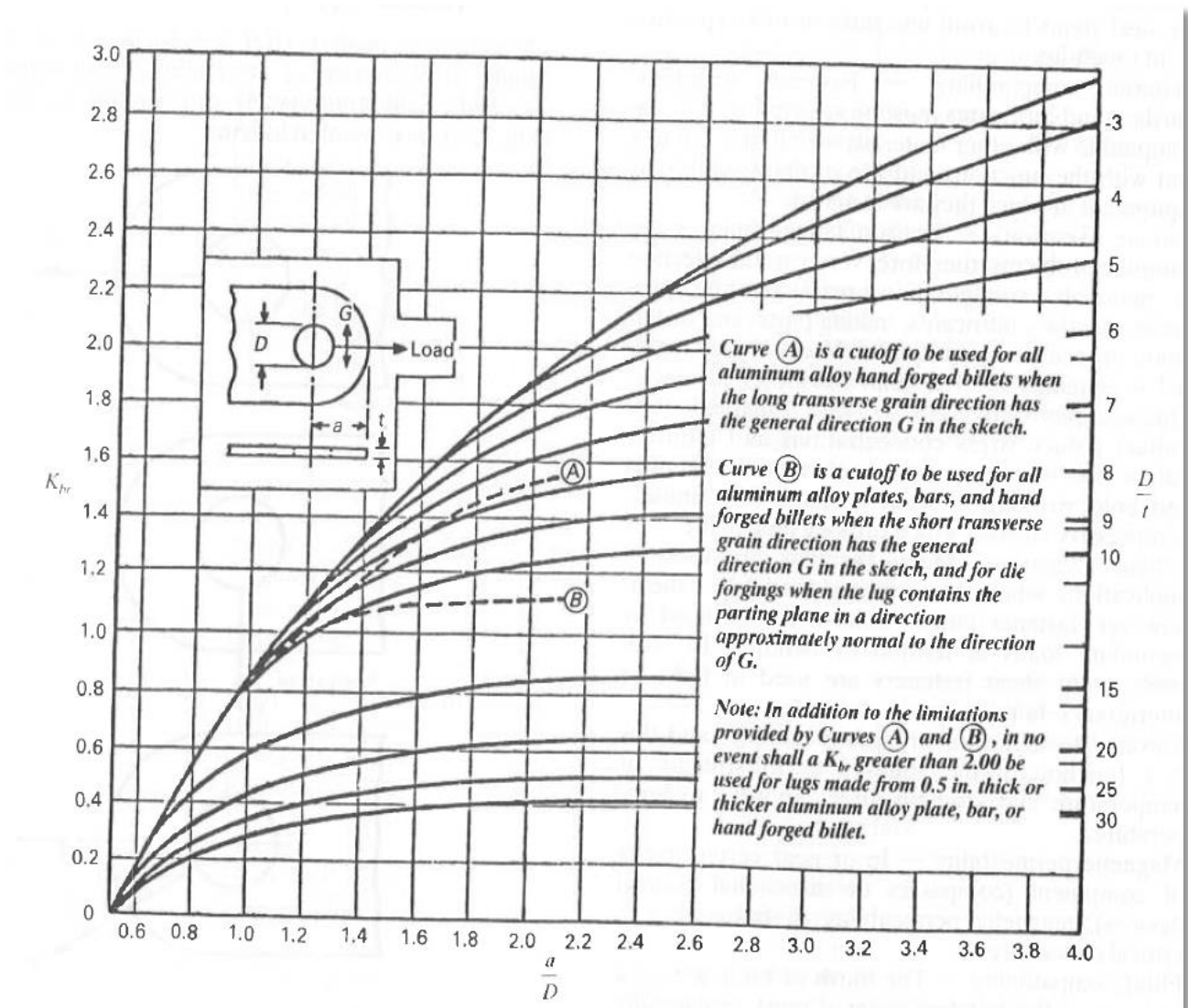
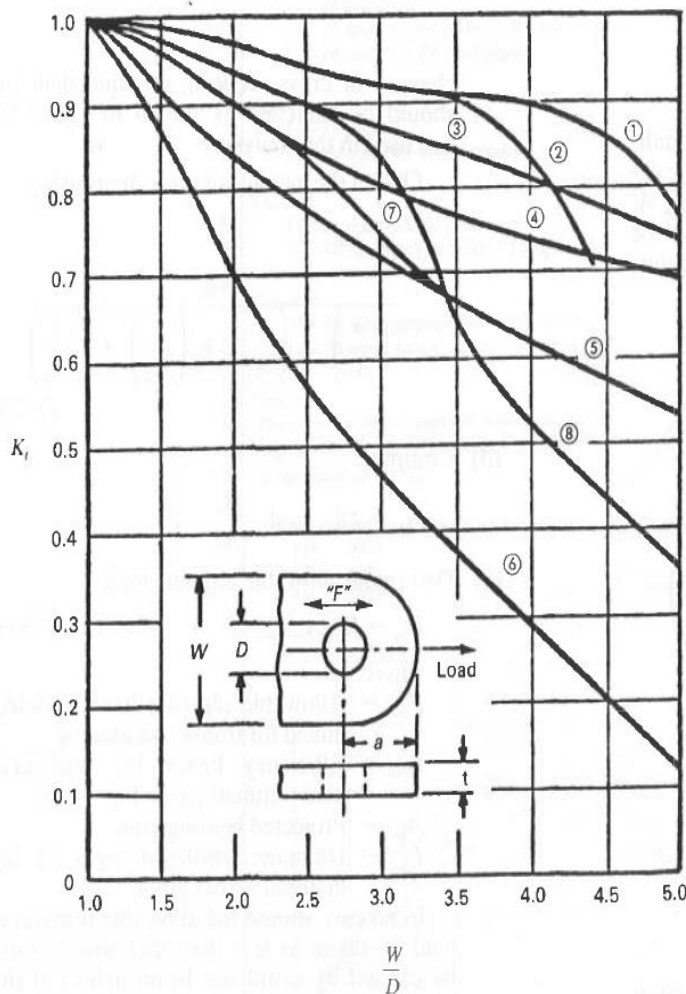


Figure 61: Shear bearing efficiency factor  $K_{br}$  [27]



Legend  $L$ ,  $LT$  and  $ST$  indicate grain in direction  $F$  in sketch:

Aluminum designation:

14S-2014

24S-2024

75S-7075

Curve ①

4130 steel

14S-T6 and 75S-T6 plate  $\leq 0.5$  in ( $L$ ,  $LT$ )

75S-T6 bar and extrusion ( $L$ )

14S-T6 hand forged billet  $\leq 144$  sq in ( $L$ )

14S-T6 and 75S-T6 die forgings ( $L$ )

Curve ②

14S-T6 and 75S-T6 plate  $> 0.5$  in,  $\leq 1$  in

75S-T6 extrusion ( $LT$ ,  $ST$ )

75S-T6 hand forged billet  $\leq 36$  sq in ( $L$ )

14S-T6 hand forged billet  $> 144$  sq in ( $L$ )

14S-T6 hand forged billet  $\leq 36$  sq in ( $LT$ )

14S-T6 and 75S-T6 die forgings ( $LT$ )

Curve ③

24S-T6 plate ( $L$ ,  $LT$ )

24S-T4 and 24S-T42 extrusion ( $L$ ,  $LT$ )

Curve ④

24S-T4 plate ( $L$ ,  $LT$ )

24S-T3 plate ( $L$ ,  $LT$ )

14S-T6 and 75S-T6 plate  $> 1$  in ( $L$ ,  $LT$ )

24S-T4 bar ( $L$ ,  $LT$ )

75S-T6 hand forged billet  $> 36$  sq in ( $L$ )

75S-T6 hand forged billet  $\leq 16$  sq in ( $LT$ )

Curve ⑤

75S-T6 hand forged billet  $> 16$  sq in ( $LT$ )

14S-T6 hand forged billet  $> 36$  sq in ( $LT$ )

Curve ⑥

Aluminum alloy plate, bar, hand forged billet, and die forging ( $ST$ )

75S-T6 bar ( $LT$ )

Curve ⑦

18-8 stainless steel, annealed

Curve ⑧

18-8 stainless steel, full hard. Note: for  $\frac{1}{4}$ ,  $\frac{1}{2}$  and  $\frac{3}{4}$  hard, interpolate between Curves ⑦ and ⑧.

Figure 62: Tension efficiency factor  $K_t$  [27]

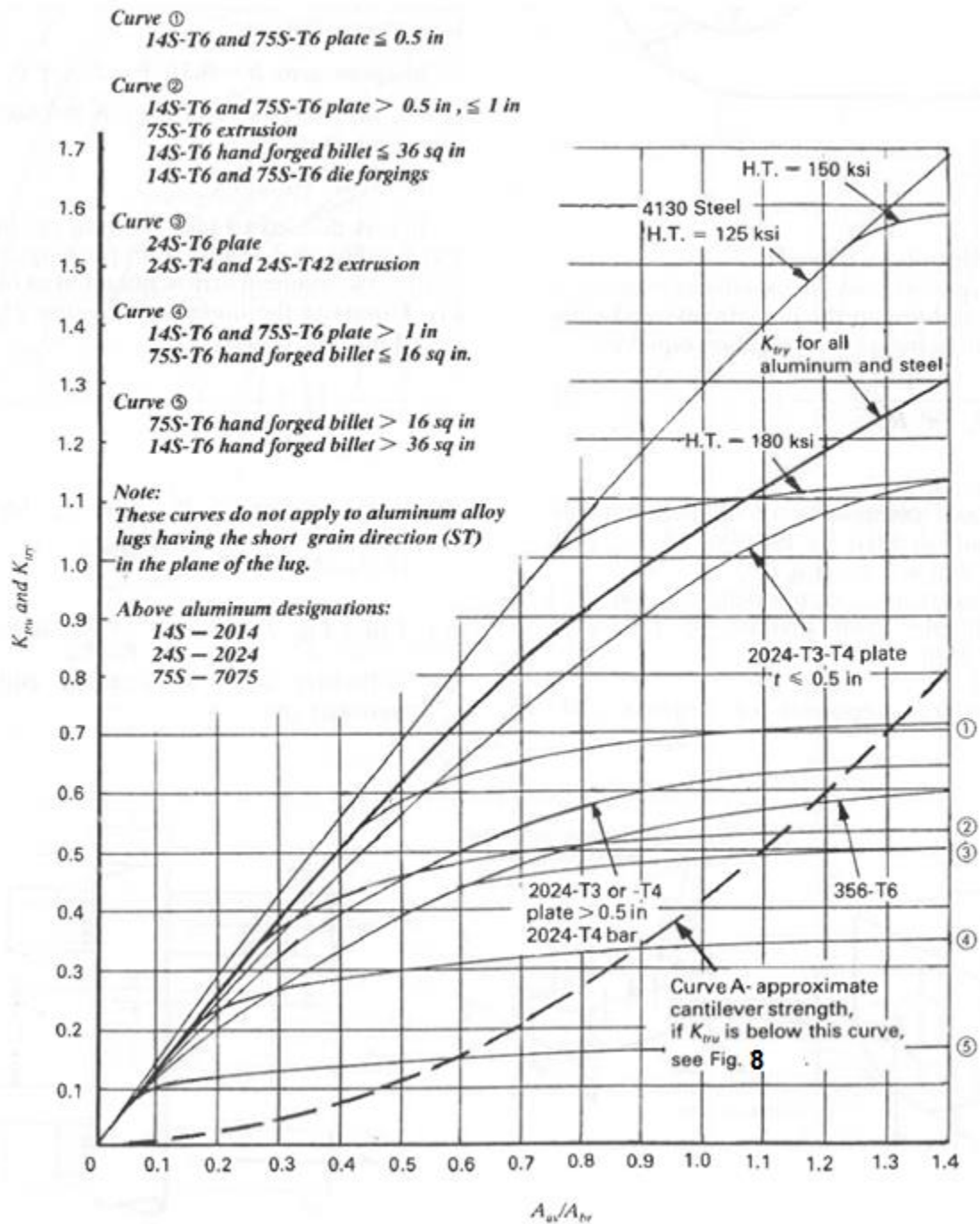


Figure 63: Transverse load efficiency factors:  $K_{ru}$  and  $K_{ry}$  [27]

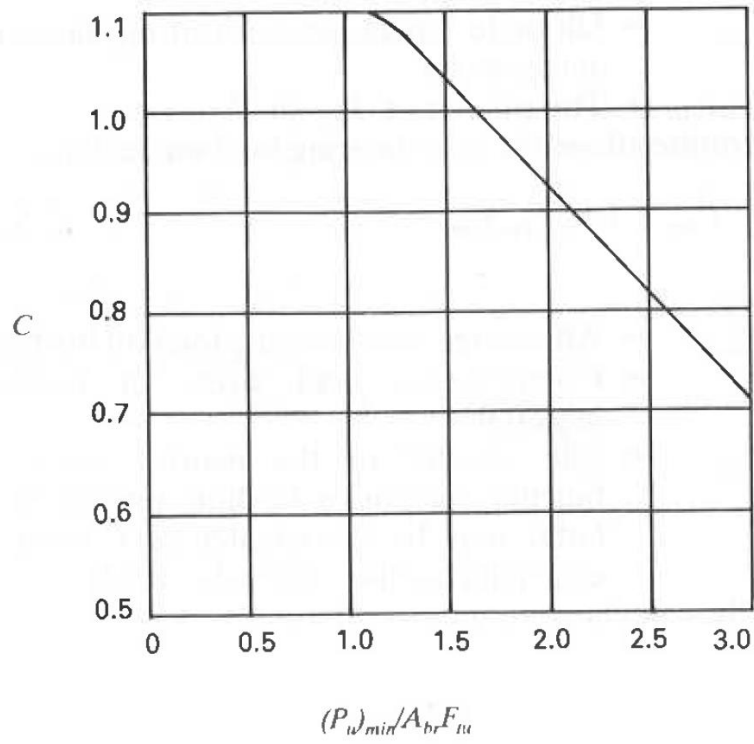


Figure 64: Variation of yield factor [27]



### 6.2.3 PIN ANALYSIS

Pin Analysis involves checking the net-section (minimum cross-section) of the pin subjected to a combination of axial, shear and bending loads. The inputs are the pin outer and inner diameter, loads on the pin and the material properties.

The calculation for pin margin of safety is shown below:

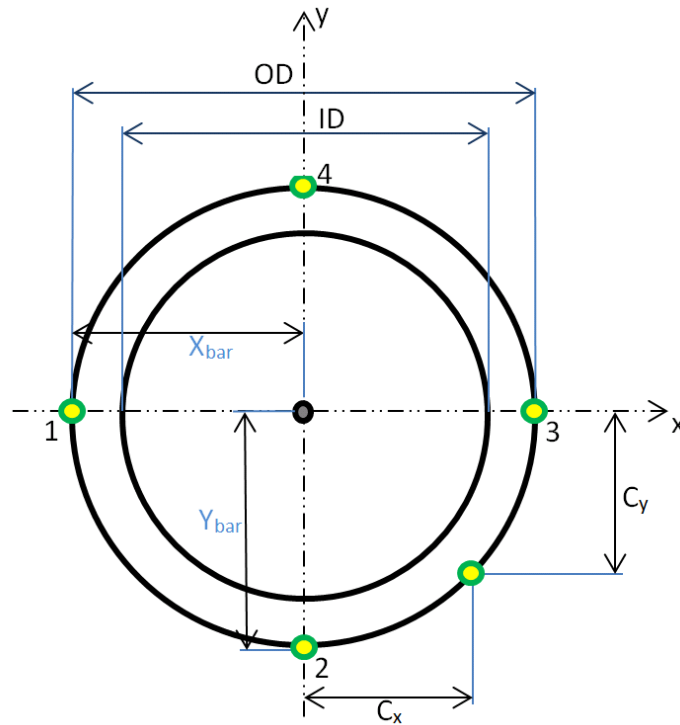


Figure 65: Pin Cross-Section

The section properties are as follows

$$C_{1x}, C_{3x} = \left( \frac{OD}{2} \right) \quad \text{Equation 45}$$

$$C_{1y}, C_{3y} = 0 \quad \text{Equation 46}$$

$$C_{2x}, C_{4x} = 0 \quad \text{Equation 47}$$

$$C_{2y}, C_{4y} = \left( \frac{OD}{2} \right) \quad \text{Equation 48}$$

$$X_{\text{bar}} = \left( \frac{OD}{2} \right) \quad \text{Equation 49}$$

$$t = \frac{(OD-ID)}{2} \quad \text{Equation 50}$$

$$A = \frac{\pi}{4} (OD^2 - ID^2) \quad \text{Equation 51}$$

$$I_{xx} = \frac{\pi}{64} [OD^4 - ID^4] \quad \text{Equation 52}$$

$$Q_{xx} = \frac{OD^3 - ID^3}{12} \quad \text{Equation 53}$$

$$Z_{xx} = \frac{I_{xx}}{C_y} \quad \text{Equation 54}$$

$$K_{xx} = \frac{2Q_{xx}}{Z_{xx}} \quad \text{Equation 55}$$

$$J_{zz} = \frac{\pi}{32} [OD^4 - ID^4] \quad \text{Equation 56}$$

The properties in the y-direction are the same as the corresponding properties in the x-direction because of the symmetric nature of the section. This is summarized in the table below

$$Y_{\text{bar}} = X_{\text{bar}} \quad \text{Equation 57}$$

$$I_{xx} = I_{yy} \quad \text{Equation 58}$$

$$Q_{xx} = Q_{yy} \quad \text{Equation 59}$$

$$Z_{xx} = Z_{yy} \quad \text{Equation 60}$$

$$K_{xx} = K_{yy} \quad \text{Equation 61}$$

The stresses on the cross section are then calculated as follows:

#### 6.2.3.1 Axial (Normal) Stress

Axial stress is defined as the stress resulting in a structural member upon application of an axial load (tension or compression) on a cross-sectional area. The average axial stress in a cross section, subjected to axial load “P” is

$$f_A = \frac{P}{A} \quad \text{Equation 62}$$

#### 6.2.3.2 Shear Stress

Shear stresses on a cross-section subjected to a shear load  $P_s$  can be determined using the following formulae.

Average shear stress	$f_s = \frac{P_s}{A}$	Equation 63
----------------------	-----------------------	-------------

Max shear stress	$f_{smax} = \frac{P_s Q}{I t}$	Equation 64
------------------	--------------------------------	-------------

where,

- $f_A$  = Average axial stress
- $P$  = Axial force
- $f_s$  = Average shear stress

- $P_s$  = Shear force
- $f_{smax}$  = Max shear stress
- $A$  = Area of the cross-section
- $I$  = Moment of inertia
- $q$  = Shear flow
- $E$  = Elastic modulus
- $L$  = Length of the member
- $f_s$  = Shear form factor  $[f_s = A/I^2 \int_A (Q^2/t^2) dA]$
- $Q$  = Semi area moment of inertia
- $t$  = Thickness of cross-section

#### 6.2.3.3 Stress Ratios

Once the various stresses due to the respective applied loads are determined, the stress ratios are calculated as follows:

$$R = \frac{\text{Applied stress}}{\text{Allowable stress}} \quad \text{Equation 65}$$

#### 6.2.3.4 Pin Margin of Safety Calculation

The stress ratios are used to calculate utilization factors, given by:

$$U_1 = \sqrt{(R_A - R_B)^2 + (R_H)^2 - (R_A - R_B)(R_H) + (R_S + R_{St})^2} \quad \text{Equation 66}$$

$$U_2 = \sqrt{(R_A + R_B)^2 + (R_H)^2 - (R_A + R_B)(R_H) + (R_S + R_{St})^2} \quad \text{Equation 67}$$

$$U_3 = \sqrt{(R_A)^2 + (R_H)^2 - (R_A)(R_H) + (R_{Smax} + R_{St})^2} \quad \text{Equation 68}$$

where,

- $U_1, U_2, U_3$  = Utilization factors
- $R_A$  = Axial stress ratio (tension or compression)
- $R_B$  = Combined bending stress ratio
- $R_H$  = Hoop stress ratio
- $R_{St}$  = Torsional shear stress ratio
- $R_S$  = Combined average shear stress ratio
- $R_{Smax}$  = Combined max shear stress ratio

The margin of safety for the cross-section can be determined using the highest utilization factor through the following equation:

$$MS = \frac{1}{U_{\max}} - 1 \quad \text{Equation 69}$$

Where,

MS = Margin of safety

$U_{\max}$  = The highest utilization factor

## 6.3 APPENDIX-III: FINITE ELEMENT MODEL DETAILS

This section presents the details of the Finite Element Models (FEM) used in the case studies.

### 6.3.1 ROLL FRAME

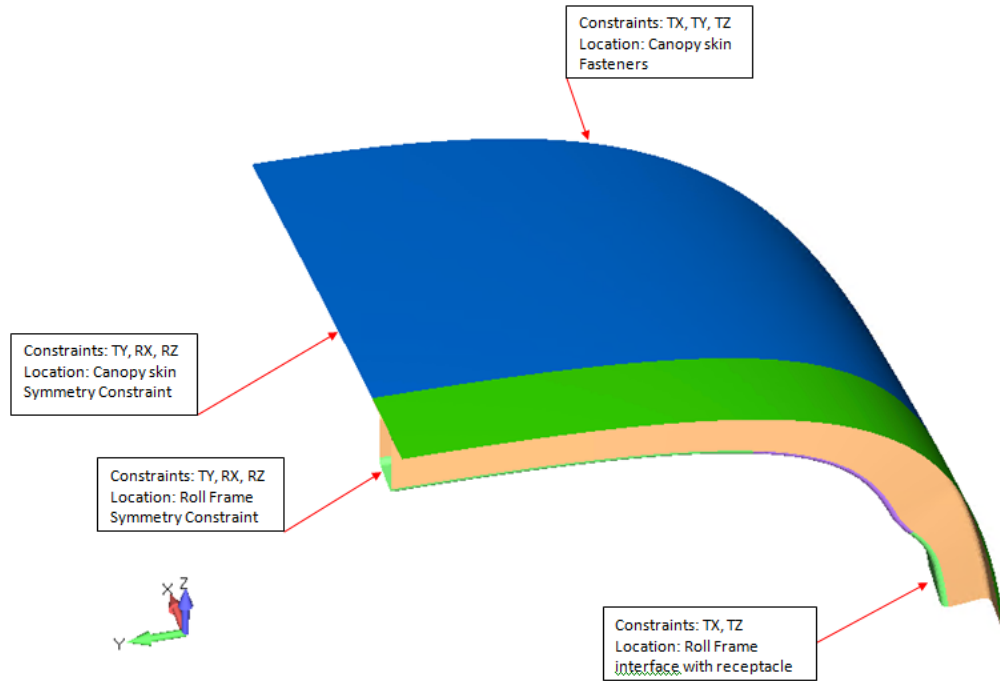


Figure 66: Roll Frame Boundary Conditions

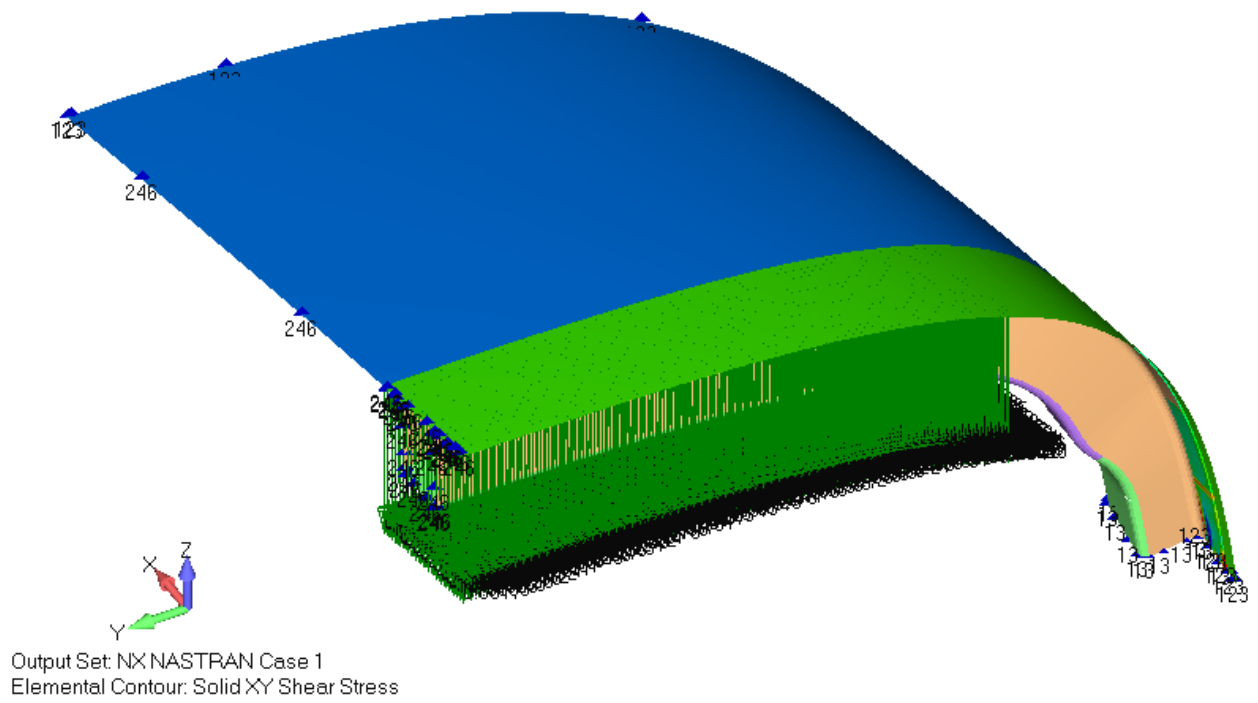


Figure 67: Roll Frame Load Distribution

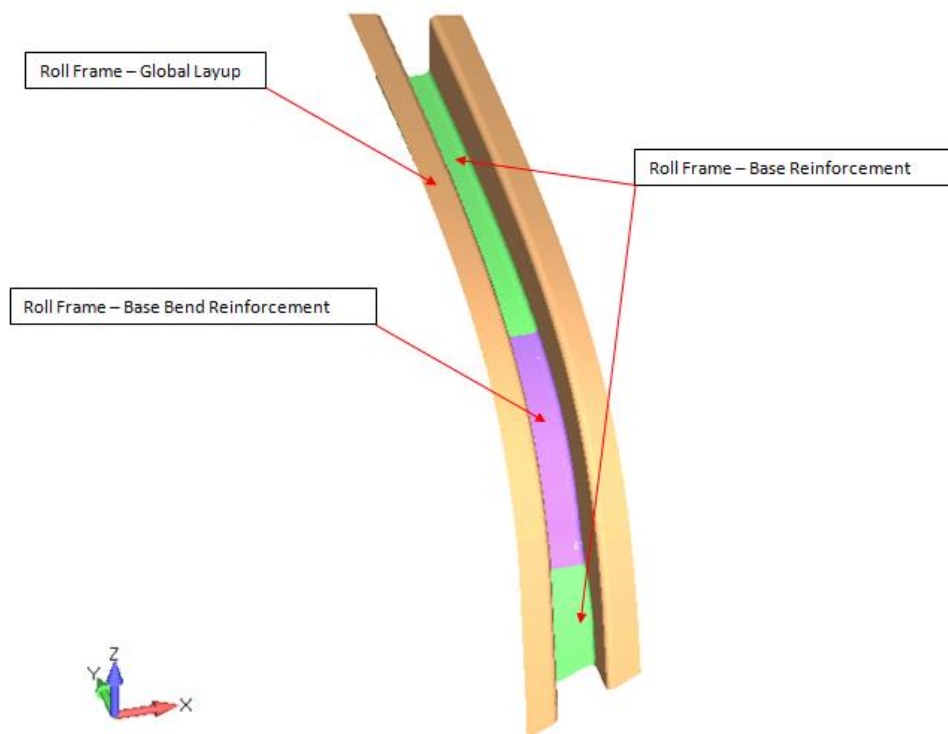


Figure 68: Roll Frame - Ply Regions

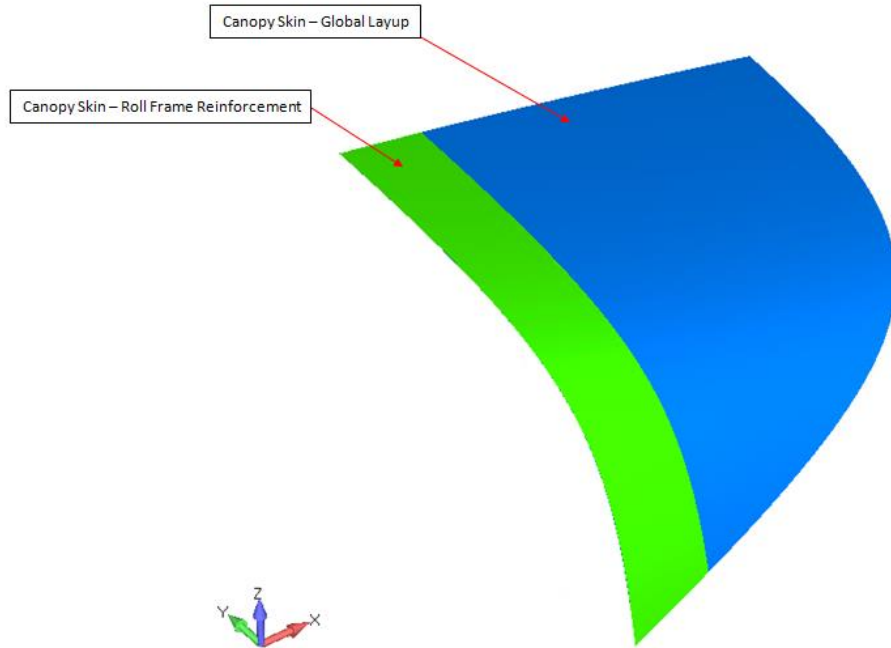


Figure 69: Canopy – Ply Regions

Table 17: Roll Frame - Model Details

Region	Element Type	# Elements
Fuselage Skin – Global Layup	4 Noded Quad	9091
Fuselage Skin –Roll cage Area	4 Noded Quad	2644
Roll Frame – Global Layup	4 Noded Quad	5783
Roll Frame - Base	4 Noded Quad	1854
Roll Frame – Base Bend	4 Noded Quad	947
Bonding Paste	8 Noded Brick	1036



### 6.3.2 NLG BAY DOOR

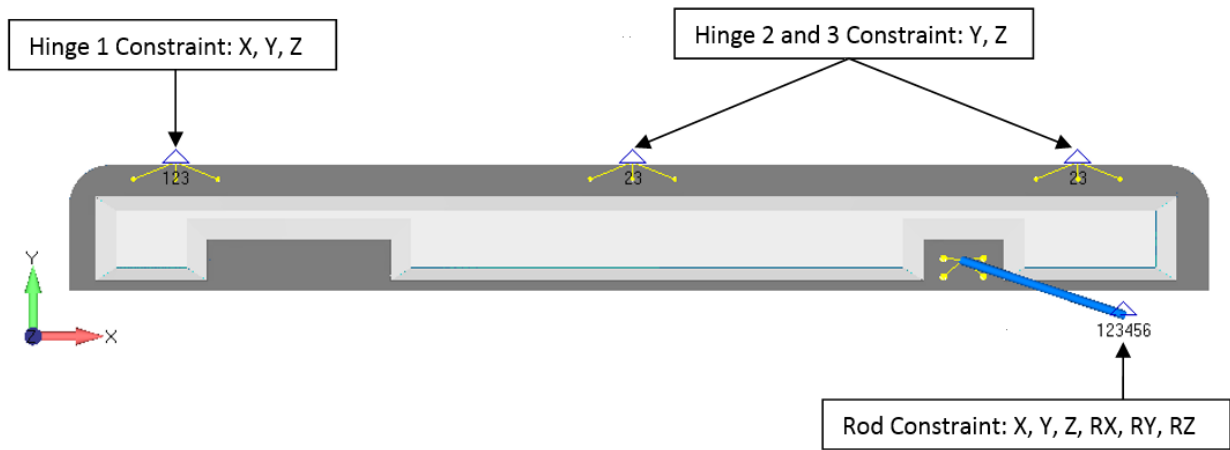


Figure 70: NLG Bay Door Boundary Conditions

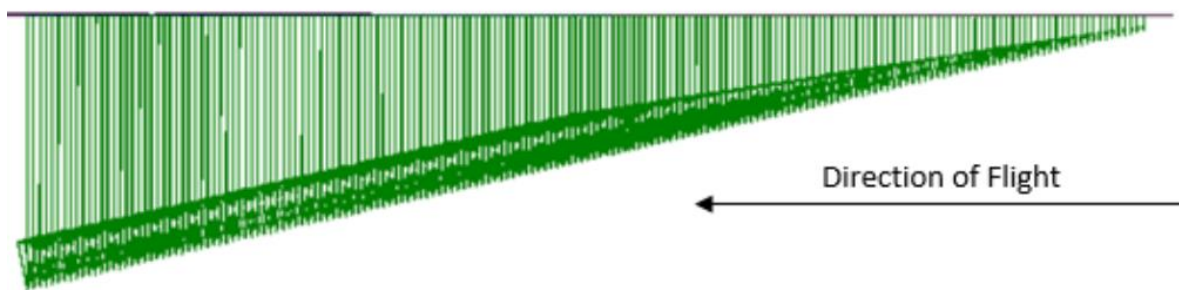


Figure 71: NLG Bay Door Load Distribution

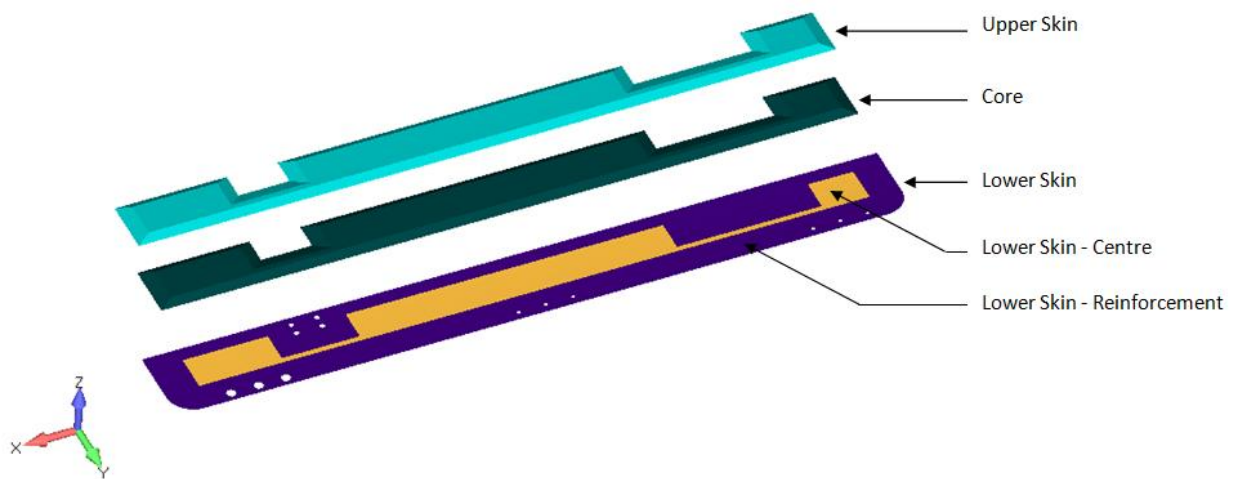


Figure 72: NLG Bay Door – Regions

Table 18: NLG Bay Door – Model Details

<b>Region</b>	<b>Element Type</b>	<b># Elements</b>
Core	8 Noded Brick	3472
Upper Skin	4 Noded Quad	2937
Lower Skin – Centre	4 Noded Quad	2244
Lower Skin – Reinforcement	4 Noded Quad	2081
Rod	2 Noded Line	1

## 7 REFERENCES

- [1] C. M. Eastman, Design for X: concurrent engineering imperatives, Springer Science & Business Media, 2012.
- [2] Department of Defense, "Military Standard Defense System Software Development (DOD-STD-2167A)," Department of Defense, Washinton D.C., 1985.
- [3] R. W. Winston, "Managing the Development of Large Software Systems," in *IEEE Wescon*, 1970.
- [4] Y. S. Ma, G. Chen and G. Thimm, "Paradigm shift: unified and associative feature-based concurrent and collaborative engineering," *Journal of Intelligent Manufacturing*, vol. 19, no. 6, pp. 625-641, 2008.
- [5] NASA, "Concurrent Engineering Guideline for Aerosspace Systems," NASA.
- [6] D. K. Sobek II, A. C. Ward and J. K. Liker, "Toyota's Principles of Set-Based Concurrent Engineering," *Sloan Management Review*, vol. 40, no. 2, pp. 67-83, 1999.
- [7] D. Raudberget, "Practical Applications of Set-Based Concurrent Engineering in Industry," *Strojniški vestnik - Journal of Mechanical Engineering*, vol. 56, no. 11, pp. 685-695, 2010.
- [8] D. K. Sobek II, A. C. Ward and J. K. Liker, "Toyota's Principles of Concurrent Engineering," *Sloan Management Review*, vol. 40, no. 2, pp. 67-83, 1999.
- [9] S. Pugh, "Concept Selection: A Method That Works," in *International Conference on Engineering Design ICED*, Rome, 1981.
- [10] M. Khan and D. G. Smith, "Overcoming Conceptual Barriers -- By Systematic Design," in *Proceedings of the Institute of Mechanical Engineers ICED*, Harrogate, 1989.
- [11] D. D. Frey, Y. Wijnia, K. Katsikopoulos, P. M. Herder, E. Subrahmanian and D. P. Clausing, "An Evaluation of the Pugh Controlled Convergence Method," in *ASME Design Engineering Technical Conference*, Las Vegas, 2007.
- [12] C. Grovers, "What and how about quality function deployment (QFD)," *Internation Journal of Production Economics*, vol. 46, no. 47, pp. 575-585, 1996.
- [13] V. Bouchereau and H. Rowlands, "Methods and Techniques to help quality function deployment (QFD)," *Benchmarking: An Internation Journal*, vol. 7, no. 1, pp. 8-19, 2000.
- [14] DRM Associates, "Customer-Focused Development with QFD," 2016. [Online]. Available: <http://www.npd-solutions.com/qfd.html>. [Accessed 10 02 2017].
- [15] J. D. Schaffer, "Multiple objective optimization with vector evaluated genetic algorithms," Vanderbilt Univ, Nashville, 1984.

- [16] C. M. Fonseca and P. J. Fleming, "Genetic Algorithms for Multiobjective Optimization: Formulation, Discussion and Generalization," in *Genetic Algorithms: Proceedings of the Fifth International Conference*, San Mateo, 1993.
- [17] E. Zitzler and L. Thiele, "Multiobjective Evolutionary Algorithms: A Comparative Case Study and the Strength Pareto Approach," *IEEE Transactions on Evolutionary Computation*, vol. 3, no. 4, pp. 257-271, 1999.
- [18] K. Deb, *Multi-Objective Optimization Using Evolutionary Algorithms*, John Wiley & Sons. Copyright. , 2001.
- [19] N. Srinivas and K. Deb, " Multi-Objective function optimization using non-dominated sorting genetic algorithms," *Evolutionary Computation*, vol. 2, no. 3, pp. 221-248, 1995.
- [20] K. Deb, S. Agrawal, A. Pratap and T. Meyarivan, "A Fast Elitist Non-Dominated Sorting Genetic Algorithm for Multi-Objective Optimization: NSGA-II," Kanpur Genetic Algorithms Laboratory (KanGAL), Indian Institute of Technology Kanpur, Kanpur.
- [21] N. Olhoff, M. P. Bendsoe and J. Rasmussen, "On CAD-integrated structural topology and design optimization," *Computer Methods in Applied Mechanics and Engineering*, vol. 89, pp. 259 - 279, 1991.
- [22] D. Brackett, I. Ashcroft and R. Hague, "Topology Optimization for Additive Manufacturing," Wolfson School of Mechanical and Manufacturing Engineering, Loughborough University, Loughborough, 2011.
- [23] United States Department of Transportation, "14 CFR Part 23, Airworthiness Standards: Normal, Utility, Acrobatic, and Commuter Category Airplanes".
- [24] Battelle Memorial Institute, "Metallic ,aterials Properties Development and Standardization (MMPDS-07)," 2012.
- [25] W. D. Pilkey and R. E. Peterson, *Peterson's Stress Concentration Factors*, New York: Wiley, 1997.
- [26] NHBB Minebea Mitsumi Group, "NHBB Rod End Bearings Astro Division," [Online]. Available: <https://nhbb.com/products/rod-end-bearings.aspx>. [Accessed 20 01 2017].
- [27] E. F. Bruhn, *Analysis and Design of Flight Vehicle Structures*.
- [28] R. M. Jones, *Mechanics of Composite Materials*, 2. Edition, Ed., Taylor and Francis.
- [29] M. C. Niu, *Composite Airframe Structures*, Hong Kong Comlit Press Ltd., 1992.
- [30] W. C. Young and R. G. Budynas, *Roark's Formulas for Stress and Strain*, 7th, Ed., McGraw-Hill.
- [31] R. Lloyd, *Metric mishap caused loss of NASA orbiter*, CNN, 1999.

- [32] D. S. B. Johnson, "Success, Failure, and NASA Culture," ASK Magazine.
- [33] M. Matousek and J. Schneider, "Untersuchungen Zur Struktur des Zicherheitproblems bei Bauwerken," Zurich, 1976.
- [34] D. W. W. Royce, "Managing the Development of Large Software Systems," in *IEEE, Wescon*, 1970.
- [35] J. R. Hauser, "How Puritan-Bennett used the House of Quality," *Sloan Management Review*, vol. 34, pp. 61-70, 1993.
- [36] W.-C. Chiang, A. Mital and A. Desai, "A generic methodology based on Six-Sigma for designing and manufacturing consumer products for functionality," *International Journal of Product Development*, vol. 7, no. 3/4, pp. 349-371, 2009.
- [37] K. Matzler and H. H. Hinterhuber, "How to make product development more successful by integrating Kano's model of customer saisfaction into quality function deployment," *Technovation*, vol. 18, no. 1, pp. 25-38, 1998.
- [38] P. Marwick, "Integrating design and manufacturing strategies for business transformation," *International Journal of Technology Management, Special Issue on Manufacturing Strategy*, pp. 355-359, 1991.
- [39] R. J. Holt and C. J. Barnes, "Proactive Design for Manufacture through decision analysis," *International Journal Product Development*, vol. 13, no. 1, pp. 67-83, 2011.
- [40] G. Pahl, W. Beitz, J. Feldhusen and -H. K. Grote, *Engineering Design: A Systematic Approach*, 3 ed., London: Springer, 2007.
- [41] A. Martins and E. M. Aspinwall, "Quality function deployment: an empirical study in the UK," *Total Quality Management*, vol. 12, no. 5, pp. 575-588, 2001.
- [42] H. Winter, "Flow Phenomenon on Plates and Airfoils of Short Span," 1936.
- [43] M. C. Niu, *Airframe Stress Analysis and Sizing*, Hong Kong Comlit Press Ltd., 1999.
- [44] J. L. Cadden and P. F. Sadesky, "Tooling for Composites," *Handbook of Composites*, pp. 556-575, 1998.
- [45] "New Hampshire Ball Bearings Inc.," 2014. [Online]. Available: [https://nhbb.com/files/catalog\\_pages/NHBB\\_RodEnd\\_and\\_Spherical\\_Bearing\\_Products\\_and\\_Engineering\\_Catalog-2014.pdf](https://nhbb.com/files/catalog_pages/NHBB_RodEnd_and_Spherical_Bearing_Products_and_Engineering_Catalog-2014.pdf). [Accessed 31 03 2017].
- [46] D. Raudberget, "Practical Applications of Set-Based Concurrent Engineering in Industry," *Strojniški vestnik - Journal of Mechanical Engineering*, vol. 56, no. 11, pp. 685 - 695, 2010.